

Balancing potency, metabolic stability and permeability in pyrrolopyrimidine based EGFR inhibitors

Jin Han^{a,b)}, Silje Henriksen^{a,c)}, Kristin G. Nørsett^{d)}, Eirik Sundby^{b)}, Bård Helge Hoff^{a)}*

^{a)}Norwegian University of Science and Technology, Department of Chemistry, Høgskoleringen 5, NO-7491 Trondheim, Norway. ^{b)}Norwegian University of Science and Technology, Institute of Chemistry and Material Technology, Faculty of Technology, 7491 Trondheim. ^{c)} Current address: Jotun Marine, Protective and Powder Coatings, Rosenvoldsgt. 19, NO-3202 Sandefjord, Norway. ^{d)}Norwegian University of Science and Technology, Department of Cancer Research and Molecular Medicine, Prinsesse Kristinas gt. 1, N-7030 Trondheim, Norway.

Corresponding author: * Bård H. Hoff, Department of Chemistry, Norwegian University of Science and Technology (NTNU), NO-7491, Norway. Email: Bard.Helge.Hoff@chem.ntnu.no, phone: ++004773593973, fax: ++004773594256.

Abstract: The present study describes our continuous effort to develop epidermal growth factor receptor (EGFR) inhibitors based on the 6-aryl-pyrrolo[2,3-*d*]pyrimidin-4-amine scaffold. The activity-ADME space has been evaluated by synthesizing 43 new structures, including four variations of the 4-amino group and 34 different substitution patterns in the 6-aryl moiety. Most of the new pyrrolopyrimidines were highly active, with twelve analogues possessing lower IC₅₀ values than the commercial drug Erlotinib in enzymatic assays. Ten EGFR inhibitors were also profiled in cell studies using the Ba/F3-EGFR^{L858R} reporter cells, and all revealed nanomolar activity. However, some of the privileged structures in terms of potency had ADME short-comings: compounds containing amides, sulfonamides, amine and hydroxymethyl substituents in the 6-aryl group had low permeability and high efflux, derivatives having (*R*)-3-amino-3-phenylpropan-1-ol at C-4 induced hERG inhibition properties, and metabolic lability was seen for compounds having (*S*)-2-methoxy-1-phenylethan-1-amine at C-4. Based on a trade-off between enzymatic activity, cellular potency and ADME properties, (*S*)-2-phenyl-2-((6-phenyl-7*H*-pyrrolo[2,3-*d*]pyrimidin-4-yl)amino)ethan-1-ol appeared as the most promising drug candidate. Cellular studies indicate this compound to have therapeutic use in EGFR driven diseases.

Keywords: EGFR; Pyrrolopyrimidine; SAR; ADME; metabolism; Erlotinib

1. Introduction

Protein kinases are an important class of enzymes which catalyse phosphorylation of specific protein substrates, thereby regulating vital cellular processes. Abnormality in expression levels or in the structure of these protein kinases plays a crucial role in a number of human diseases. Kinases are especially attractive targets for treatment of cancer diseases [1, 2] The membrane bound epidermal growth factor receptor tyrosine kinase (EGFR) has been one of the more investigated kinase, since EGFR amplification or mutation has been noted in lung [1, 3], breast [2], pancreatic [4], ovarian [5], prostate [6], and head and neck [7] cancers. However, development of new kinase drug candidates is increasingly difficult, and a late focus on absorption, distribution, metabolism, excretion and toxicology (ADMET) is regarded as one of the main reasons for drug failure [8, 9]. Kinase inhibitors tend to have higher molecular weight and be more lipophilic than other classes of drugs [10], which could lead to suboptimal properties in terms of solubility and permeability [11], but also to toxicity [12]. Attractive kinase inhibitors could have a moderate kinase selectivity [13, 14] causing side effects [15]. Moreover, patients receiving EGFR therapy are likely to have undergone other type of chemotherapy increasing the risk of organ failure [16]. Thus, avoiding potential ADMET pitfalls early on in development is important. Most small molecular based EGFR inhibitors are based on aniline substituted quinazolines. For this class of drug candidates ADMET data is available as input for drug developmental programs [16-18]. We have focused our development on chiral benzylamine based pyrrolo[2,3-*d*]pyrimidines as EGFR inhibitors [19-21]. Only three pyrrolopyrimidines based EGFR inhibitors have reached clinical trials, namely PKI-166 [22], AEE-788 [23, 24], and TAK-285 [25, 26], see Figure 1.

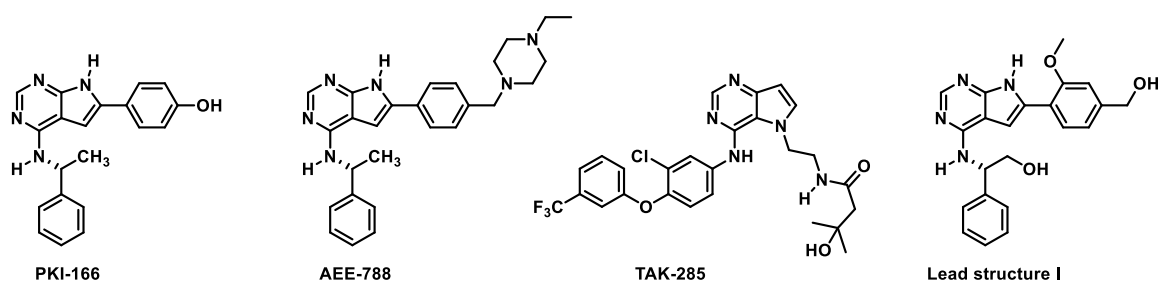


Figure 1. Pyrrolopyrimidine-based EGFR inhibitors.

Our lead compound **I** [20] (Figure 1), which possessed high *in vitro* enzymatic and cellular activity, was unfortunately a substrate of the breast cancer resistant protein and the P-glycoprotein ABC-transporters, making further development challenging [21]. Herein, we describe our continuous effort to identify new EGFR inhibitor candidates with improved ADME profile.

2. Results and discussion

2.1 Design

At the onset of this study, our main concern with the lead structure **I** was metabolism at the 4-positioned benzylic alcohol and at the 2-methoxy group. However, as the project proceeded it was evident that the challenge with **I** was mediocre permeability and a high efflux, while human liver microsome assay indicated the molecule to be stable to phase I oxidative metabolism. Thus, the drug discovery process was thereafter motivated by desire to improve permeability while maintaining on target potency.

Initially, we focused on identifying bioisosteres for the 2-methoxy and the 4-hydroxymethyl groups. The 4-benzylic function is directed towards the active site entrance, which might allow for some flexibility in terms of substituent size. Thus, we included a range of hydrogen bond acceptor and donor groups of different size at the 3- and 4-position of the 6-aryl group. At the 2-position we set on to synthesise compounds with ether functionalities varying in size and electronic properties.

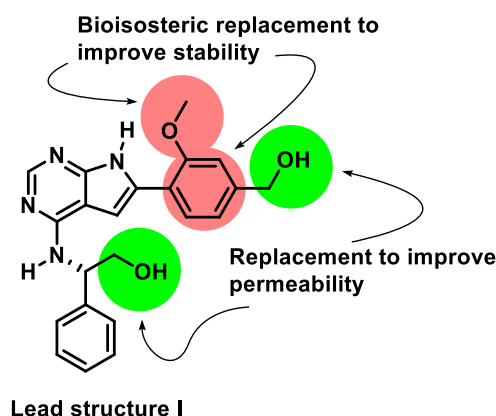
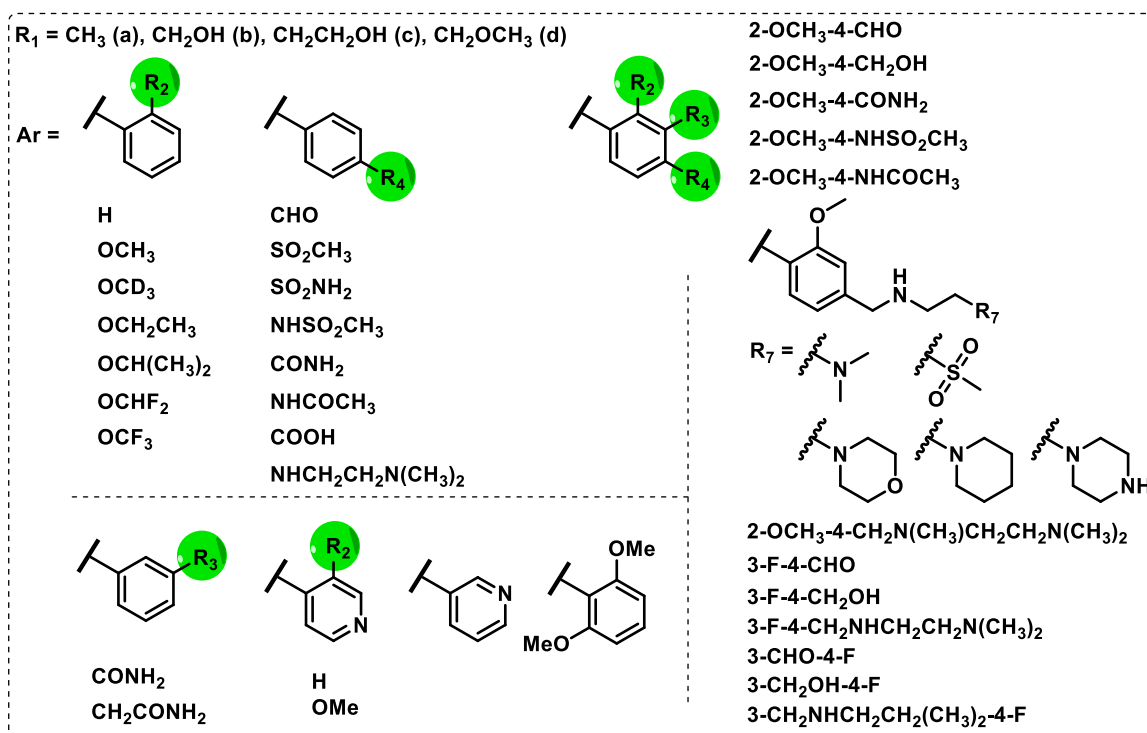
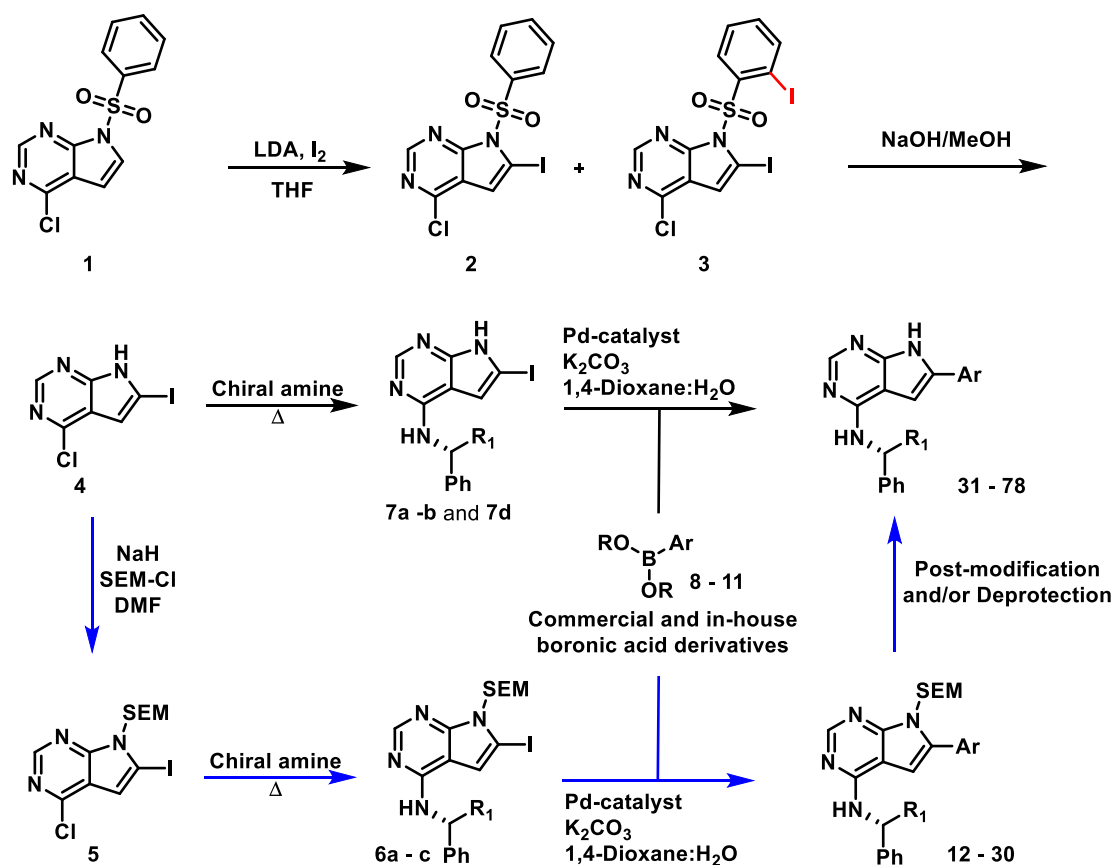


Figure 2. Lead structure **I**, and structural elements subjected to further evaluation.

As the project proceeded various strategies were attempted to improve the activity/ADME properties of the compounds including: fluorine insertion; deuteration; solubilizing tails; replacement of the 6-aryl group by pyridines; and varying the amine part of the molecule.

2.2 Chemistry

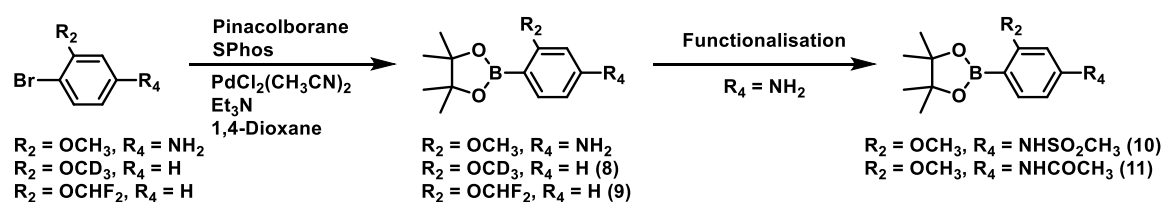
The synthesis of all EGFR inhibitors were performed starting with 4-chloro-6-iodo-7*H*-pyrrolo[2,3-*d*]pyrimidine (**4**), which in turn was obtained in two steps from the precursor **1**, see Scheme 1. Iodination of **1** gave a 9 : 1 mixture of compound **2** and **3**, which upon pyrrole deprotection gave the key intermediate **4** in 89 % yield. Two alternative routes were used for C-4 and C-6 functionalisation of the pyrrolo[2,3-*d*]pyrimidine core. The shortest method includes amination of **4** to yield the derivatives **7**, followed by a Suzuki coupling to give the target inhibitor structures. Although containing only two steps, this pathway has the drawbacks of low reactivity in both the amination and in the Suzuki coupling.



Scheme 1. Synthesis of functionalized pyrrolo[2,3-*d*]pyrimidines. Reagents: SEM-deprotection i) TFA, CH_2Cl_2 , ii) sat. Aqueous NaHCO_3 , THF.

Therefore, we installed the *N*-2-trimethylsilylethoxymethyl (*N*-SEM) protection on the pyrrol to give the intermediate **5**. With the SEM-protected pyrrolopyrimidine derivatives,

both the amination and the cross-coupling reaction proceeded more smoothly. Purification by silica-gel chromatography was also more facile. The Suzuki reaction was performed mainly with XPhos/Xphos Pd G2 as catalyst system. In contrast, standard conditions using Pd(PPh₃)₄ proved inefficient also on typically good substrates. Low reactivity in the Suzuki coupling was observed between pyridinylboronic acids and **6a-b**. Besides pyrrole protection, a change in catalyst system from XPhos/Xphos Pd G2 to the ferrocene based PdCl₂(dppf) catalyst improved the processes. When more complex 6-aryl substitution patterns were targeted, in-house synthesized arylboronic esters (**8-11**) were used, see Scheme 2. These were synthesised by boronylation of aryl bromides with pinacolborane using the PdCl₂(CH₃CN)₂ / SPhos catalyst system [27] with yields ranging from 64 – 81 %. Importantly, this system successfully transformed aryl bromides with amines and sterically hindered *ortho*-substituents to the corresponding arylboronic esters in good yield. The required *N*-substitution pattern in **10** and **11** could be introduced either prior or after the boronylation.



Scheme 2. Synthesis of boronic esters **8-11**. Functionalisation to: **10**: CH₃SO₂Cl, CH₂Cl₂; **11**: Ac₂O, CH₂Cl₂.

Some of the kinase inhibitors were made by post-modification of 6-aryl-7*H*-pyrrolo[2,3-*d*]pyrimidin-4-amines structures having aldehyde substituents in the 3- and 4-position of the 6-aryl group. These reactions involved conventional reduction using sodium borohydride to the corresponding benzylic alcohols and reductive aminations. A two-step reductive amination protocol via the imine followed by NaBH₄ reduction was found more efficient than the one-step method using NaBH(OAc)₃.

2.3 EGFR kinase inhibition

In our previous work, combination of 2-methoxy and 4-hydroxymethyl as 6-aryl substituents resulted in favourable ligand-protein interactions and high EGFR inhibitory properties [21]. Nevertheless, both the methoxy group and the polar benzyl alcohol function could easily be afflicted by metabolic inactivation *in vivo*. Initially, the benzyl alcohol at the 4-position of the 6-aryl ring was replaced with amide, methyl sulfone, sulfone amide, methyl sulfone amide, acetamide, *meta*-carboxamide and pyridine, while using (*R*)-1-phenylethan-1-amine as the C-4 substituent, see Figure 3. All these derivatives displayed high inhibitory properties with IC₅₀ below 1 nM. Especially attractive was derivative **34** bearing a methylsulfone and the sulfonamide **37**. Erlotinib in this assay had an IC₅₀ value of 0.4±0.2 nM. We were also encouraged to find that the pyridine derivative **39** was active. This allows for tuning of both metabolic stability and solubility. Turning to the 2-position

which has been insufficiently investigated previously, enzymatic EGFR assays showed that ethoxy, isopropoxy and OCHF₂ groups were all well tolerated, while the trifluoromethoxy group resulted in lower potency. Four di-substituted derivatives, **46-49**, were also evaluated and displayed promising activity. However, only in case of the *N*¹,*N*¹-dimethylethane-1,2-diamine substituted **49** an obvious improvement in activity was seen as compared to the mono-substituted analogues.

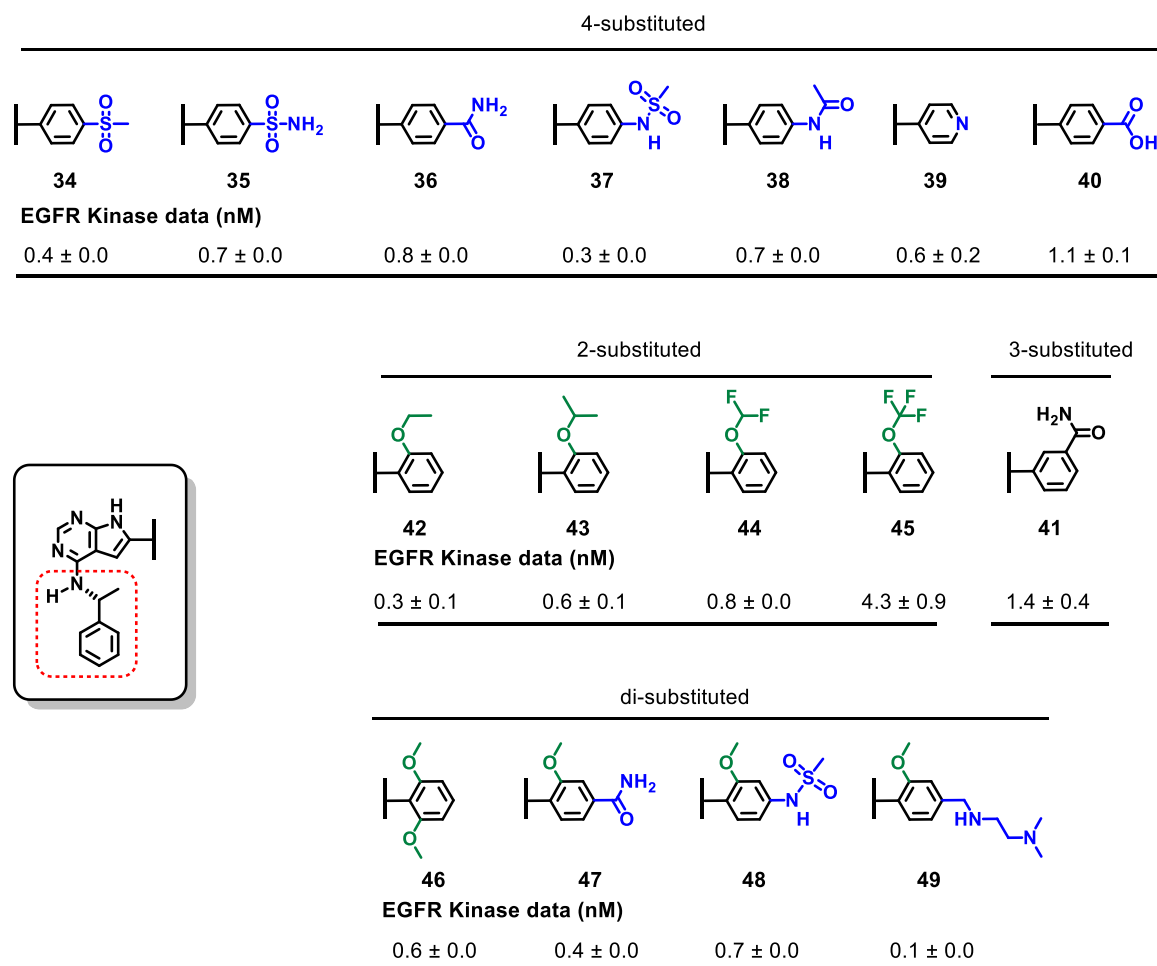


Figure 3. Effect of variation of the 6-aryl group on the EGFR IC₅₀ value (nM) for pyrrolopyrimidines containing (*R*)-1-phenylethan-1-amine as C-4 substituent.

In our previous study on pyrrolopyrimidine-based EGFR inhibitors, an improvement of potency was seen when substituting (*R*)-1-phenylethan-1-amine at C-4 with the (*S*)-2-amino-2-phenylethan-1-ol group. As a starting point we evaluated the previously discovered unsubstituted compound **50** and the 2-methoxy derivative **51** for metabolic stability and permeability. Both compounds were found highly permeable by Caco-2 assays (P_{app} (**50**) = 30.3×10^{-6} cm/s, P_{app} (**51**) = 26.4×10^{-6} cm/s), while compound **50** had higher stability in human liver microsome assays ($t_{1/2}$ (**50**) = 109 min, $t_{1/2}$ (**51**) = 29.6 min). Based on this background, we analysed additional derivatives having the (*S*)-2-amino-2-phenylethan-1-ol, see Figure 4. Several of the potency inducing 6-aryl groups identified in the first series (Figure 3) was chosen, but also new substitution patterns: a deuterated derivative, **52**, designed to slow metabolism; the amide **56** as a bioisoster for the benzyl alcohol function;

compounds containing pyridines (**60-62**) and solubilizing tails (**63-68**) to address solubility and protein binding. Again, most derivatives were highly potent, but an additional increase in potency on introducing the (*S*)-2-amino-2-phenylethan-1-ol was hardly seen. This could be due to enthalpy-entropy compensating effects, in which the favourable binding energy is compensated by unfavourable entropy losses due to more tight binding [28, 29].

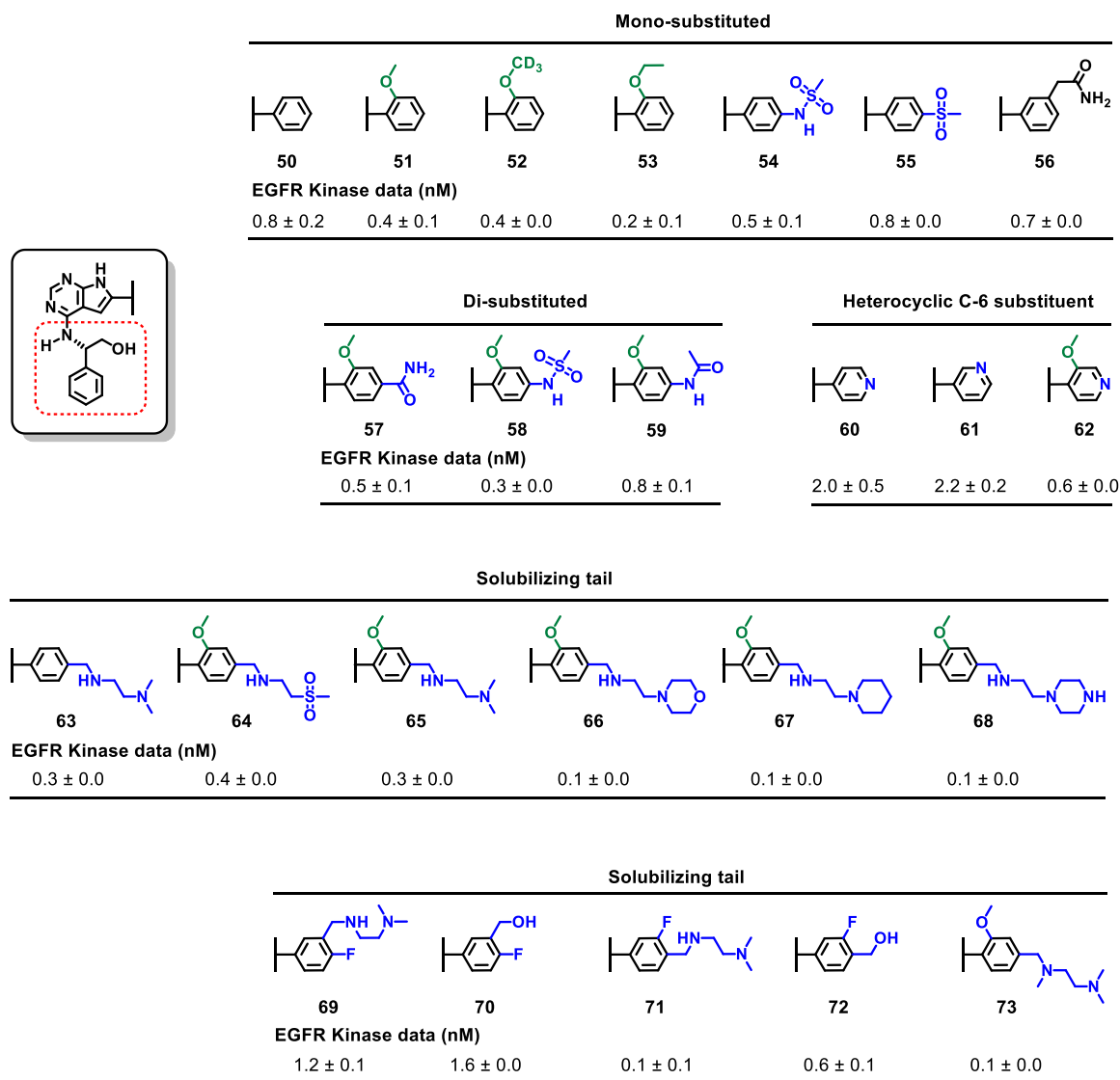


Figure 4. Effect of variation of the 6-aryl group on EGFR IC₅₀ value (nM) for pyrrolopyrimidines containing (*S*)-2-amino-2-phenylethan-1-ol as C-4 substituent.

During ADME evaluation of the derivatives mentioned above, it became evident that the more polar compounds had low permeability and a high efflux ratio. Incorporation of fluorine adjacent to hydrogen bond donors has previously been shown as an efficient strategy to improve permeability [30], thus derivatives **69-72** were prepared.

Compounds **69** and **70** having a 4-fluoro substituent showed IC₅₀ values of 1.2 and 1.6 nM, respectively. However, higher activity was observed for derivatives **71** and **72** substituted with a fluorine in position 3. Compound **73** with a *N*¹,*N*²,*N*²-trimethylethane-1,2-diamine group was also highly active.

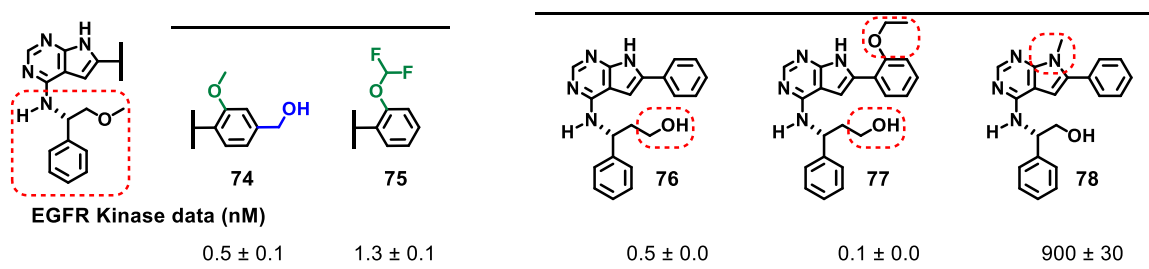


Figure 5. EGFR IC₅₀ value (nM) for pyrrolopyrimidines **74-78**.

Five other compounds evaluated by kinase assay are shown in Figure 5. The (*S*)-2-methoxy-1-phenylethan-1-amine containing compounds **74** and **75** had IC₅₀ values of 0.5 and 1.3 nM, respectively. This scaffold was not further investigated due to the low metabolic stability seen for compound **75**. Compound **76**, with (*R*)-3-amino-3-phenylpropan-1-ol at C-4, was designed to improve contacts in the DFG motif by hydrogen bonding to polar residues, and as compared to derivative **50**, an improvement in EGFR activity was seen. Furthermore, an additional gain in potency was obtained when installing a 2-ethoxy substituent (compound **77**). Unfortunately, this scaffold induced hERG inhibition. The *N*-methyl substituted compound **78** was made to confirm SAR information and as a model compound for ADME studies. As anticipated, removing the pyrrole NH-group gave a high IC₅₀-value.

2.4 SAR and *in-silico* evaluation

The SAR information based on this and our previous work on pyrrolopyrimidines is summarised in Figure 6.

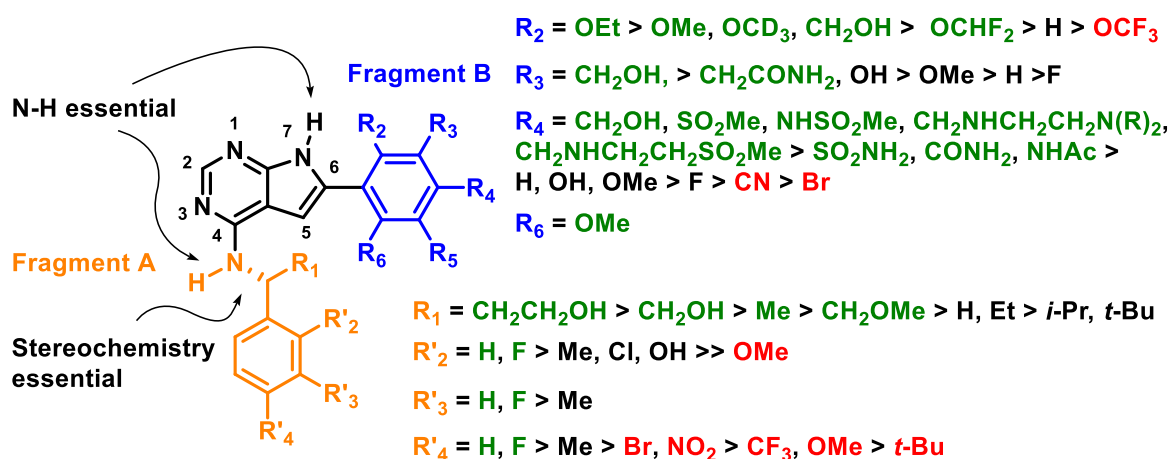


Figure 6. Structure-activity relationships identified in this and previous study [19, 20]. Colour code: green: induce potency; black: minor effects; red: reduce potency.

In short, for Fragment A, the activity was highest when having a hydroxymethyl or hydroxyethyl substituent as R₁, which is explained by hydrogen interactions to the DFG motif. The discussion of the effect of hydroxyl group on activity is complicated by the possibility of intramolecular hydrogen bonding. Compounds **50**, **53** and **77** were subjected to a conformational search using MacroModel and the OPLS3 force field. The search gave conformations with lowest energy which displayed intermolecular hydrogen bonds between the hydroxyl groups and the pyrimidine N-3 for all compounds tested, see Supplementary Material. The intramolecular hydrogen bond would reduce desolvation cost, but the required reorganisation of hydrogen bonding, as judged from docking and dynamics, would somewhat limit the positive impact on binding. Unsubstituted phenyl or fluorinated substituents are preferred in the aromatic part [20], while the activity is highly dependent on correct stereochemistry as also seen in the thienopyrimidine series of compounds [31]. Substitution of the 6-aryl group (Fragment B) improved EGFR potency when having polar groups in the 4-position. The same substituent can also be placed in 3-position. Evaluation of 2-substitution patterns confirmed the ethoxy substituent to have the highest positive impact on activity, and also that larger substituents as isopropoxy and difluoromethoxy were well tolerated. A drop in potency was noted for the trifluoromethoxy analogue, which might indicate that minor size changes or electronic properties are of importance. Finally, methylating the pyrrole NH group removed most activity.

Selected derivatives were investigated for their binding interactions with EGFR by induced-fit docking with the Schrödinger Maestro suite [32-34] using the crystal structure 4WKQ at 1.85 Å resolution [35]. The docking revealed compounds **53**, **65**, **76**, and **77** to have very similar binding mode. Docking scores were -10.63, -11.00, -11.42 and -10.77 kcal/mol, respectively. The docked structure of compound **77** is shown in Figure 7. The main interactions were between the pyrimidine N-1 involved in hydrogen bonding with the backbone NH of Met793, and the pyrimidine N-3 nitrogen which engaged in water mediated hydrogen bonding. For derivatives **53**, **76** and **77**, a hydrogen bond between the hydroxyl group in the R₁ side chain and Asp855 was noticed, while compound **65** is bonded to Thr854.

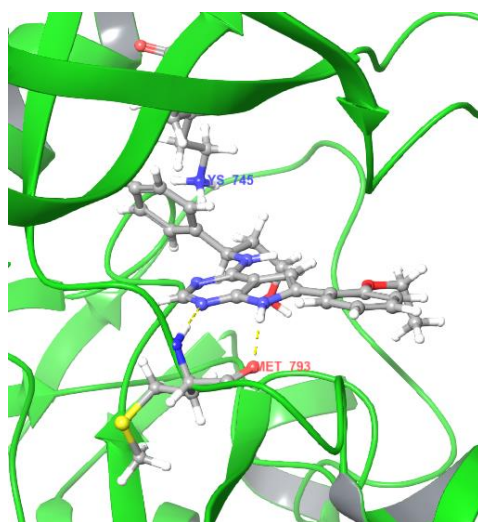


Figure 7. Docking of compound **77** using crystal structure 4WKQ [35].

In contrast, the highest docking score for compound **50** was for a pose in which the pyrrole NH and the pyrimidine N-1 promote binding via a network of water molecules to Thr790, Gln791 and Thr854. We also found a docking pose with similar binding mode as that shown for **77** in Figure 7, but being 1.36 kcal/mol higher in energy. Both binding modes are shown in the Supplementary Material. Although we cannot exclude the possibility of an alternative binding mode, the rather consistent SAR data indicate that all derivatives bind in a very similar way.

The poses with the best docking scores were then evaluated by 10 ns molecular dynamics using the Desmond suite, the OPL-3 force field and the TIP4P solvent model [36]. An interaction plot following dynamics for compound **77** is shown in Figure 8.

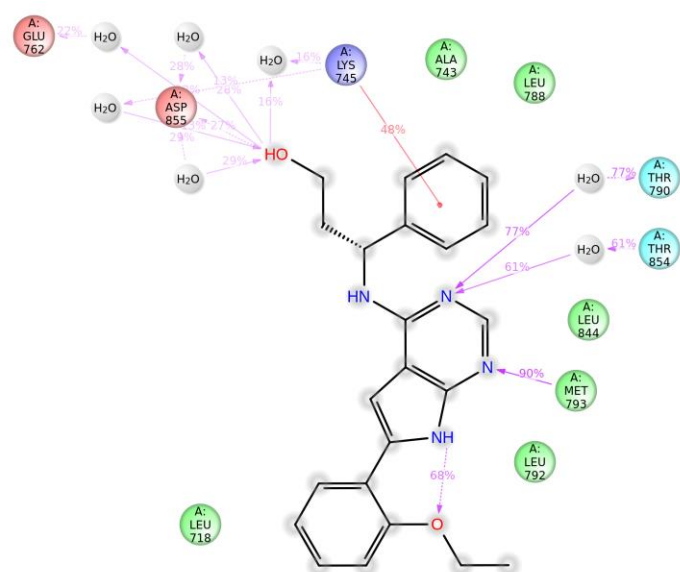


Figure 8. Ligand-EGFR contacts for compound **77** during 10 ns of molecular dynamics. Highlighted amino acids are within 5 Å distance from the docked ligand. (Dynamics for compounds **50**, **53** and **76** are given in the Supplementary Material). The colours indicate residue type: green – lipophilic residues; red – acidic residues; blue – polar residues; purple – basic residues. The lines indicate contacts with the enzyme. Only interactions that occur more than 10 % of the 10 ns simulation time are shown. Ligand atoms that are exposed to solvent are marked with grey spheres.

Dynamics showed all these compounds to interact via N-1 to Met793. The pyrrole NH in case of compound **65** and **76** is found to interact with the oxygen of Met793. However, in compounds **53** and **77** the pyrrole NH instead was indicated to have intramolecular hydrogen bonding with the ether functionalities at the 6-aryl group. On one hand, if this interaction is also present in the unbound state, desolvation will be less costly. On the other side, an intramolecular hydrogen bond would prevent the pyrrole NH from taking part in EGFR binding. However, a potency increase was seen going from unsubstituted to 2-methoxy and 2-ethoxy substituted 6-aryls. It could be that this is solely due to weak lipophilic interactions, which could be under estimated in docking protocols. Alternatively,

the substituent or the indicated intramolecular hydrogen bond could induce a slight alteration of the position of the 4-amino group causing stronger binding in this part.

Further, compounds **53**, **65**, **76** and **77** were indicated to have hydrogen bonding from N-3 via water molecules to different residues, mainly Thr854 and Cys775. In the 4-amino part (Fragment A) differences were noticed as compared to the docked structures. Lys745 forms a cation- π interaction with the aromatic ring. This interaction was found to be most prominent in the ether containing derivatives **53** and **77**. Lys745 also together with Asp855 and other residues form hydrogen bonding networks with the hydroxyl group at the R₁ side chain. The higher activity of **76** and **77** as compared to derivatives **50** and **53** could thus be due to these extended hydrogen bonding networks.

High potency was seen for all derivatives containing solubilizing tails at the 4-position of the 6-aryl group. An interaction plot from dynamics of derivative **65** is shown in Figure 9. The *N,N'*-dimethylethane-1,2-diamine substituent is indicated to be hydrogen bonded via several water molecules to Asp800, Cys797, and Pro794, which might explain the high activity of these derivatives.

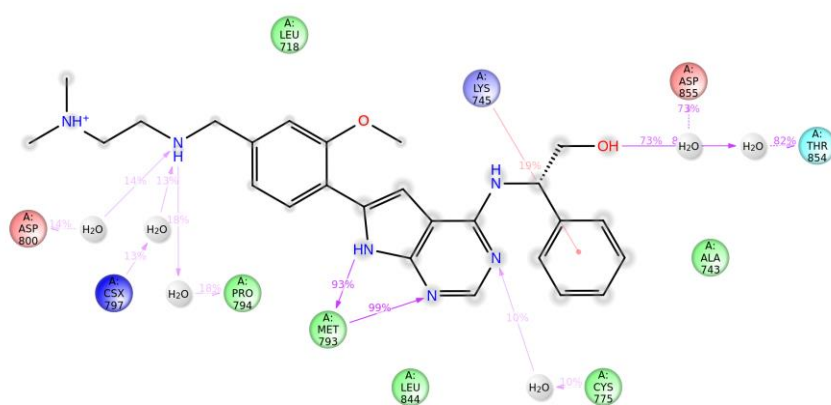
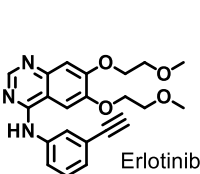
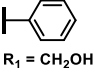
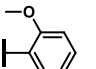
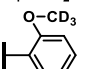
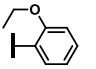
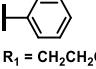
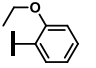
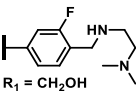
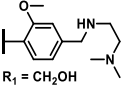
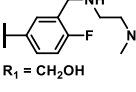
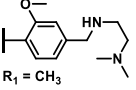


Figure 9. Ligand-EGFR contacts for compound **65** during 10 ns of molecular dynamics. Highlighted amino acids are within 5 Å distance from the docked ligand. The colours indicate residue type: green – lipophilic residues; red – acidic residues; blue – polar residues; purple – basic residues. The lines indicate contacts with the enzyme. Only interactions that occur more than 10 % of the 10 ns simulation time are shown. Ligand atoms that are exposed to solvent are marked with grey spheres.

2.5 ADME profiling

A summary of the ADME profile of some of the drug candidates is given in Table 1, while additional data for other compounds is provided in the Supplementary Material.

Table 1. Summary of key ADME data for the new EGFR inhibitors. Compounds are sorted by the P_{app} values. Additional data is provided in Supplementary Material.

Comp.	Structures	P_{app} A-B ($10^{-6} \text{ cm s}^{-1}$) ^{a)}	Efflux ratio ^{a)}	HLM $t_{1/2}$ [min] ^{b)}	Protein binding (fu) ^{c)}	Solubility (μM) ^{d)}
Erlotinib		38.8	0.80	31.7	0.12	20
50	 $R_1 = \text{CH}_2\text{OH}$	30.3	1.17	109	0.02	>100
51	 $R_1 = \text{CH}_2\text{OH}$	26.4	1.34	29.6	0.02	10.5
52	 $R_1 = \text{CH}_2\text{OH}$	23.4	1.02	44.1	<0.01	11.5
53	 $R_1 = \text{CH}_2\text{OH}$	24.0	0.79	22.9	-	37.5
76	 $R_1 = \text{CH}_2\text{CH}_2\text{OH}$	24.5	1.32	67.0	0.02	12.9
77	 $R_1 = \text{CH}_2\text{CH}_2\text{OH}$	23.4	0.88	23.7	0.01	12.2
71	 $R_1 = \text{CH}_2\text{OH}$	2.0	3.30	87.8	0.23	>100
65	 $R_1 = \text{CH}_2\text{OH}$	2.1	4.62	95.4	0.68	>100
69	 $R_1 = \text{CH}_2\text{OH}$	1.6	5.90	103	-	>100
49	 $R_1 = \text{CH}_3$	2.7	6.77	46.9	-	>100

a) Determined by Caco-2 assay.

b) Time study using pooled human liver microsomes (HLM) at 3 μM concentration.

c) Protein binding is given as fraction unbound (fu).

d) Solubility was measured as turbidimetric aqueous solubility.

High Caco-2 permeability (P_{app}) and efflux ratio close to unity were seen for the less polar compounds **50-53**, **76** and **77**. Derivatives containing the *N,N'*-dimethylethane-1,2-diamine solubilizing tail (**49**, **65**, **69** and **71**) had a 10 fold lower permeability in the A-B direction, but also reasonable efflux values. Thus, the major challenge with the pyrrolopyrimidines as EGFR inhibitors was related to balancing the potency versus the permeability of the compounds. Many of the most potent inhibitors had a high efflux,

mainly due to a low P_{app} in the A-B direction. This was the case for compounds bearing amide or sulfonamide type substituents, which could indicate that hydrogen bond acceptors lowers permeability. High efflux was also seen in a series of N5-substituted pyrrolo[3,2-*d*]pyrimidine EGFR inhibitors containing amides and the methylsulfonyl functional group [37].

A rational prediction of efflux effects is challenging due to the multitude of possible transporter proteins involved [38, 39], and for some previously investigated classes of pyrrolopyrimidines no clear system can be seen [40]. However, in this homogenous series of compounds (28 investigated for permeability, Supplementary Material) correlation with physiochemical properties gave a decent fit with polar surface area, see Figure 10. One outlier was identified, compound **68** containing a piperazine group in the solubilizing tail. The low efflux ratio value is due to extremely low P_{app} in the B-A direction, indicating this compound to be a substrate or inhibitor of specific ABC transporter.

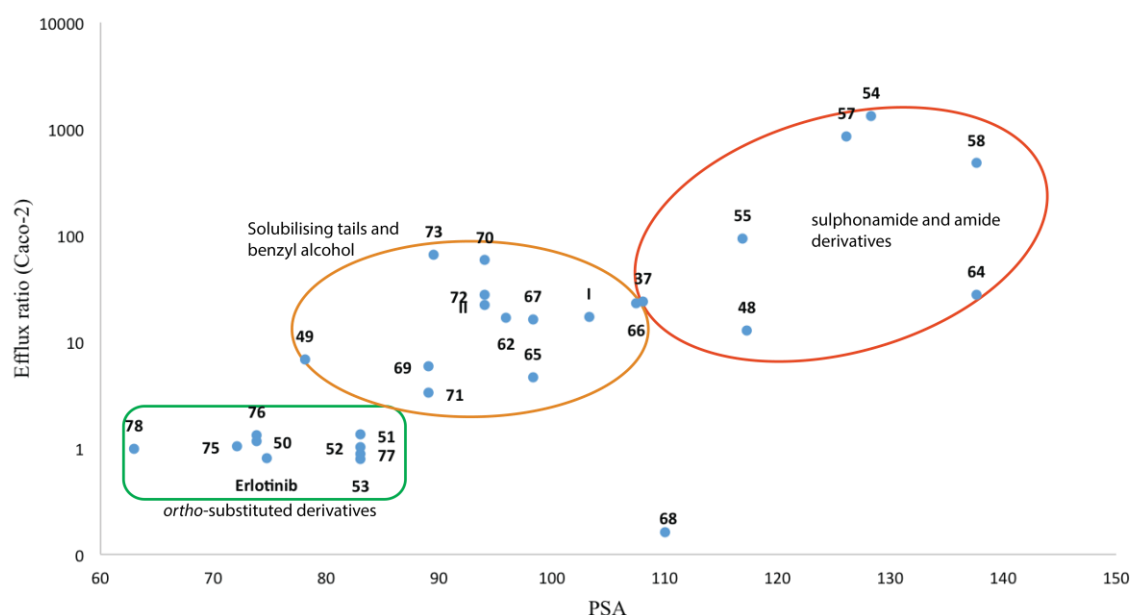


Figure 10. Efflux ratio (Caco-2) as a function polar surface area (n = 28).

The metabolic stability of the EGFR inhibitors and selected model compounds (29 derivatives) were evaluated in human liver microsomes (HLM) assay at 3 μ M test concentration. A graphical representation of the key findings in this part of the study is shown in Figure 11. As a point of reference, the unsubstituted phenyl analogue **50** had a half-life of 109 min. The 2-methoxy derivative **51** had a stability comparable to that of Erlotinib, which is somewhat on the low side [41]. Higher stability was seen for the *d*₃-methoxy analogue **52**, possibly due to a kinetic isotope effect [42]. Based on previous reports we anticipated that the difluoromethoxy [43] or the ethoxy substituted derivatives could be used as more stable bioisostere for the methoxy analogue. Whereas compounds with both substituents maintained a high EGFR activity, no improvement in half-life was detected for the difluoromethoxy compound **44** and the ethoxy compound **53**. Upon varying

the 4-substituent of the 6-aryl group (R_4) most amides and benzyl alcohol containing derivatives had higher stability than the reference **50**. Moreover, although the 2-methoxy group is a metabolic soft spot, including substituents in position 4 increases the stability of all molecules containing this functionality. Compounds containing solubilizing tails generally had a high stability. The most labile compound of these was the piperidine substituted analogue **67** (half-life: 40 min). Fluorine was inserted in an attempt to improve the stability and permeability of the benzylalcohol and benzylamine containing derivatives (compounds **69-72**). Only in one case a direct comparison of stability could be made, indicating that an adjacent fluorine has a slight negative impact on stability. A well-known trick to improve stability of drug candidates is to reduce the electron content of the aromatic ring by insertion of heteroatoms [44]. Thus, also in this study replacing the 2-methoxyphenyl with the corresponding pyridine derivative **62** increase the half-life considerably.

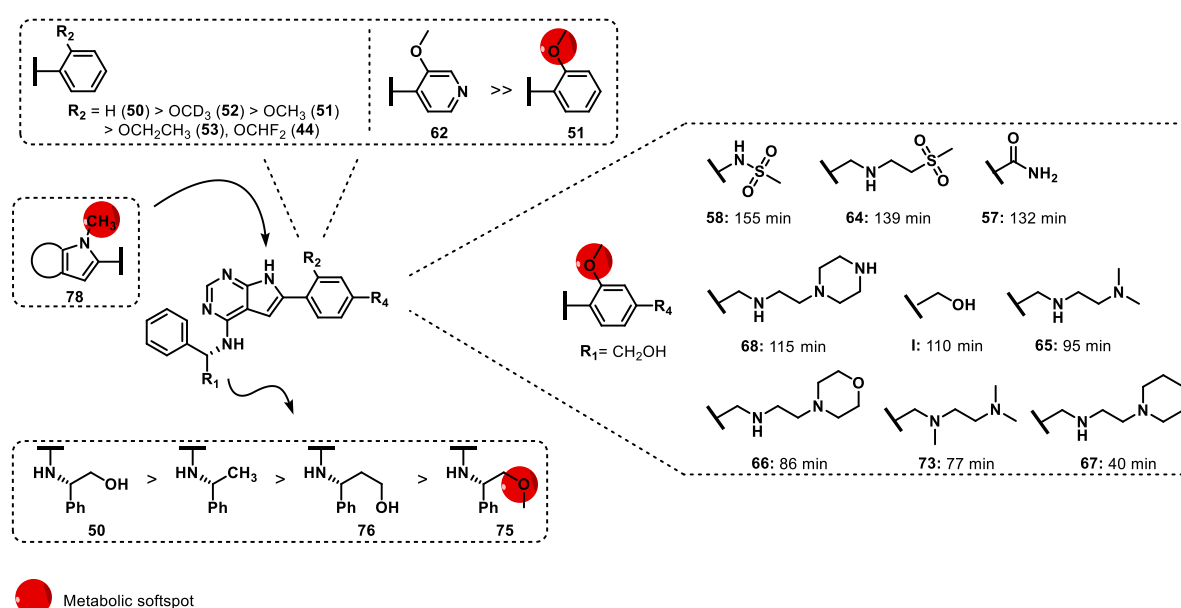


Figure 11. Illustration of the relative stability and metabolic soft spots based on HLM data.

Concerning the effect of the 4-amino group on metabolic stability a few guidelines could be drawn. Comparing data for three analogues containing the (*R*)-1-phenylethan-1-amine fragment (compound **37**, **48** and **49**) with the stability of the corresponding (*S*)-2-amino-2-phenylethan-1-ol containing compounds (**54**, **58** and **65**) indicate that the latter group improves stability. The highly active EGFR inhibitors based on (*R*)-2-amino-2-phenylpropanol, **76** and **77**, had a half-life of 67 and 23 minutes, respectively, which is lower than compound **50**. The (*S*)-2-methoxy-1-phenylethan-1-amine unit in compound **75** was found especially labile. The *N*-methyl derivative **78** is not an EGFR inhibitor, but was included as a model substance for evaluating ADME properties. The stability was considerably lower than the reference compound **50**, indicating the *N*-methyl group as the metabolic soft spot. Detailed data is provided in the Supplementary Material.

To attain on target activity *in vivo* the drug candidates must possess high bioavailability. A graphical method for evaluating bioavailability (% F) based on Caco-2 and HLM data have been developed by Mandagere et al. [45], which categorise molecules into high, medium and low bioavailability classes. We adopted the approach on our data, see Figure 12.

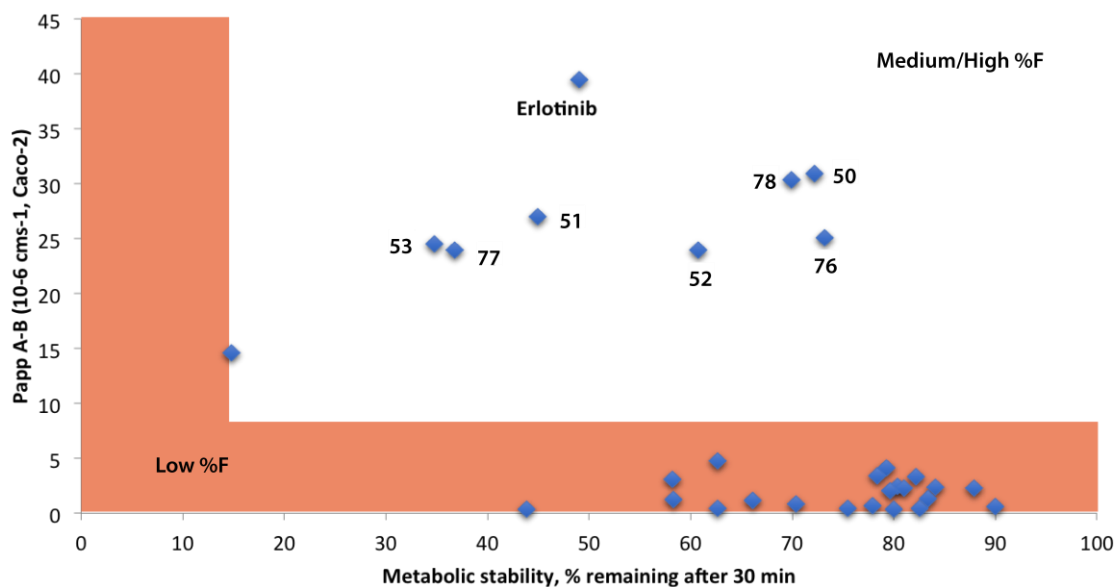


Figure 12. Estimation of bioavailability using a graphical oral bioavailability map.

The method predicts (*S*)-2-amino-2-phenylethan-1-ol containing molecules possessing nonpolar substituents (**50-53**) and the (*R*)-2-amino-2-phenylpropan-1-ol containing structures **76** and **77** to have medium bioavailability. Note that compound **78** has very low EGFR potency.

High protein binding was seen for several of the candidate structures. However, this is also the case for the EGFR/HER2 inhibitor Lapatinib [16], and 45 % of newly approved drugs had protein binding above 95 % [46]. By including a solubilizing tail in the inhibitor structure, protein binding was efficiently reduced, but the permeability drops probably as a result of higher polarity.

The hERG potassium voltage-gated ion channel is essential for cardiac re-polarisation. Thus, inhibiting hERG can give rise to potentially fatal toxicity. Ten compounds were evaluated by IC_{50} titration. For eight of these IC_{50} was $> 25 \mu M$, see Table 2. However, upon including the 1-phenyl-2-amino-3-propanol scaffold as present in compound **76** and **77** higher activity was seen, indicating possible toxic issues with these agents.

Table 2. hERG inhibition data for the new EGFR inhibitors. Additional data is provided in Supplementary Material.

Comp.	Erlotinib	50	51	52	65	71	76	77
hERG inhibition	>25 (n=17)	>25 (n=12)	>25 (n=15)	>25 (n=12)	>25 (n=14)	>25 (n=14)	22 (n=17)	11 (n=12)
IC₅₀ (μM)^{a)}								

^{a)}hERG channel inhibition (IC₅₀) was done at concentrations 0.008, 0.04, 0.2, 1, 5 and 25 μM.

2.6 Kinase selectivity profile

The kinase selectivity profile of five compounds (**50**, **51**, **53**, **71** and **76**) representing different structural elements was evaluated in assays towards 50 additional kinases at 500 nM test concentration. The selectivity as analysed by the Gini-method [47] was rather similar (Gini coefficient from 0.57-0.62). Another way of quantifying selectivity, which assumes that low inhibitory activity is clinically irrelevant, is the so called selectivity score [48]. It is calculated by dividing the number of kinases showing inhibition above a set limit by the total number of kinases evaluated. Thus, a non-selective inhibitor has a selectivity score close to unity, while a selective inhibitor has a score close to zero. Employing 50 % inhibition as the threshold for the calculation, the compounds follows the selectivity order: **76** (0.08) > **53** (0.10) > Erlotinib (0.16) > **50** (0.18) > **51** (0.20) > **71** (0.25). Figure 13 illustrates the degree of inhibition for **76**, **50** and **71** towards 15 of the kinases sorted by the activity displayed by the least selective compound **71**.

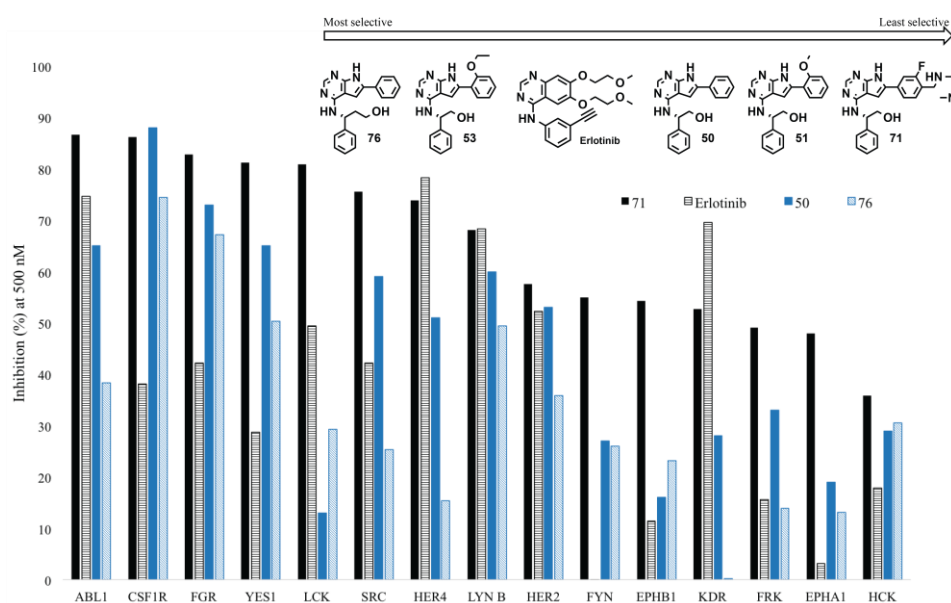


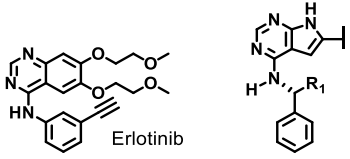
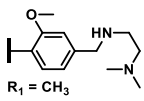
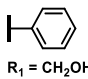
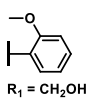
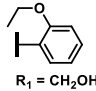
Figure 13. Inhibition profile of compounds **71**, **50**, **76** and Erlotinib towards 15 kinases sorted by the activity of compound **71**. Data for additional kinases for these compounds, **51** and **53** is provided in Supplementary Material)

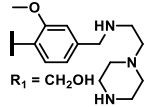
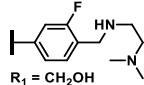
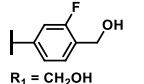
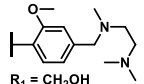
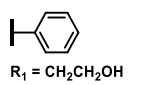
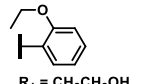
Evidently, the solubilizing tail in **71** increase activity towards a number of kinases. This was also noted in one of our structurally related furopyrimidine compound [49]. On one hand this might lead to undesired off-target related toxicity, on the other side having activity towards several kinases in the same pathway might be beneficial in a therapeutic setting.

2.7 Cell assays

The new EGFR inhibitors were compared with the reference drug Erlotinib in proliferation studies with two cell lines; A-431 harbouring overexpressed EGFR-wild type, and a genetically engineered cancer model cell, Ba/F3-EGFR^{L858R}, containing the activating L858R mutant form (see Table 3). Except compound **68** (IC₅₀ 396 nM) all compounds were highly sensitive towards the Ba/F3-EGFR^{L858R} cells with IC₅₀ in the range as Erlotinib (IC₅₀ 75-158 nM). This proves on-target activity also in cells. In assay towards the more complex A-431 cell line, the activity was high for derivative **50**, **51** and **76**, but considerable lower than Erlotinib for the other derivatives tested. Interestingly, compound **71** displaying excellent EGFR activity in enzymatic studies and also high inhibition towards a number of kinases including HER2 and HER4, had a mediocre activity towards the A-431 cell line.

Table 3. Cell proliferation study of selected pyrrolopyrimidines towards Ba/F3-EGFR^{L858R} and A-431 cells.

Comp.	Structure	Ba/F3-EGFR ^{L858R} (nM) ^{a)}	A-431 (μM) ^{b)}
Erlotinib		87±5	0.4±0.1 (n=9)
49		90±3	5.0±0.0
50		127±29 ^{c)}	0.3±0.1 (n=6)
51		134±22 ^{c)}	0.4±0.1 ^{d)}
53		98±1	9.2±3.9

68	 R ₁ = CH ₂ OH	396±50	6.2±3.1
71	 R ₁ = CH ₂ OH	142±12	>10
72	 R ₁ = CH ₂ OH	158±44	5.8±4.6
73	 R ₁ = CH ₂ OH	77±12	>10
76	 R ₁ = CH ₂ CH ₂ OH	75±14	0.8±0.3
77	 R ₁ = CH ₂ CH ₂ OH	99±1	4.9±4.2

^{a)}Each IC₅₀ is the result of three independent replicates.

^{b)}Unless otherwise stated IC₅₀ is the result of three replicates.

^{c)}Data is taken from ref. [20] (Erlotinib had an IC₅₀ of 142±65 nM).

^{d)}Data is taken from ref. [20] (Erlotinib had an IC₅₀ of 0.4±0.1 μM).

Based on a trade-off between enzymatic and cellular activity and ADME properties the previously identified compound **50** appears as the most promising drug candidate. Table 4 summarises other cell proliferation data for compound **50**.

Table 4. Cell proliferation data of compound **50** and Erlotinib towards various cancer cell lines.

Cancer type	Cell line	IC ₅₀ (μM)	
		Erlotinib	Comp. 50
Lung	PC-9	< 0.1	< 0.1
	A-549	>100	>100
Breast	AU-565	3.3±0.6 ^{a)}	2.5±0.4 ^{a)}
Ovarian	C-33A	0.9±0.0 ^{a)}	0.7±0.0 ^{a)}
Head&Neck	CAL-27	1.3±0.6 ^{a)}	2.7±0.6 ^{a)}
	FaDu	>11	>33
Leukaemia	K-562	55±9 ^{a)}	15±2 ^{a)}

Pancreatic

BxPC3

1.9±0.2

15±1

a) Data taken from ref. [20]

Erlotinib and compound **50** were highly potent towards the PC-9 lung cancer cells harbouring the EGFR E746-A750 deletion mutation. In contrast, both compounds were found inactive towards A-549, which have wild type EGFR, but mutated RAS [50]. Fairly similar potency was seen towards the AU-565 breast cancer cell line and the cervix carcinoma cell line C-33A [20]. The decent potency detected for the latter cell line is surprising giving this cell line's low expression of EGFR [51-53], indicating that alternative cytotoxicity mechanisms might be operating. In line with what seen for structurally related analogues [21], compound **50** was moderately active towards CAL-27 cells, but inactive towards the FaDu cells. Compound **50** also had a low potency towards the leukaemia K-562 cell line and the pancreatic cell line BxPC3. Overall the cell proliferation studies on compound **50** indicate that the major use of this compound as single agent is in EGFR driven diseases.

3. Conclusion

The goal of this work was to identify pyrrolopyrimidine-based EGFR inhibitors for medical use. Thus, starting from our own lead structure, we have performed a SAR study involving 43 new structures. The SAR study revealed that *ortho*-ethoxy groups and amine based solubilizing tails in *para*-position of the 6-aryl moiety, and a (*R*)-3-amino-3-phenylpropan-1-ol at C-4 boosted potency. Based on this collection of new structures and two previously identified compounds, various ADME assays were used to identify the most promising drug candidate. Permeability was investigated by the Caco-2 method for 28 of the inhibitors. Overall, the efflux ratio correlated well with polar surface area of the molecules, and compounds bearing polar functionalities at the 6-aryl ring, especially amides and sulphonamides, increased drug efflux ratio and reduced permeability. Metabolic stability (HLM), investigated for 29 of the derivatives, showed that sites most prone to metabolism were the *ortho*-methoxyphenyl group at C-6, and (*S*)-2-methoxy-1-phenylethan-1-amine at C-4. The metabolic stability of the *ortho*-methoxy compound could be increased by bioisosteric substitution with a deuteromethoxy group, whereas no improvement was seen using the difluoromethoxy substituent. hERG inhibition was generally low, but two compounds bearing the (*R*)-3-amino-3-phenylpropan-1-ol group at C-4, had $IC_{50} < 25 \mu M$, indicating toxicity issues with this scaffold. Ten compounds were subjected to proliferation assays using Ba/F3-EGFR^{L858R} and A-431 cells. Whereas high activity was seen for the former cell line, only a few was potent in the A-431 cells. Further, five of the EGFR inhibitors were compared in assays towards a panel of 50 kinases, revealing that amine containing solubilizing tails at *para*-position of the 6-aryl group reduced selectivity. On background of all these studies, (*S*)-2-phenyl-2-((6-phenyl-7*H*-pyrrolo[2,3-*d*]pyrimidin-4-yl)amino)ethan-1-ol (**50**) appeared as the most promising drug candidate. The high potency

displayed in Ba/F3-EGFR^{L858R} reporter cells, A-431 and PC9 cell proliferation studies indicate this compound to have potential therapeutic use in EGFR driven diseases.

4. Experimental

4.1 General

Xhos, 2nd generation XPhos, NaBH₄, (*R*)-1-phenylethan-1-amine and (*S*)-2-amino-2-phenylethan-1-ol and the arylboronic acid derivatives except 2-(3-(4,4,5,5-tetramethyl-1,3,2-dioxaborolan-2-yl)phenyl)acetamide (Activate Scientific) and **8-11** (in house prepared) were from Sigma Aldrich. (*R*)-3-Amino-3-phenylpropan-1-ol was from Fluorochem.. Silica-gel column chromatography was performed using silica-gel 60A from Fluka, pore size 40-63 μ m. Celite 545 from Fluka was also used. (*S*)-2-Methoxy-1-phenylethanamine [54], and compounds **1**, **7a-b**, **7d**, **31-33**, **50** and **51** [20], were prepared and characterized in other studies from our laboratory. The Supplementary Material contains experimental and analytical data on synthesis of 4-bromo-3-methoxyaniline, 1-bromo-2-(methoxy-*d*₃)benzene and compounds **3** and **8-11**.

4.2 Analyses

¹H and ¹³C NMR spectra were recorded with Bruker Avance 600 and 400 spectrometer operating at 600/400 MHz and 150/100 MHz, respectively. ¹⁹F NMR was performed on a Bruker Avance 600 operating at 564 MHz. For ¹H and ¹³C NMR chemical shifts are in ppm rel. to tetramethylsilane (TMS) calibrated using DMSO-*d*₆ or TMS, while for ¹⁹F NMR the shift values were calibrated using hexafluorobenzene. Coupling constants are in hertz. The pyrrole NH signal (δ : 12.2-10.2 ppm), the NH at C-4 (δ : 7.9-7.7 ppm and the hydroxyl group at R₁ in compounds **52 - 73** and **78** (δ : 4.99-4.95 ppm) disappeared after D₂O exchange. Other exchangeable protons are mentioned for each specific compound. HPLC (Agilent 110-Series) with a G1379A degasser, G1311A Quatpump, G1313A ALS autosampler and a G1315D Agilent detector (230 nm) was used to determine the purity of the synthesised compounds. All compounds evaluated for EGFR inhibitory potency had a purity of $\geq 96\%$. Conditions: Poroshell C18 (100 \times 4.6 mm) column, flow rate 0.8 mL/min, elution starting with water/CH₃CN (90/10), 5 min isocratic elution, then linear gradient elution for 35 min ending at CH₃CN/water (100/0). The software used with the HPLC was Agilent ChemStation. Accurate mass determination (ESI) was performed on an Agilent G1969 TOF MS instrument equipped with a dual electrospray ion source. Accurate mass determination in positive and negative mode was performed on a "Synapt G2-S" Q-TOF instrument from Waters. Samples were ionized by the use of an ASAP probe, no chromatography separation was used before the mass analysis. FTIR spectra were recorded on a Thermo Nicolet Avatar 330 infrared spectrophotometer. All melting points are uncorrected and measured by a Stuart automatic melting point SMP40 apparatus.

4.3 *In vitro* EGFR (ErbB1) inhibitory potency

The compounds were supplied in a 10 mM DMSO solution, and enzymatic EGFR (ErbB1) inhibition potency was determined by Reaction Biology Corp. using their biochemical kinase assay at 10 μ M ATP concentration. All compounds were first tested for their inhibitory activity at 100 nM in duplicates. The potency observed at 100 nM was used to set starting point of the IC₅₀ titration curve, in which three levels were used 100, 1000 or 10000 nM. The IC₅₀ values reported are based on the average of at least 2 titration curves (minimum 20 data points), and were calculated from activity data with a four parameter logistic model using SigmaPlot (Windows Version 12.0 from Systat Software, Inc.) Unless stated otherwise the ATP concentration used was equal to K_m. The average standard deviation for single point measurements were <4 %.

4.4 *In vitro* kinase panel

The compounds were supplied in a 10 mM DMSO solution, and enzymatic kinase inhibition potency was determined by Invitrogen (LifeTechnology) using their Z'-LYTE[®] assay technology [55], at 500 nM in duplicates. ATP concentration used was equal to K_m, except when this service was not provided and other concentrations had to be used.

4.5 ADME and cell studies

ADME studies, including solubility, Caco-2 assay, human liver microsome metabolic assay, hERG inhibition and protein binding were performed as previously described [21].

Cell proliferation studies with the PC-9, FaDu and BXPC-3 cells were performed as described in reference [21], while protocols for the Ba/F3 EGFR^{L858R} cell proliferation studies can be found in reference [20].

Proliferation study with the A-549 cell line was performed by Reaction Biology Corp: The A549 cell line was obtained from American Type Culture Collection (Manassas, VA). Staurosporine was obtained from Selleckchem. Cell Titer-Glo[®] Luminescent cell viability assay reagent was obtained from Promega (Madison, WI). A549, cell line was cultured in F-12K medium supplemented with 10 % FBS. 100 μ g/ml penicillin and 100 μ g/ml streptomycin. Cultures were maintained at 37 °C in a humidified atmosphere of 5 % CO₂ and 95 % air. The test compound, Erlotinib and Staurosporine (positive control) were all dissolved in DMSO in 10 mM stock. Culture medium (10 μ l) was added to each well of 384 well cell culture plates. The compounds were diluted in a source plate in DMSO at 3 fold serial dilutions starting at 10 mM, total 10 doses. The compounds (0.25 μ l) were delivered from source plate to each well of the cell culture plates by Echo 550. Then, 250 μ l of culture medium containing 5000 cells were added to the wells of the cell culture plates. The cells were incubated with the compounds at 37 °C, 5 % CO₂ for 72 hours. 25 μ l of Cell Titer Glo reagent (25 μ l) was added to each well according to the instruction of the kit. The contents were mixed on an orbital shaker for 2 minutes and incubated at room temperature for 10 minutes to stabilize luminescent signal. Luminescence was recorded by Envision 2104 Multilabel Reader (PerkinElmer, Santa Clara, CA). The maximum luminescence for

each cell line in the absence of test compound, but in the presence of 0.4 % DMSO, was similarly recorded after incubation for 72 hours. The number of viable cells in the culture was determined based on quantitation of the ATP present in each culture well. The percentage growth after 72 hours (*%-growth*) was calculated as follows: $100 \% \times (\textit{luminescence } t = 72 \text{ hours} / \textit{luminescence } \textit{untreated}, t = 72 \text{ hours})$.

4.6 General procedures

4.6.1 General procedure for thermal amination of pyrrolo[2,3-*d*]pyrimidines

The 4-chloropyrrolopyrimidine (**4** or **5**) (0.12 - 2.0 g) was mixed with the selected amine (2-3 eq) and *n*-BuOH (2 - 30 mL) and agitated at 145 °C for 1 - 24 h under N₂ atmosphere. The mixture was then cooled to ambient temperature, concentrated *in vacuo*, diluted with water and extracted with EtOAc (2 × 30 - 100 mL). The combined organic phases were washed with saturated aq. NaCl solution (15 - 60 mL), dried over anhydrous Na₂SO₄, filtered and concentrated *in vacuo*. The crude material was purified by silica-gel column chromatography.

4.6.2 General procedure for Suzuki cross-coupling on pyrrolo[2,3-*d*]pyrimidines

The 6-iodopyrrolopyrimidine (**6a** - **6c**, **7a** - **7b** or **7d**) (50 - 350 mg) was mixed with the selected arylboronic acid (1.2 eq), fine powdered K₂CO₃ (3 eq), XPhos (5 mol %) / 2nd generation XPhos precatalyst (5 mol %) system or PdCl₂(dppf) (5 mol %) and mixture with degassed 1,4-dioxane/H₂O (1/1 by vol. %, 2-8 mL). The reaction was then stirred at 100 °C for 0.5 - 10 hours under N₂ atmosphere. The solvent was removed and the product was diluted with H₂O (25 - 100 mL) and extracted with EtOAc (50 - 120 mL), several times if required. The combined organic phases were washed with saturated aq. NaCl solution (30 mL), dried over anhydrous Na₂SO₄, filtered and concentrated *in vacuo*. Purification was performed as described for each individual compound.

4.6.3 General procedure for reductive amination of pyrrolo[2,3-*d*]pyrimidines

The 6-aryl aldehydes (**19**, **23**, **24**, **31** - **33**) (16.6 - 100 mg) were dissolved in anhydrous CH₂Cl₂ (1 - 5 mL) and the respective amine (1.2 eq) was added and stirred at 20 °C for 1 - 4 hours until full conversion to the imine as determined by ¹H NMR spectroscopy. Solvent was removed *in vacuo* and the crude product was dissolved in MeOH (4-10 mL) and NaBH₄ (1.8 - 2.3 eq) was added and stirred for 2 - 4 hours until completed reduction. The reaction mixture was diluted with H₂O (10 - 30 mL) and the mixture was extracted with EtOAc (40 - 100 mL). The combined organic phases were washed with saturated aq. NaCl (10-30 mL), dried over anhydrous Na₂SO₄, filtered and concentrated *in vacuo*. Purification was performed as described for each individual compound.

4.6.4 General procedure for SEM-deprotection of pyrrolo[2,3-*d*]pyrimidines

Compounds (50 - 200 mg) were dissolved in CH₂Cl₂ (10 - 20 mL) and TFA (2 - 4 mL) was added and stirred at 50 °C for 3-6 hours until full conversion determined by ¹H NMR at which time the solvent was removed *in vacuo*. The crude material was dissolved in THF (10 - 20 mL) and saturated aq NaHCO₃ (10 - 20 mL) solution was added and stirred for 6 - 12 hours. The mixture was then extracted with EtOAc (50 - 150 mL) and the combined organic phases were washed with saturated aq NaCl (10 - 40 mL), dried over anhydrous Na₂SO₄, filtered and concentrated *in vacuo*. Purification was performed as described for each individual compound.

4.7 Synthesis of intermediates

4.7.1 4-Chloro-6-iodo-7*H*-pyrrolo[2,3-*d*]pyrimidine (**4**) [20].

4-Chloro-7-(phenylsulfonyl)-7*H*-pyrrolo[2,3-*d*]pyrimidine (**1**) [20], (5.42 g, 18.5 mmol) was iodinated as previously described [20]. This gave a 9 : 1 mixture of **2** and **3** (6.0 g) which was mixed with THF (125 mL) and 5 M NaOH solution in MeOH (21 mL). After 2 hours stirring at room temperature, a saturated aqueous NH₄Cl-solution (125 mL) was added and the mixture concentrated. The formed precipitate was collected by filtration and washed with water. Trituration from boiling acetonitrile (1 g/10 mL) gave 3.96 g (14.2 mmol, 77 %) of **4** as a white solid, mp 219 °C (dec.) (lit.[20] 220 °C); ¹H NMR (400 MHz, DMSO-*d*₆) δ: 12.57 (s, 1H), 8.51 (s, 1H), 6.88 (s, 1H). The ¹H NMR data is in agreement with that previously reported [20].

4.7.2 4-Chloro-6-iodo-7-((2-(trimethylsilyl)ethoxy)methyl)-7*H*-pyrrolo[2,3-*d*]pyrimidine (**5**) [56].

4-Chloro-6-iodo-7*H*-pyrrolo[2,3-*d*] (2.02 g, 7.24 mmol) and sodium hydride (210 mg, 8.45 mmol) were added dry DMF (70 mL) under nitrogen atmosphere and cooled to 0 °C. 2-(Trimethylsilyl)ethoxymethyl chloride (1.69 mL, 9.36 mmol) was added dropwise over 30 min at 0 °C and stirred at 22 °C for 1 hour. The reaction mixture was added water (150 mL) and extracted with EtOAc (2 x 150 mL), dried over Na₂SO₄ and concentrated *in vacuo*. Column chromatography on silica gel (EtOAc/*n*-pentane 1/1, R_f = 0.78) gave **5** in 2.43 g (5.92 mmol, 81 %) as a clear oil that solidified upon drying *in vacuo*. ¹H NMR (400 MHz, DMSO-*d*₆) δ: 8.63 (s, 1H), 7.12 (s, 1H), 5.62 (s, 2H), 3.54 (t, *J* = 8.4, 2H), 0.83 (t, *J* = 8.4, 2H), -0.10 (s, 9H); ¹³C NMR (100 MHz, DMSO-*d*₆) δ: 152.5, 150.7, 149.1, 118.5, 109.7, 91.5, 73.4, 66.1, 17.0, -1.4 (3C); HRMS (APCI/ASAP, *m/z*): 409.9955 (calcd. C₁₂H₁₈N₃OSiCl, 409.9952, [M+H]⁺).

4.7.3 (R)-6-Iodo-N-(1-phenylethyl)-7-((2-(trimethylsilyl)ethoxy)methyl)-7H-pyrrolo[2,3-d]pyrimidin-4-amine (6a)

Compound **6a** was prepared as described in Section 4.6.1, starting with **5** (506 mg, 1.24 mmol) and (*R*)-1-phenylethan-1-amine (449 mg, 3.71 mmol, 3 eq.). The reaction time was 3 hours. Purification by silica-gel column chromatography (*n*-pentane/EtOAc, 8/2, R_f = 0.49) gave 456 mg (0.923 mmol, 75 %) of a pale foam; HPLC purity: 98 %, t_R = 30.3 min; $[\alpha]_D^{20}$ = -195.6 (*c* 1.00, DMSO); $^1\text{H NMR}$ (600 MHz, CDCl_3 -TMS) δ : 8.27 (s, 1H), 7.41 - 7.40 (m, 2H), 7.36 - 7.33 (m, 2H), 7.28 - 7.25 (m, 1H), 6.66 (s, 1H), 5.57 (s, 2H), 5.52 - 5.47 (m, 1H), 3.58 - 3.55 (m, 2H), 1.64 (d, J = 6.8, 3H), 0.98 - 0.89 (m, 2H), -0.06 (s, 9H); $^{13}\text{C NMR}$ (150 MHz, CDCl_3 -TMS) δ : 154.2, 152.6, 152.4, 143.8, 128.9 (2C), 127.5, 126.2 (2C), 109.5, 105.2, 77.8, 73.2, 66.5, 50.2, 22.9, 17.9, -1.3 (3C); IR (neat, cm^{-1}): 3273, 2945, 1594, 1450, 1295, 1080, 833, 746, 697; HRMS (APCI/ASAP, m/z): 495.1082 (calcd. $\text{C}_{20}\text{H}_{28}\text{N}_4\text{OSi}$, 495.1077 $[\text{M}+\text{H}]^+$).

4.7.4 (S)-2-((6-Iodo-7-((2-(trimethylsilyl)ethoxy)methyl)-7H-pyrrolo[2,3-d]pyrimidin-4-yl)amino)-2-phenylethan-1-ol (6b)

Compound **6b** was prepared as described in Section 4.6.1, starting with **5** (1.02 g, 2.05 mmol) and (*S*)-2-amino-2-phenylethan-1-ol (844 mg, 6.15 mmol, 3 eq.). The reaction time was 6 hours. Purification by silica-gel column chromatography (EtOAc/*n*-pentane, 6/4, R_f = 0.24) gave 896 mg (1.76 mmol, 86 %) of a white foam; HPLC purity: 99 %, t_R = 25.6 min; $[\alpha]_D^{20}$ = -187.2 (*c* 1.00, DMSO); $^1\text{H NMR}$ (400 MHz, $\text{DMSO}-d_6$) δ : 8.04 (s, 1H), 7.83 - 7.81 (m, 1H), 7.41 - 7.39 (m, 2H), 7.31 - 7.28 (m, 2H), 7.22 - 7.17 (m, 2H), 5.48 - 5.37 (m, 1H), 5.45 (s, 2H), 4.97 - 4.94 (m, 1H), 3.76 - 3.67 (m, 2H), 3.51 - 3.47 (m, 2H), 0.82 - 0.78 (m, 2H), -0.11 (s, 9H); $^{13}\text{C NMR}$ (100 MHz, $\text{DMSO}-d_6$) δ : 154.4, 151.9, 151.4, 141.6, 128.0 (2C), 126.9 (2C), 126.7, 110.2, 104.9, 79.5, 72.5, 65.4, 64.9, 56.1, 17.1, -1.3 (3C); HRMS (APCI/ASAP, m/z): 511.1031 (calcd. $\text{C}_{20}\text{H}_{28}\text{N}_4\text{O}_2\text{Si}$, 511.1026 $[\text{M}+\text{H}]^+$).

4.7.5 (R)-3-((6-Iodo-7-((2-(trimethylsilyl)ethoxy)methyl)-7H-pyrrolo[2,3-d]pyrimidin-4-yl)amino)-3-phenylpropan-1-ol (6c)

Compound **6c** was prepared as described in Section 4.6.1, starting with **5** (152 mg, 0.371 mmol) and (*R*)-3-amino-3-phenylpropan-1-ol (121 mg, 0.800 mmol, 2 eq.). The reaction time was 20 hours. Purification by silica-gel column chromatography (EtOAc/*n*-pentane, 6/4, R_f = 0.24) gave 190 mg (0.361 mmol, 97 %) of a white foam; HPLC purity: 99 %, t_R = 25.9 min; $[\alpha]_D^{20}$ = -190.1 (*c* 1.00, DMSO); $^1\text{H NMR}$ (400 MHz, CDCl_3 -TMS) δ : 8.28 (s, 1H), 7.42 - 7.36 (m, 4H), 7.34 - 7.29 (m, 1H), 6.66 (s, 1H), 5.61 - 5.55 (m, 1H), 5.59 (s, 2H), 5.23 - 5.22 (m, 1H), 3.77 - 3.75 (m, 1H), 3.70 - 3.64 (m, 1H), 3.60 - 3.56 (m, 2H), 2.31 - 2.23 (m, 1H), 2.03 - 1.95 (m, 1H), 1.61 (s, br, 1H), 0.94 - 0.90 (m, 2H), -0.05 (s, 9H); $^{13}\text{C NMR}$ (100 MHz, CDCl_3 -TMS) δ : 154.7, 152.2, 152.0, 142.3, 129.2 (2C), 128.0, 126.8 (2C), 109.2, 105.2, 78.2, 73.3, 66.6, 58.5, 52.0, 39.4, 17.9, -1.3 (3C); HRMS (APCI/ASAP, m/z): 524.1093 (calcd. $\text{C}_{21}\text{H}_{30}\text{N}_4\text{O}_2\text{Si}$, 524.1098 $[\text{M}+\text{H}]^+$).

4.8 SEM-protected pyrrolopyrimidines

4.8.1 (*R*)-*N*-(1-Phenylethyl)-6-(pyridin-4-yl)-7-((2-(trimethylsilyl)ethoxy)methyl)-7*H*-pyrrolo[2,3-*d*]pyrimidin-4-amine (**12**)

Compound **12** was prepared as described in Section 4.6.2, starting with **6a** (150 mg, 0.30 mmol), pyridin-4-ylboronic acid (52 mg, 0.430 mmol) and using PdCl₂(dppf) (10 mg, 0.014 mmol, 0.05 eq.) as catalyst. The reaction time was 2 hours. Purification by silica-gel column chromatography (EtOAc/*n*-pentane, 2/1, R_f = 0.32) gave 123 mg (0.280 mmol, 61 %) of a yellow oil. HPLC purity: 99 %, t_R = 30.8 min; [α]_D²⁰ = -189.9 (c 1.00, DMSO); ¹H NMR (600 MHz, CDCl₃-TMS) δ: 8.67 - 8.66 (m, 2H), 8.40 (s, 1H), 7.66 - 7.65 (m, 2H), 7.44 - 7.43 (m, 2H), 7.37 - 7.34 (m, 2H), 7.29 - 7.24 (m, 1H), 6.62 (s, 1H), 5.61 - 5.57 (m, 3H), 5.59 - 5.53 (m, 1H), 3.79 - 3.76 (m, 2H), 1.67 (d, J = 6.8, 3H), 0.99 - 0.96 (m, 2H), -0.02 (s, 9H); ¹³C NMR (150 MHz, DMSO-*d*₆) δ: 155.8, 153.3, (2C), 150.4, (2C), 143.9, 139.3, 135.5, 128.9, (2C), 127.5, 126.2, 122.9, 103.0, 100.5, 70.8, 66.9, 50.5, 22.9, 18.1, -1.3 (3C); IR (neat, cm⁻¹): 3262, 2945, 2353, 1591, 1468, 1303, 1073, 730, 697; HRMS (APCI/ASAP, m/z): 446.2376 (calcd. C₂₅H₃₂N₅OSi, 446.2376 [M+H]⁺).

4.8.2 (*S*)-2-((6-(2-(Methoxy-*d*₃)phenyl)-7-((2-(trimethylsilyl)ethoxy)methyl)-7*H*-pyrrolo[2,3-*d*]pyrimidin-4-yl)amino)-2-phenylethan-1-ol (**13**)

Compound **13** was prepared as described in Section 4.6.2, starting with **6b** (90 mg, 0.237 mmol) and 2-(2-(methoxy-*d*₃)phenyl)-4,4,5,5-tetramethyl-1,3,2-dioxaborolane (**8**) (68 mg, 0.284 mmol). The reaction time was 1 hour. Purification by silica-gel column chromatography (CH₂Cl₂/MeOH, 19/1, R_f = 0.20) gave 91 mg (0.209 mmol, 88 %) of a clear oil; HPLC purity: 99 %, t_R = 15.1 min; ¹H NMR (400 MHz, CDCl₃-TMS) δ: 8.35 (s, 1H), 7.44 - 7.37 (m, 6H), 7.35 - 7.30 (m, 1H), 7.05 - 7.01 (m, 1H), 6.99 - 6.97 (m, 1H), 6.36 (s, 1H), 5.48 (s, 2H), 5.34 - 5.30 (m, 1H), 4.13 - 3.99 (m, 2H), 3.38 - 3.34 (m, 2H), 0.77 - 0.73 (m, 2H), -0.13 (s, 9H); NH and OH was not seen; ¹³C NMR (100 MHz, CDCl₃-TMS) δ: 157.4, 155.9, 151.7, 151.2, 140.0, 135.3, 132.6, 130.7, 129.3 (2C), 128.3, 127.0 (2C), 121.0, 120.7, 111.1, 103.5, 99.6, 71.5, 68.5, 66.4, 64.4, 59.3, 17.9, -1.3 (3C).

4.8.3 (*S*)-2-((6-(2-Ethoxyphenyl)-7-((2-(trimethylsilyl)ethoxy)methyl)-7*H*-pyrrolo[2,3-*d*]pyrimidin-4-yl)amino)-2-phenylethan-1-ol (**14**)

Compound **14** was prepared as described in Section 4.6.2, starting with **6b** (100 mg, 0.196 mmol) and (2-ethoxyphenyl)boronic acid (49 mg, 0.294 mmol). Purification by silica-gel column chromatography (EtOAc/*n*-pentane, 3/2, R_f = 0.34) gave 90 mg (0.178 mmol, 90 %) of a colourless oil; HPLC purity: 99 %, t_R = 27.3 min; [α]_D²⁰ = -102.1 (c 0.50, DMSO); ¹H NMR (400 MHz, CDCl₃-TMS) δ: 8.38 (s, 1H), 7.44 - 7.31 (m, 7H), 7.04 - 6.96 (m, 2H), 6.34 (s, 1H), 5.53 (s, 2H), 5.47 - 5.46 (m, 1H), 5.36 - 5.33 (m, 1H), 4.12 - 4.03 (m, 4H), 3.34 - 3.30 (m, 2H), 1.29 (t, J = 7.0, 3H), 0.75 - 0.70 (m, 2H), -0.15 (s, 9H); ¹³C NMR (100 MHz, CDCl₃-TMS) δ: 156.6, 155.9, 151.7, 151.4, 140.1, 135.8, 132.7, 130.6, 129.3 (2C),

128.3, 127.0 (2C), 121.1, 120.9, 112.2, 103.7, 99.0, 71.6, 68.6, 66.3, 64.1, 59.2, 17.9, 14.9, -1.4 (3C).

4.8.4 (S)-2-(3-(4-((2-Hydroxy-1-phenylethyl)amino)-7-((2-(trimethylsilyl)ethoxy)methyl)-7H-pyrrolo[2,3-d]pyrimidin-6-yl)phenyl)acetamide (15)

Compound **15** was prepared as described in Section 4.6.2, starting with **6b** (75 mg, 0.147 mmol), PdCl₂(dppf) (10.5 mg, 0.015 mmol, 0.05 eq.) and 2-(3-(4,4,5,5-tetramethyl-1,3,2-dioxaborolane-2-yl)acetamide (59 mg, 0.224 mmol). Purification by silica-gel column chromatography (EtOAc/MeOH, 94/6, R_f = 0.16) gave 63 mg (0.121 mmol, 83 %) of a yellow foam. ¹H NMR (400 MHz, DMSO-*d*₆) δ: 8.45 (s, 1H), 7.91 - 7.87 (m, 1H), 7.79 - 7.76 (m, 1H), 7.62 - 7.57 (m, 3H), 7.40 - 7.36 (m, 2H), 7.35 - 7.29 (m, 3H), 7.20 - 7.17 (m, 2H), 7.04 - 6.99 (m, 1H), 5.86 (s, br, 2H), 5.56 (s, 2H), 5.46 - 5.40 (m, 1H), 5.02 - 4.99 (m, 1H), 3.74 - 3.71 (m, 2H), 3.54 - 3.50 (m, 2H), 0.81 - 0.77 (m, 2H), -0.13 (s, 9H).

4.8.5 (S)-2-Phenyl-2-((6-(pyridin-4-yl)-7-((2-(trimethylsilyl)ethoxy)methyl)-7H-pyrrolo[2,3-d]pyrimidin-4-yl)amino)ethan-1-ol (16)

Compound **16** was prepared as described in Section 4.6.2, starting with **6b** (150 mg, 0.294 mmol), PdCl₂(dppf) (11 mg, 15.0 μmol, 5 mol %) and pyridin-4-ylboronic acid (54 mg, 0.441 mmol). The reaction time was 1 hour. Purification by silica-gel column chromatography (EtOAc, R_f = 0.17) gave 124 mg (0.271 mmol, 92 %) of a colourless film; HPLC purity: 99 %, t_R = 25.8 min; ¹H NMR (400 MHz, DMSO-*d*₆) δ: 8.68 - 8.65 (m, 2H), 8.41 (s, 1H), 7.65 - 7.63 (m, 2H), 7.44 - 7.42 (m, 2H), 7.35 - 7.31 (m, 2H), 7.30 - 7.25 (m, 1H), 6.59 (s, 1H), 5.63 - 5.58 (m, 3H), 5.55 - 5.52 (m, 1H), 3.81 - 3.77 (m, 2H), 3.56 - 3.53 (m, 2H), 0.90 - 0.86 (m, 2H), -0.11 (s, 9H).

4.8.6 (S)-2-Phenyl-2-((6-(pyridin-3-yl)-7-((2-(trimethylsilyl)ethoxy)methyl)-7H-pyrrolo[2,3-d]pyrimidin-4-yl)amino)ethan-1-ol (17)

Compound **17** was prepared as described in Section 4.6.2, starting with **6b** (80 mg, 0.157 mmol), PdCl₂(dppf) (6 mg, 7.85 μmol, 0.05 eq.) and pyridin-3-ylboronic acid (29 mg, 0.235 mmol). The reaction time was 4 hours. Purification by silica-gel column chromatography (EtOAc, R_f = 0.21) gave 70 mg (0.151 mmol, 96 %) of a pale film. ¹H NMR (400 MHz, DMSO-*d*₆) δ: 8.89 (s, 1H), 8.63 - 8.61 (m, 1H), 8.16 (s, 1H), 8.14 - 8.12 (m, 1H), 7.97 - 7.95 (m, 1H), 7.55 - 7.52 (m, 1H), 7.44 - 7.42 (m, 2H), 7.33 - 7.29 (m, 2H), 7.23 - 7.20 (m, 1H), 7.08 (s, br, 1H), 5.52 (s, 2H), 5.47 - 5.42 (m, 1H), 5.00 - 4.97 (m, 1H), 3.76 - 3.70 (m, 2H), 3.58 - 3.54 (m, 2H), 0.84 - 0.80 (m, 2H), -0.12 (s, 9H); ¹³C NMR (100 MHz, DMSO-*d*₆) δ: 155.8, 152.3, 152.0, 148.9, 148.8, 141.7, 139.7, 135.5, 133.1, 128.1 (2C), 127.9, 127.0 (2C), 126.7, 123.7, 101.0, 70.2, 65.6, 64.9, 56.2, 17.2, -1.4 (3C).

4.8.7 (S)-2-((6-(3-Methoxypyridin-4-yl)-7-((2-(trimethylsilyl)ethoxy)methyl)-7H-pyrrolo[2,3-d]pyrimidin-4-yl)amino)-2-phenylethan-1-ol (18)

Compound **18** was prepared as described in Section 4.6.2, starting with **6b** (200 mg, 0.392 mmol), PdCl₂(dppf) (14 mg, 0.020 μmol, 0.05 eq.) and 3-methoxy-4-(4,4,5,5-tetramethyl-1,3,2-dioxaborolan-2-yl)pyridine (138 mg, 0.588 mmol). The reaction time was 1 hour. Purification by silica-gel column chromatography (EtOAc, R_f = 0.14) gave 161 mg (0.328 mmol, 84 %) of a colourless film. ¹H NMR (400 MHz, DMSO-*d*₆) δ: 8.54 (s, 1H), 8.32 - 8.31 (m, 1H), 8.14 (s, 1H), 7.97 - 7.95 (m, 1H), 7.51 - 7.50 (m, 1H), 7.43 - 7.41 (m, 2H), 7.31 - 7.29 (m, 2H), 7.23 - 7.20 (m, 1H), 7.02 (s, br, 1H), 5.46 - 6.42 (m, 1H), 5.44 (s, 2H), 4.99 - 4.96 (m, 1H), 3.93 (s, 3H), 3.78 - 3.69 (m, 2H), 3.32 - 3.30 (m, 2H), 0.69 - 0.65 (m, 2H), -0.18 (s, 9H); The SEM-protected intermediate **18** was used without further purification.

4.8.8 (S)-4-(4-((2-Hydroxy-1-phenylethyl)amino)-7-((2-(trimethylsilyl)ethoxy)methyl)-7H-pyrrolo[2,3-d]pyrimidin-6-yl)-3-methoxybenzaldehyde (19)

Compound **19** was prepared as described in Section 4.6.2, starting with **6b** (511 mg, 1.00 mmol) and (4-formyl-2-methoxyphenyl)boronic acid (216 mg, 1.20 mmol). The reaction time was 2 hours. Purification by silica-gel column chromatography (EtOAc/*n*-pentane, 7/3, R_f = 0.29) gave 456 mg (0.879 mmol, 88 %) of a yellow solid. mp 169 - 171 °C; [α]_D²⁰ = -238.1 (c 1.00, DMSO); ¹H NMR (400 MHz, DMSO-*d*₆) δ: 10.07 (s, 1H), 8.14 (s, 1H), 7.91 - 7.89 (m, 1H), 7.70 - 7.68 (m, 1H), 7.65 - 7.64 (m, 2H), 7.43 - 7.41 (m, 2H), 7.32 - 7.29 (m, 2H), 7.23 - 7.21 (m, 1H), 6.94 (s, 1H), 5.47 - 5.38 (m, 3H), 4.97 (t, *J* = 5.7, 1H), 3.89 (s, 3H), 3.78 - 3.71 (m, 2H), 3.32 - 3.25 (m, 2H), 0.66 - 0.62 (m, 2H), -0.19 (s, 9H); ¹³C NMR (100 MHz, DMSO-*d*₆) δ: 192.6, 157.3, 155.7, 152.0, 151.4, 141.7, 137.4, 132.1, 131.5, 128.0 (2C), 127.1 (2C), 126.9, 126.7, 122.7, 110.8, 102.9, 102.2, 70.7, 65.3, 64.9, 59.6, 55.8, 17.0, -1.5 (3C); HRMS (APCI/ASAP, *m/z*): 519.2348 (calcd. C₂₈H₃₅N₄O₄Si, 519.2348 [M+H]⁺).

4.8.9 (S)-2-((6-(2-Methoxy-4-(((2-morpholinoethyl)amino)methyl)phenyl)-7-((2-(trimethylsilyl)ethoxy)methyl)-7H-pyrrolo[2,3-d]pyrimidin-4-yl)amino)-2-phenylethan-1-ol (20)

Compound **20** was prepared as described in Section 4.6.3, starting with **19** (200 mg, 0.386 mmol) and 2-morpholinoethan-1-amine (0.15 mL, 15 mg, 1.157 mmol). This gave 217 mg (0.343 mmol, 89 %) of a pale solid. ¹H NMR (400 MHz, DMSO-*d*₆) δ: 8.10 (s, 1H), 7.70 - 7.49 (m, 1H), 7.43 - 7.41 (m, 2H), 7.33 - 7.28 (m, 3H), 7.23 - 7.19 (m, 1H), 7.13 (s, 1H), 7.02 - 7.00 (m, 1H), 6.73 (s, br, 1H), 5.46 - 5.41 (m, 1H), 5.38 - 5.31 (m, 2H), 4.97 - 4.95 (m, 1H), 3.79 - 3.70 (m, 7H), 3.57 - 3.55 (m, 4H), 3.26 - 3.22 (m, 2H), 2.63 (t, *J* = 6.4, 2H), 2.41 (t, *J* = 6.4, 2H), 2.35 - 2.33 (m, 4H), 0.65 - 0.61 (m, 2H), -0.19 (s, 9H), NH was not seen; ¹³C NMR (100 MHz, DMSO-*d*₆) δ: 156.8, 155.5, 152.9, 151.5, 143.8, 141.9, 133.1, 131.5, 128.1 (2C), 127.0 (2C), 126.7, 119.9, 118.8, 110.9, 107.3, 100.5, 70.5, 68.3, 66.2,

65.3, 65.0, 58.0, 57.5, 56.4, 55.4, 53.5, 53.0, 45.3, 17.1, -1.5 (3C); The SEM-protected intermediate **20** was used without further purification.

4.8.10 (S)-2-((6-(2-Methoxy-4-(((2-(piperidin-1-yl)ethyl)amino)methyl)phenyl)-7-((2-(trimethylsilyl)ethoxy)methyl)-7H-pyrrolo[2,3-d]pyrimidin-4-yl)amino)-2-phenylethan-1-ol (21)

Compound **21** was prepared as described in Section 4.6.3, starting with **19** (160 mg, 0.308 mmol) and 2-(piperidin-1-yl)ethan-1-amine (0.13 mL, 16 mg, 0.925 mmol). Purification by silica-gel column chromatography (CH₂Cl₂/MeOH, 85/15, R_f = 0.11) gave 174 mg (0.343 mmol, 90 %) of a pale solid. ¹H NMR (400 MHz, DMSO-*d*₆) δ: 8.10 (s, 1H), 7.77 - 7.75 (m, 1H), 7.43 - 7.41 (m, 2H), 7.33 - 7.28 (m, 3H), 7.23 - 7.19 (m, 1H), 7.13 (s, 1H), 7.01 - 7.00 (m, 1H), 6.73 (s, br, 1H), 5.46 - 5.41 (m, 1H), 5.38 - 5.32 (m, 2H), 4.98 - 4.95 (m, 1H), 3.76 - 3.71 (m, 7H), 3.25 - 3.21 (m, 2H), 2.62 - 2.57 (m, 2H), 2.38 - 2.35 (m, 2H), 2.31 - 2.28 (m, 4H), 1.50 - 1.45 (m, 4H), 1.39 - 1.34 (m, 2H), 0.64 - 0.60 (m, 2H), -0.19 (s, 9H), NH was not seen; ¹³C NMR (100 MHz, DMSO-*d*₆) δ: 156.8, 155.5, 151.5, 143.9, 141.9, 133.1, 131.4, 128.0 (2C), 127.0 (2C), 126.7, 119.9, 118.8, 110.9, 102.9, 110.5, 70.5, 65.3, 64.9, 59.8, 58.3, 55.4, 54.2 (2C), 53.0, 45.7, 25.7 (2C), 24.2, 17.1, 14.1, -1.5 (3C).

4.8.11 (S)-2-((6-(2-Methoxy-4-(((2-(piperazin-1-yl)ethyl)amino)methyl)phenyl)-7-((2-(trimethylsilyl)ethoxy)methyl)-7H-pyrrolo[2,3-d]pyrimidin-4-yl)amino)-2-phenylethan-1-ol (22)

Compound **22** was prepared as described in Section 4.6.3, starting with **19** (160 mg, 0.308 mmol) and 2-(piperazin-1-yl)ethan-1-amine (0.13 mL, 12 mg, 0.925 mmol). This gave 186 mg (0.296 mmol, 96 %) of a pale solid. ¹H NMR (400 MHz, DMSO-*d*₆) δ: 8.10 (s, 1H), 7.78 - 7.76 (m, 1H), 7.45 - 7.41 (m, 2H), 7.32 - 7.28 (m, 3H), 7.23 - 7.19 (m, 1H), 7.13 (s, 1H), 7.02 - 6.99 (m, 1H), 6.73 (s, br, 1H), 5.47 - 5.42 (m, 1H), 5.37 - 5.31 (m, 2H), 4.99 - 4.96 (m, 1H), 3.76 - 3.70 (m, 7H), 3.25 - 3.21 (m, 2H), 2.67 - 2.65 (m, 4H), 2.62 - 2.59 (m, 2H), 2.39 - 2.35 (m, 2H), 2.33 - 2.32 (m, 1H), 2.28 - 2.24 (m, 4H), 0.64 - 0.60 (m, 2H), -0.19 (s, 9H), NH was not seen; SEM-protected intermediate **22** was used further without purification.

4.8.12 (S)-2-Fluoro-5-(4-((2-hydroxy-1-phenylethyl)amino)-7-((2-(trimethylsilyl)ethoxy)methyl)-7H-pyrrolo[2,3-d]pyrimidin-6-yl)benzaldehyde (23)

Compound **23** was prepared as described in Section 4.6.2, starting with **6b** (300 mg, 0.588 mmol) and (4-fluoro-3-formylphenyl)boronic acid (148 mg, 0.882 mmol). The reaction time was 1 hour. Purification by silica-gel column chromatography (EtOAc/*n*-pentane, 3/2, R_f = 0.27) gave 260 mg (0.513 mmol, 87 %) of a yellow foam; mp 146 - 148 °C; HPLC purity: 99 %, t_R = 27.1 min; [α]_D²⁰ = -227.6 (c 0.99, DMSO); ¹H NMR (400 MHz, CDCl₃-TMS) δ: 10.39 (s, 1H), 8.36 (s, 1H), 8.18 - 8.16 (m, 1H), 8.05 - 8.02 (m, 1H), 7.42 - 7.39 (m, 4H), 7.36 - 7.33 (m, 1H), 7.30 - 7.25 (m, 1H), 6.51 (s, 1H), 5.73 - 5.66 (m, 1H), 5.55 - 5.49 (m, 2H), 5.39 - 4.35 (m, 1H), 4.12 - 4.03 (m, 2H), 3.75 - 3.71 (m, 2H), 1.02 - 0.98 (m,

2H), -0.02 (s, 9H), OH not observed; ^{13}C NMR (100 MHz, CDCl_3 -TMS) δ : 186.8 (d, $J = 6.0$), 156.0, 152.4, 152.2, 139.8, 136.8 (d, $J = 9.9$), 136.6, 129.6, 129.3 (2C), 128.8 (d, $J = 3.8$), 128.3, 126.9 (2C), 124.5 (d, $J = 8.9$), 117.2 (d, $J = 21.2$), 112.2, 103.3, 99.1, 70.8, 68.2, 66.8, 58.8, 18.1, -1.3 (3C).

4.8.13 (S)-2-Fluoro-4-(4-((2-hydroxy-1-phenylethyl)amino)-7-((2-(trimethylsilyl)ethoxy)methyl)-7H-pyrrolo[2,3-d]pyrimidin-6-yl)benzaldehyde (24)

Compound **24** was prepared as described in Section 4.6.2, starting with **6b** (300 mg, 0.588 mmol) and (3-fluoro-4-formylphenyl)boronic acid (148 mg, 0.882 mmol). The reaction time was 1 hour. Purification by silica-gel column chromatography (EtOAc/n -pentane, 7/3, $R_f = 0.32$) gave 252 mg (0.500 mmol, 85 %) of a yellow foam; $[\alpha]_{\text{D}}^{20} = -218.5$ (c 0.50, DMSO); ^1H NMR (400 MHz, $\text{DMSO}-d_6$) δ : 10.25 (s, 1H), 8.19 (s, 1H), 8.09 - 8.07 (m, 1H), 7.98 - 7.94 (m, 1H), 7.83 - 7.80 (m, 1H), 7.76 - 7.74 (m, 1H), 7.44 - 7.42 (m, 2H), 7.33 - 7.29 (m, 3H), 7.24 - 7.20 (m, 1H), 5.63 - 5.57 (m, 2H), 5.47 - 5.42 (m, 1H), 5.01 - 4.98 (m, 1H), 3.76 - 3.73 (m, 2H), 3.66 - 3.61 (m, 2H), 0.88 - 0.84 (m, 2H), -0.09 (s, 9H); ^{13}C NMR (100 MHz, $\text{DMSO}-d_6$) δ : 187.3, 166.1 (d, $J = 261.2$), 156.1, 153.0, 152.5, 145.3, 141.5, 133.9, 130.0, 128.1 (2C), 127.0 (2C), 126.8, 124.3, 122.5 (d, $J = 9.2$), 115.2 (d, $J = 22.5$), 103.0, 70.4, 67.0, 65.8, 64.9, 56.2, 17.2, -1.4 (3C).

4.8.14 (S)-2-((6-(3-(((2-(Dimethylamino)ethyl)amino)methyl)-4-fluorophenyl)-7-((2-(trimethylsilyl)ethoxy)methyl)-7H-pyrrolo[2,3-d]pyrimidin-4-yl)amino)-2-phenylethan-1-ol (25)

Compound **25** was prepared as described in Section 4.6.3, starting with **23** (98 mg, 0.192 mmol) and N,N' -dimethylethane-1,2-diamine (40.0 μL , 51 mg, 0.577 mmol). Purification by silica-gel column chromatography ($\text{CH}_2\text{Cl}_2/\text{MeOH}/\text{NH}_3$, 90/10/1, $R_f = 0.10$) gave 127 mg (0.219 mmol, 74 %) of a light yellow solid; HPLC purity: 99 %, $t_R = 27.3$ min; $[\alpha]_{\text{D}}^{20} = -99.1$ (c 0.50, DMSO); ^1H NMR (400 MHz, CHCl_3 -TMS) δ : 8.36 (s, 1H), 7.70 - 7.68 (m, 1H), 7.65 - 7.61 (m, 1H), 7.45 - 7.38 (m, 4H), 7.36 - 7.32 (m, 1H), 7.13 - 7.09 (m, 1H), 6.44 (s, 1H), 5.56 - 5.53 (m, 3H), 5.38 - 5.34 (m, 1H), 5.30 (s, 1H), 4.12 - 4.01 (m, 2H), 3.90 (s, 2H), 3.74 - 3.70 (m, 2H), 2.73 (t, $J = 6.2$, 2H), 2.44 (t, $J = 6.2$, 2H), 2.20 (s, 6H), 0.98 - 0.94 (m, 2H), -0.03 (s, 9H) NH was not seen; ^{13}C NMR (100 MHz, CHCl_3 -TMS) δ : 161.8 (d, $J = 239.9$), 155.9, 152.2, 151.8, 140.0, 138.5 (d, $J = 24.9$), 131.5 (d, $J = 4.9$), 129.6, 129.5 (d, $J = 8.7$), 129.3 (2C), 128.3, 126.9 (2C), 115.6 (d, $J = 22.7$), 112.1, 103.4, 98.1, 70.8, 68.4, 66.7, 59.1, 59.0, 47.4, 46.8, 45.6 (2C), 18.2, -1.25 (3C); HRMS (APCI/ASAP, m/z): 579.3273 (calcd. $\text{C}_{31}\text{H}_{44}\text{N}_6\text{O}_2\text{FSi}$, 579.3279 $[\text{M}+\text{H}]^+$).

4.8.15 (S)-2-((6-(4-Fluoro-3-(hydroxymethyl)phenyl)-7-((2-(trimethylsilyl)ethoxy)methyl)-7H-pyrrolo[2,3-d]pyrimidin-4-yl)amino)-2-phenylethan-1-ol (26)

To a solution of (S)-2-fluoro-5-(4-((2-hydroxy-1-phenylethyl)amino)-7-((2-(trimethylsilyl)ethoxy)methyl)-7H-pyrrolo[2,3-d]pyrimidin-6-yl)benzaldehyde (**23**) (100 mg, 0.197 mmol) in a mixture of MeOH (5 mL) and THF (10 mL), NaBH₄ (22.5 mg, 0.597 mmol) was added. The reaction mixture was stirred at 20 °C for 4 hours at which time the solvent was removed *in vacuo*. The reaction mixture was diluted with H₂O (20 mL) and extracted with EtOAc (2 × 20 mL). The combined organic phases were washed with saturated aq. NaCl solution (15 mL), dried over anhydrous Na₂SO₄, filtered and concentrated *in vacuo*. Purification by silica-gel column chromatography (EtOAc, R_f = 0.31) gave 75 mg (0.148 mmol, 75 %) of a pale solid; HPLC purity: 99 %, t_R = 24.6 min; [α]_D²⁰ = -140.5 (c 0.50, DMSO); ¹H NMR (400 MHz, CDCl₃-TMS) δ: 8.35 (s, 1H), 7.78 - 7.75 (m, 1H), 7.68 - 7.64 (m, 1H), 7.44 - 7.31 (m, 5H), 7.15 - 7.11 (m, 1H), 6.42 (s, 1H), 5.59 - 5.58 (m, 1H), 5.52 (s, 2H), 5.38 - 5.34 (m, 1H), 4.81 (s, 2H), 4.12 - 4.01 (m, 2H), 3.74 - 3.70 (m, 2H), 0.98 - 0.94 (m, 2H), -0.04 (s, 9H); OH groups not observed; ¹³C NMR (100 MHz, CDCl₃-TMS) δ: 160.8 (d, J = 249.4), 155.9, 152.3, 151.8, 139.9, 138.1, 130.3, 130.2, 129.3 (2C), 128.6, 128.3, 126.9 (2C), 115.9, 115.7, 103.3, 98.2, 77.4, 70.8, 68.3, 66.7, 59.4, 59.0, 18.2, -1.3 (3C).

4.8.16 (S)-2-((6-(4-(((2-(Dimethylamino)ethyl)amino)methyl)-3-fluorophenyl)-7-((2-(trimethylsilyl)ethoxy)methyl)-7H-pyrrolo[2,3-d]pyrimidin-4-yl)amino)-2-phenylethan-1-ol (27)

Compound **27** was prepared as described in Section 4.6.3, starting with **24** (100 mg, 0.197 mmol) and *N,N'*-dimethylethane-1,2-diamine (40.0 μL, 51 mg, 0.577 mmol). Purification by silica-gel column chromatography (CH₂Cl₂/MeOH/NH₃, 90/10/1, R_f = 0.16) gave 107 mg (0.183 mmol, 93 %) of a colourless oil; HPLC purity: 98 %, t_R = 17.8 min; [α]_D²⁰ = -134.1 (c 0.50, DMSO); ¹H NMR (400 MHz, CHCl₃-TMS) δ: 8.37 (s, 1H), 7.48 - 7.38 (m, 7H), 7.36 - 7.32 (m, 1H), 6.46 (s, 1H), 5.57 - 5.55 (m, 3H), 5.38 - 5.35 (m, 1H), 4.12 - 4.02 (m, 2H), 3.89 (s, br, 2H), 3.76 - 3.72 (m, 2H), 2.73 (t, J = 6.2, 2H), 2.45 (t, J = 6.2, 2H), 2.21 (s, 6H), 0.99 - 0.95 (m, 2H), -0.02 (s, 9H); ¹³C NMR (100 MHz, CHCl₃-TMS) δ: 161.3 (d, J = 260.4), 156.0, 152.4, 152.0, 139.9, 137.8, 132.3 (d, J = 25.7), 130.8 (d, J = 5.0), 129.3 (2C), 127.7 (d, J = 16.1), 128.3, 126.9 (2C), 124.8, 115.9 (d, J = 24.0), 103.3, 98.4, 70.8, 68.3, 66.8, 59.2, 58.9, 47.3, 46.8, 45.6 (2C), 18.1, -1.25 (3C).

4.8.17 (S)-2-((6-(3-Fluoro-4-(hydroxymethyl)phenyl)-7-((2-(trimethylsilyl)ethoxy)methyl)-7H-pyrrolo[2,3-d]pyrimidin-4-yl)amino)-2-phenylethan-1-ol (28)

To a solution of (S)-2-fluoro-4-(4-((2-hydroxy-1-phenylethyl)amino)-7-((2-(trimethylsilyl)ethoxy)methyl)-7H-pyrrolo[2,3-d]pyrimidin-6-yl)benzaldehyde (**24**) (100 mg, 0.197 mmol) in a mixture of MeOH (5 mL) and THF (10 mL) NaBH₄ (23 mg, 0.597 mmol) was added. The reaction mixture was stirred at 20 °C for 2.5 hours at which time

the solvent was removed *in vacuo*. The reaction mixture was diluted with H₂O (20 mL) and extracted with EtOAc (2 × 35 mL). The combined organic phases were washed with saturated aq. NaCl solution (15 mL), dried over anhydrous Na₂SO₄, filtered and concentrated *in vacuo*. Purification by silica-gel column chromatography (EtOAc, R_f = 0.24) gave 95 mg (0.187 mmol, 95 %) of a pale solid; ¹H NMR (400 MHz, DMSO-*d*₆) δ: 8.15 (s, 1H), 7.93 - 7.91 (m, 1H), 7.61 - 7.53 (m, 3H), 7.44 - 7.42 (m, 2H), 7.33 - 7.29 (m, 2H), 7.23 - 7.19 (m, 1H), 7.04 (s, br, 1H), 5.52 (s, 2H), 5.44 - 5.41 (m, 1H), 4.60 (s, br, 2H), 3.77 - 3.73 (m, 2H), 3.63 - 3.58 (m, 2H), 0.87 - 0.83 (m, 2H), -0.09 (s, 9H).

4.8.18 (S)-2-((6-(4-(((2-(Dimethylamino)ethyl)(methyl)amino)methyl)-2-methoxyphenyl)-7-((2-(trimethylsilyl)ethoxy)methyl)-7H-pyrrolo[2,3-*d*]pyrimidin-4-yl)amino)-2-phenylethan-1-ol (29)

To a solution of (S)-4-(4-((2-hydroxy-1-phenylethyl)amino)-7-((2-(trimethylsilyl)ethoxy)methyl)-7H-pyrrolo[2,3-*d*]pyrimidin-6-yl)-3-methoxybenzaldehyde (**19**) (100 mg, 0.192 mmol) in 2,2,2-trifluoroethanol (4 mL) was added *N*¹,*N*¹,*N*²-trimethylethane-1,2-diamine (42 μL, 12 mg, 0.578 mmol) and molecular sieve (0.2 g, 4Å). The reaction mixture was stirred at 40 °C for 12 hours at which time the solvent was removed *in vacuo*. The crude product was dissolved in MeOH (10 mL) and NaBH₄ (22 mg, 0.529 mmol) was added and the mixture stirred for 3 hours. Upon completion, all solvent was removed and the crude material was extracted with EtOAc (2 × 50 mL) and H₂O (2 × 30 mL). The combined organic phases were washed with saturated aq. NaCl solution (15 mL), dried over anhydrous Na₂SO₄, filtered and concentrated *in vacuo*. Purification by silica-gel column chromatography (CH₂Cl₂/MeOH/NH₃, 90/10/1, R_f = 0.19) gave 93 mg (0.154 mmol, 80 %) of a pale solid; ¹H NMR (400 MHz, DMSO-*d*₆) δ: 8.11 (s, 1H), 7.78 - 7.76 (m, 1H), 7.43 - 7.41 (m, 2H), 7.34 - 7.28 (m, 3H), 7.23 - 7.19 (m, 1H), 7.10 (s, 1H), 7.00 - 6.98 (m, 1H), 6.75 (s, br, 1H), 5.47 - 5.41 (m, 1H), 5.38 - 5.32 (m, 2H), 4.98 - 4.95 (m, 1H), 3.78 - 3.71 (m, 2H), 3.76 (s, 3H), 3.55 (s, 2H), 3.25 - 3.20 (m, 2H), 2.47 - 2.38 (m, 4H), 2.20 (s, 3H), 2.14 (s, 6H), 0.64 - 0.60 (m, 2H), -0.19 (s, 9H).

4.8.19 (R)-3-((6-(2-Ethoxyphenyl)-7-((2-(trimethylsilyl)ethoxy)methyl)-7H-pyrrolo[2,3-*d*]pyrimidin-4-yl)amino)-3-phenylpropan-1-ol (30)

Compound **30** was prepared as described in Section 4.6.2, starting with **6c** (100 mg, 0.191 mmol) and (2-ethoxyphenyl)boronic acid (47 mg, 0.286 mmol). Purification by silica-gel column chromatography (EtOAc/*n*-pentane, 6/4, R_f = 0.32) gave 97 mg (0.187 mmol, 98 %) of a colourless oil; HPLC purity: 98 %, t_R = 27.6 min; [α]_D²⁰ = -105.2 (*c* 0.50, DMSO); ¹H NMR (600 MHz, CDCl₃-TMS) δ: 8.40 (s, 1H), 7.44 - 7.36 (m, 6H), 7.33 - 7.29 (m, 1H), 7.03 - 6.96 (m, 2H), 6.29 (s, 1H), 5.64 - 5.59 (m, 1H), 5.52 (s, 2H), 5.13 - 5.12 (m, 1H), 4.05 (q, *J* = 7.0, 2H), 3.80 - 3.70 (m, 2H), 3.35 - 3.31 (m, 2H), 2.32 - 2.23 (m, 2H), 2.03 - 1.95 (m, 1H), 1.30 (t, *J* = 7.0, 3H), 0.75 - 0.70 (m, 2H), -0.15 (s, 9H); ¹³C NMR (100 MHz, CDCl₃-TMS) δ: 156.6, 155.9, 151.8, 151.4, 142.7, 135.6, 132.7, 130.6, 129.2 (2C), 127.9, 126.9 (2C), 121.1, 120.9, 112.1, 103.3, 98.7, 71.6, 66.3, 64.0, 58.4, 51.8, 39.7, 17.8, 14.9, -1.4 (3C).

4.9 EGFR inhibitor structures

4.9.1 (*R*)-6-(4-(Methylsulfonyl)phenyl)-*N*-(1-phenylethyl)-7*H*-pyrrolo[2,3-*d*]pyrimidin-4-amine (34)

Compound **34** was prepared as described in Section 4.6.2, starting with **7a** (300 mg, 0.824 mmol) and (4-(methylsulfonyl)phenyl)boronic acid (198 mg, 0.988 mmol). The reaction time was 4 hours. Purification by silica-gel column chromatography (THF/Et₂O, 1/1, *R_f* = 0.23) gave 244 mg (0.622 mmol, 76 %) of a pale solid; mp 326 - 327 °C (dec.); HPLC purity: 99 %, *t_R* = 19.7 min; [α]_D²⁰ = -362.1 (*c* 1.00, DMSO); ¹H NMR (400 MHz, DMSO-*d*₆) δ : 12.26 (s, 1H), 8.11 (s, 1H), 8.03 - 7.95 (m, 5H), 7.45 - 7.43 (m, 2H), 7.33 - 7.29 (m, 3H), 7.22 - 7.18 (m, 1H), 5.55 - 5.48 (m, 1H), 3.24 (s, 3H), 1.55 (d, *J* = 7.0, 3H); ¹³C NMR (100 MHz, DMSO-*d*₆) δ : 155.4, 152.7, 152.0, 145.3, 138.7, 136.5, 131.5, 128.2 (2C), 127.8 (2C), 126.5, 126.0 (2C), 124.8 (2C), 104.0, 99.0, 48.7, 43.6, 22.8; IR (neat, cm⁻¹): 3377, 3356, 2982, 1593, 1478, 1315, 1295, 1144, 1089, 818, 764, 699; HRMS (APCI/ASAP, *m/z*): 393.1380 (calcd. C₂₁H₂₁N₄O₂S, 393.1385 [M+H]⁺).

4.9.2 (*R*)-4-(4-((1-Phenylethyl)amino)-7*H*-pyrrolo[2,3-*d*]pyrimidin-6-yl)benzenesulfonamide (35)

Compound **35** was prepared as described in Section 4.6.2, starting with **7a** (260 mg, 0.714 mmol) and (4-sulfamoylphenyl)boronic acid (178 mg, 0.884 mmol). The reaction time was 23 hours. Purification by silica-gel column chromatography (THF/Et₂O, 7/3, *R_f* = 0.23), followed by crystallization from EtOAc (15 mL) gave 260 mg (0.660 mmol, 90 %) of a white solid; mp 306 - 307 °C (dec.); HPLC purity: 99 %, *t_R* = 18.5 min; [α]_D²⁰ = -342.9 (*c* 0.99, DMSO); ¹H NMR (400 MHz, DMSO-*d*₆) δ : 12.18 (s, 1H), 8.09 (s, 1H), 7.94 - 7.90 (m, 3H), 7.88 - 7.85 (m, 2H), 7.44 - 7.42 (m, 2H), 7.35 (s, br, 2H), 7.33 - 7.29 (m, 2H), 7.26 (s, 1H), 7.22 - 7.18 (m, 1H), 5.54 - 5.47 (m, 1H), 1.55 (d, *J* = 7.0, 3H); ¹³C NMR (100 MHz, DMSO-*d*₆) δ : 155.3, 152.4, 151.9, 145.3, 142.2, 134.9, 131.8, 128.2 (2C), 126.5, 126.4 (2C), 126.0 (2C), 124.6 (2C), 103.9, 98.3, 48.7, 22.8; IR (neat, cm⁻¹): 3361, 3060, 2977, 1592, 1477, 1334, 1312, 1155, 1094, 898, 768, 697; HRMS (APCI/ASAP, *m/z*): 394.1335 (calcd. C₂₀H₂₀N₅O₂S, 394.1338 [M+H]⁺).

4.9.3 (*R*)-4-(4-((1-Phenylethyl)amino)-7*H*-pyrrolo[2,3-*d*]pyrimidin-6-yl)benzamide (36)

Compound **36** was prepared as described in Section 4.6.2, starting with **7a** (300 mg, 0.824 mmol) and (4-carbamoylphenyl)boronic acid (164 mg, 0.988 mmol). The reaction time was 10 hours. Purification by silica-gel column chromatography (THF, *R_f* = 0.20), followed by recrystallization from MeOH (10 mL) gave 197 mg (0.551 mmol, 71 %) of a white solid; mp 323 - 325 °C (dec.); HPLC purity: 99 %, *t_R* = 18.1 min; [α]_D²⁰ = -343.1 (*c* 1.00, DMSO); ¹H NMR (400 MHz, DMSO-*d*₆) δ : 12.11 (s, 1H), 8.08 (s, 1H), 7.95 - 7.93 (m, 3H), 7.87 - 7.84 (m, 3H), 7.44 - 7.43 (m, 2H), 7.33 - 7.29 (m, 3H), 7.22 - 7.18 (m, 2H), 5.54 - 5.47 (m, 1H), 1.54 (d, *J* = 7.0, 3H); ¹³C NMR (100 MHz, DMSO-*d*₆) δ : 167.3, 155.2, 152.2, 151.8,

145.4, 134.3, 132.46, 132.48, 128.2 (4C), 126.4, 126.0 (2C), 124.0 (2C), 103.9, 97.5, 48.7, 22.8; IR (neat, cm^{-1}): 3346, 3117, 2961, 1668, 1590, 1491, 1387, 1142, 841, 765, 702; HRMS (APCI/ASAP, m/z): 358.1662 (calcd. $\text{C}_{21}\text{H}_{20}\text{N}_5\text{O}$, 358.1668 $[\text{M}+\text{H}]^+$).

4.9.4 (*R*)-*N*-(4-(4-((1-Phenylethyl)amino)-7*H*-pyrrolo[2,3-*d*]pyrimidin-6-yl)phenyl)methanesulfonamide (**37**)

Compound **37** was prepared as described in Section 4.6.2, starting with **7a** (301 mg, 0.826 mmol) and (4-(methylsulfonamido)phenyl)boronic acid (213 mg, 0.988 mmol). The reaction time was 8 hours. Purification by silica-gel column chromatography (THF/Et₂O, 1/1, $R_f = 0.26$) gave 254 mg (0.624 mmol, 76 %) of a pale solid; mp 260 - 261 °C; HPLC purity: 97 %, $t_R = 19.5$ min; $[\alpha]_D^{20} = -325.6$ (c 1.00, DMSO); ¹H NMR (400 MHz, DMSO-*d*₆) δ : 11.99 (s, 1H), 9.87 (s, br, 1H), 8.06 (s, 1H), 7.82 - 7.80 (m, 1H), 7.77 - 7.75 (m, 2H), 7.44 - 7.40 (m, 2H), 7.32 - 7.27 (m, 4H), 7.21 - 7.17 (m, 1H), 7.04 (s, 1H), 5.54 - 5.47 (m, 1H), 3.04 (s, 3H), 1.54 (d, $J = 7.0$, 3H); ¹³C NMR (100 MHz, DMSO-*d*₆) δ : 155.0, 151.7, 151.5, 145.5, 137.5, 133.1, 128.2 (2C), 127.5, 126.4, 126.1 (2C), 125.5 (2C), 120.1 (2C), 103.9, 95.5, 48.7, 39.4, 22.9; IR (neat, cm^{-1}): 3426, 3387, 3288, 3125, 2967, 2874, 1592, 1473, 1330, 1297, 1151, 969, 829, 749, 701; HRMS (APCI/ASAP, m/z): 408.1487 (calcd. $\text{C}_{21}\text{H}_{22}\text{N}_5\text{O}_2\text{S}$, 408.1494 $[\text{M}+\text{H}]^+$).

4.9.5 (*R*)-*N*-(4-(4-((1-Phenylethyl)amino)-7*H*-pyrrolo[2,3-*d*]pyrimidin-6-yl)phenyl)acetamide (**38**)

Compound **38** was prepared as described in Section 4.6.2, starting with **7a** (302 mg, 0.829 mmol) and (4-acetamidophenyl)boronic acid (187 mg, 1.04 mmol). The reaction time was 10 hours. Purification by silica-gel column chromatography (Et₂O/THF, 6/4, $R_f = 0.10$), followed by recrystallization from acetonitrile (20 mL) gave 267 mg (0.719 mmol, 83 %) of a pale solid, mp 307 - 308 °C; HPLC purity: 99 %, $t_R = 18.5$ min; $[\alpha]_D^{20} = -373.2$ (c 1.02, DMSO); ¹H NMR (400 MHz, DMSO-*d*₆) δ : 11.93 (s, 1H), 10.02 (s, 1H), 8.04 (s, 1H), 7.78 - 7.76 (m, 1H), 7.72 - 7.70 (m, 2H), 7.66 - 7.60 (m, 2H), 7.44 - 7.42 (m, 2H), 7.32 - 7.28 (m, 2H), 7.21 - 7.17 (m, 1H), 7.01 - 7.00 (m, 1H), 5.53 - 5.46 (m, 1H), 2.07 (s, 3H), 1.53 (d, $J = 7.0$, 3H); ¹³C NMR (100 MHz, DMSO-*d*₆) δ : 168.3, 154.9, 151.5, 151.4, 145.6, 138.5, 166.4, 128.2 (2C), 126.6, 126.4, 126.1 (2C), 125.0 (2C), 119.3 (2C), 103.9, 95.2, 48.7, 24.1, 22.9; IR (neat, cm^{-1}): 3416, 3268, 3110, 2972, 2859, 1694, 1584, 1507, 1497, 1492, 1313, 1245, 1134, 836, 746, 693; HRMS (APCI/ASAP, m/z): 372.1819 (calcd. $\text{C}_{22}\text{H}_{21}\text{N}_5\text{O}$, 372.1824 $[\text{M}+\text{H}]^+$).

4.9.6 (*S*)-2-Phenyl-2-(((6-(pyridin-4-yl)-7*H*-pyrrolo[2,3-*d*]pyrimidin-4-yl)amino)ethan-1-ol (**39**)

Compound **39** was prepared as described in Section 4.6.4 starting with **12** (123 mg, 0.280 mmol). Purification by silica-gel column chromatography (THF/Et₂O, 1/1, $R_f = 0.22$). This gave 49 mg (0.160 mmol, 71 %) of a yellow solid, mp 264 - 266 °C; HPLC purity: 99 %, $t_R = 19.5$ min; $[\alpha]_D^{20} = -325.6$ (c 1.00, DMSO); ¹H NMR (400 MHz, DMSO-*d*₆) δ : 11.99 (s, 1H), 9.87 (s, br, 1H), 8.06 (s, 1H), 7.82 - 7.80 (m, 1H), 7.77 - 7.75 (m, 2H), 7.44 - 7.40 (m, 2H), 7.32 - 7.27 (m, 4H), 7.21 - 7.17 (m, 1H), 7.04 (s, 1H), 5.54 - 5.47 (m, 1H), 3.04 (s, 3H), 1.54 (d, $J = 7.0$, 3H); ¹³C NMR (100 MHz, DMSO-*d*₆) δ : 155.0, 151.7, 151.5, 145.5, 137.5, 133.1, 128.2 (2C), 127.5, 126.4, 126.1 (2C), 125.5 (2C), 120.1 (2C), 103.9, 95.5, 48.7, 39.4, 22.9; IR (neat, cm^{-1}): 3426, 3387, 3288, 3125, 2967, 2874, 1592, 1473, 1330, 1297, 1151, 969, 829, 749, 701; HRMS (APCI/ASAP, m/z): 408.1487 (calcd. $\text{C}_{21}\text{H}_{22}\text{N}_5\text{O}_2\text{S}$, 408.1494 $[\text{M}+\text{H}]^+$).

$t_R = 18.9$ min; $[\alpha]_D^{20} = -298.5$ (c 1.00, DMSO); $^1\text{H NMR}$ (600 MHz, $\text{CDCl}_3\text{-TMS}$) δ : 12.98 (s, 1H), 8.69 - 8.68 (m, 2H), 8.43 (s, 1H), 7.61 - 7.60 (m, 2H), 7.47 - 7.46 (m, 2H), 7.40 - 7.37 (m, 2H), 7.31 - 7.28 (m, 1H), 6.82 (s, 1H), 5.60 - 5.58 (m, 1H), 1.72 (d, $J = 6.8$, 3H), NH not observed; $^{13}\text{C NMR}$ (150 MHz, $\text{DMSO-}d_6$) δ : 156.0, 152.7, 152.3, 150.7 (2C), 143.7, 139.2, 132.8, 129.0 (2C), 127.7, 126.3 (2C), 119.3 (2C), 104.5, 98.0, 50.6, 22.9; IR (neat, cm^{-1}): 3429, 2971, 1588, 1475, 1311, 1143, 773, 763, 703; HRMS (APCI/ASAP, m/z): 316.1563 (calcd. $\text{C}_{19}\text{H}_{18}\text{N}_5$, 316.1562 $[\text{M}+\text{H}]^+$).

4.9.1 (*R*)-4-(4-((1-Phenylethyl)amino)-7*H*-pyrrolo[2,3-*d*]pyrimidin-6-yl)benzoic acid (40)

Compound **40** was prepared as described in Section 4.6.2, starting with **7a** (150 mg, 0.412 mmol), $\text{PdCl}_2(\text{dppf})$ (15 mg, 0.021 μmol , 0.05 eq.) and 4-boronobenzoic boronic acid (89.0 mg, 0.535 mmol). The reaction time was 24 hours. Saturated NH_4Cl was used in the work-up. Purification by silica-gel column chromatography ($\text{CH}_2\text{Cl}_2/\text{MeOH}/\text{NH}_3$, 95/5/1, $R_f = 0.18$) gave 21 mg (0.045 mmol, 11 %) of a pale solid, mp 267 - 270 $^\circ\text{C}$ (dec.); HPLC purity: 98 %, $t_R = 15.2$ min; $^1\text{H NMR}$ (400 MHz, $\text{DMSO-}d_6$) δ : 12.92 (s, 1H), 12.07 (s, 1H), 8.10 (s, 1H), 7.90 - 7.88 (m, 2H), 7.82 - 7.79 (m, 2H), 7.44 - 7.43 (m, 2H), 7.32 - 7.29 (m, 3H), 7.22 - 7.18 (m, 2H), 5.55 - 5.48 (m, 1H), 1.54 (d, $J = 7.0$, 3H); $^{13}\text{C NMR}$ (100 MHz, $\text{DMSO-}d_6$) δ : 169.3, 155.1, 152.4, 151.8, 145.4, 134.3, 132.8, 132.6, 128.2 (4C), 126.4, 126.1 (2C), 124.2 (2C), 103.9, 97.5, 48.7, 22.8; HRMS (APCI/ASAP, m/z): 359.1470 (calcd. $\text{C}_{21}\text{H}_{18}\text{N}_4\text{O}_2$, 359.1468 $[\text{M}+\text{H}]^+$).

4.9.2 (*R*)-3-(4-((1-Phenylethyl)amino)-7*H*-pyrrolo[2,3-*d*]pyrimidin-6-yl)benzamide (41)

Compound **41** was prepared as described in Section 4.6.2, starting with **7a** (303 mg, 0.832 mmol) and (3-carbamoylphenyl)boronic acid (165 mg, 0.998 mmol). The reaction time was 6 hours. Purification by silica-gel column chromatography (THF, $R_f = 0.23$), followed by crystallization from EtOAc (70 mL) gave 230 mg (0.643 mmol, 77 %) of a white solid, mp 242 - 243 $^\circ\text{C}$ (EtOAc); HPLC purity: 98 %, $t_R = 18.2$ min; $[\alpha]_D^{20} = -265.2$ (c 0.50, DMSO); $^1\text{H NMR}$ (400 MHz, $\text{DMSO-}d_6$) δ : 12.05 (s, 1H), 8.33 (s, 1H), 8.07 (s, 1H), 8.00 (s, br, 1H), 7.93 - 7.91 (m, 1H), 7.82 - 7.80 (m, 1H), 7.77 - 7.75 (m, 1H), 7.53 - 7.49 (m, 1H), 7.44 - 7.43 (m, 3H), 7.33 - 7.29 (m, 2H), 7.22 - 7.18 (m, 2H), 5.54 - 5.46 (m, 1H), 1.54 (d, $J = 7.0$, 3H); $^{13}\text{C NMR}$ (100 MHz, $\text{DMSO-}d_6$) δ : 167.7, 155.1, 151.9, 151.7, 145.5, 135.0, 133.0, 131.9, 128.9, 128.1 (2C), 126.8, 126.4, 126.0 (2C), 125.9, 124.1, 103.9, 96.8, 48.7, 22.9; IR (neat, cm^{-1}): 3367, 3150, 2977, 1660, 1589, 1444, 1344, 1147, 771, 699; HRMS (APCI/ASAP, m/z): 358.1662 (calcd. $\text{C}_{21}\text{H}_{20}\text{N}_5\text{O}$, 358.1668 $[\text{M}+\text{H}]^+$).

4.9.3 (*R*)-6-(2-Ethoxyphenyl)-*N*-(1-phenylethyl)-7*H*-pyrrolo-[2,3-*d*]pyrimidin-4-amine (42)

Compound **42** was prepared as described in Section 4.6.2, starting with **7a** (200 mg, 0.550

mmol) and (2-ethoxyphenyl)boronic acid (109 mg, 0.660 mmol). The reaction time was 1 hour. Purification by silica-gel column chromatography (EtOAc/*n*-pentane, 4/1, $R_f=0.24$), followed by trituration from pentane and a further crystallisation from acetonitrile (90 mg in 1 mL) gave 60 mg (0.17 mmol, 31 %) of a white solid, mp 154 °C; HPLC purity: 96 %, $t_R = 23.5$ min; $[\alpha]_D^{20} = -275.3$ (*c* 1.00, DMSO); $^1\text{H NMR}$ (600 MHz, DMSO- d_6) δ : 11.58 (s, 1H), 8.05 (s, 1H), 7.76 (d, $J = 8.2$, 1H), 7.72 - 7.69 (m, 1H), 7.44 - 7.42 (m, 2H), 7.32 - 7.29 (m, 2H), 7.29 - 7.25 (m, 1H), 7.21 - 7.17 (m, 1H), 7.17 (m, 1H), 7.13 - 7.11 (m, 1H), 7.03 - 6.99 (m, 1H), 5.58 - 5.50 (m, 1H), 4.19 (q, $J = 6.9$, 2H), 1.55 (d, $J = 7.0$, 3H), 1.45 (t, $J = 6.9$, 3H); $^{13}\text{C NMR}$ (150 MHz, DMSO- d_6) δ : 155.3, 155.0, 151.5, 150.7, 145.6, 130.3, 128.4, 128.1 (2C), 127.6, 126.4, 126.1 (2C), 120.7, 120.6, 112.8, 103.5, 99.6, 63.7, 48.6, 22.8, 14.7. IR (neat, cm^{-1}): 3214, 2974, 2359, 1575, 1446, 1313, 1244, 1124, 1032, 749, 698. HRMS (APCI/ASAP, *m/z*): 359.1867 (calcd. $\text{C}_{22}\text{H}_{23}\text{N}_4\text{O}$, 359.1872 $[\text{M}+\text{H}]^+$).

4.9.4 (*R*)-6-(2-Isopropoxyphenyl)-*N*-(1-phenylethyl)-7*H*-pyrrolo[2,3-*d*]pyrimidin-4-amine (43)

Compound **43** was prepared as described in Section 4.6.2, starting with **7a** (200 mg, 0.550 mmol) and (2-isopropoxyphenyl)boronic acid (119 mg, 0.660 mmol). The reaction time was 1 hour. Purification by silica-gel column chromatography (EtOAc/*n*-pentane, 4/1, $R_f = 0.26$), trituration from pentane and finally crystallisation from Et₂O (70 mg in 40 mL) gave 31 mg (0.08 mmol, 15 %) of a white solid, mp 186 - 187 °C; HPLC purity: 96 %, $t_R = 23.5$ min; $[\alpha]_D^{20} = -256.7$ (*c* 1.00, DMSO); $^1\text{H NMR}$ (600 MHz, DMSO- d_6) δ : 11.52 (s, 1H), 8.05 (s, 1H), 7.76 (d, $J = 8.3$, 1H), 7.70 - 7.68 (m, 1H), 7.44 - 7.42 (m, 2H), 7.32 - 7.29 (m, 2H), 7.28 - 7.24 (m, 1H), 7.21 - 7.18 (m, 1H), 7.15 - 7.14 (m, 1H), 7.15 - 7.12 (m, 1H), 7.01 - 6.98 (m, 1H), 5.59 - 5.52 (m, 1H), 4.75 - 4.66 (m, 1H), 1.56 (d, $J = 7.0$, 3H), 1.39 - 1.37 (m, 6H); $^{13}\text{C NMR}$ (150 MHz, DMSO- d_6) δ : 155.0, 154.3, 151.4, 150.6, 145.6, 130.4, 128.3, 128.1 (2C), 127.9, 126.4, 126.1 (2C), 121.5, 120.5, 114.4, 103.5, 99.6, 70.3, 48.6, 22.8, 21.9 (2C); IR (neat, cm^{-1}): 3216, 2966, 2358, 1579, 1448, 1309, 1248, 1127, 950, 753, 699. HRMS (APCI/ASAP, *m/z*): 373.2023 (calcd. $\text{C}_{23}\text{H}_{25}\text{N}_4\text{O}$, 373.2028 $[\text{M}+\text{H}]^+$).

4.9.5 (*R*)-6-(2-(Difluoromethoxy)phenyl)-*N*-(1-phenylethyl)-7*H*-pyrrolo[2,3-*d*]pyrimidin-4-amine (44)

Compound **44** was prepared as described in Section 4.6.2, starting with **7a** (170 mg, 0.470 mmol) and 2-(2-(difluoromethoxy)phenyl)-4,4,5,5-tetramethyl-1,3,2-dioxaborolane (**9**) (300 mg, 1.11 mmol). The reaction time was 1 hour. Purification by silica-gel column chromatography (EtOAc/*n*-pentane, 4/1, $R_f = 0.28$) gave 129 mg (0.340 mmol, 73 %) of a pale yellow solid, mp 103 - 105 °C; HPLC purity: 97 %, $t_R = 22.6$ min; $[\alpha]_D^{20} = -247.5$ (*c* 1.00, DMSO); $^1\text{H NMR}$ (600 MHz, DMSO- d_6) δ : 11.86 (s, 1H), 8.08 (s, 1H), 7.95 (d, $J = 8.2$, 1H), 7.82 - 7.80 (m, 1H), 7.43 - 7.42 (m, 2H), 7.40 - 7.37 (m, 1H), 7.34 - 7.32 (m, 1H), 7.32 - 7.29 (m, 3H), 7.25 (t, $J = 73.6$, 1H), 7.21 - 7.18 (m, 1H), 7.17 (s, 1H), 5.55 - 5.50 (m, 1H), 1.54 (d, $J = 7.1$, 3H); $^{13}\text{C NMR}$ (150 MHz, DMSO- d_6) δ : 155.2, 152.0, 151.0, 147.7, 145.5, 128.7, 128.5, 128.3, 128.2 (2C), 126.4, 126.1 (2C), 125.5, 123.6, 119.0, 116.7 (t, J

= 258.1), 103.7, 110.8, 48.6, 22.7; ^{19}F NMR (564 MHz, DMSO- d_6) δ : -83.2 (d, $J = 74.4$); IR (neat, cm^{-1}): 2977, 2358, 1589, 1475, 1311, 1205, 1106, 1036, 751, 699; HRMS (APCI/ASAP, m/z): 381.1527 (calcd. $\text{C}_{21}\text{H}_{19}\text{N}_4\text{OF}_2$, 381.1527 $[\text{M}+\text{H}]^+$).

4.9.6 (*R*)-*N*-(1-Phenylethyl)-6-(2-(trifluoromethoxy)phenyl)-7*H*-pyrrolo[2,3-*d*]pyrimidin-4-amine (45)

Compound **45** was prepared as described in Section 4.6.2, starting with **7a** (200 mg, 0.470 mmol) and (2-(trifluoromethoxy)phenyl)boronic acid (136 mg, 0.660 mmol). The reaction time was 1 hour. Purification by silica-gel column chromatography (EtOAc/*n*-pentane, 4/1, $R_f = 0.38$) gave 141 mg (0.350 mmol, 64 %) of a pale green solid, mp 101 - 103 °C; HPLC purity: 99 %, $t_R = 23.8$ min; $[\alpha]_D^{20} = -273.7$ (c 1.00, DMSO); ^1H NMR (600 MHz, DMSO- d_6) δ : 11.99 (s, 1H), 8.09 (s, 1H), 7.99 (d, $J = 8.2$, 1H), 7.86 - 7.83 (m, 1H), 7.51 - 7.44 (m, 3H), 7.43 - 7.42 (m, 2H), 7.33 - 7.29 (m, 2H), 7.21 - 7.18 (m, 1H), 7.14 (s, 1H), 5.57 - 5.49 (m, 1H), 1.54 (d, $J = 7.0$, 3H); ^{13}C NMR (150 MHz, DMSO- d_6) δ : 155.3, 152.2, 151.1, 145.4, 145.4, 144.9, 129.3, 128.8, 128.2 (2C), 127.9, 127.7, 126.4, 126.1 (2C), 125.7, 121.8, 120.1 (q, $J = 257.4$), 103.7, 100.6, 48.6, 22.7; ^{19}F NMR (564 MHz, DMSO- d_6) δ : -58.2; IR (neat, cm^{-1}): 2971, 2353, 1580, 1470, 1309, 1245, 1218, 1160, 754, 698; HRMS (APCI/ASAP, m/z): 399.1429 (calcd. $\text{C}_{21}\text{H}_{18}\text{N}_4\text{OF}_3$, 399.1433 $[\text{M}+\text{H}]^+$).

4.9.7 (*R*)-6-(2,6-Dimethoxyphenyl)-*N*-(1-phenylethyl)-7*H*-pyrrolo[2,3-*d*]pyrimidin-4-amine (46)

Compound **46** was prepared as described in Section 4.6.2, starting with **7a** (298 mg, 0.820 mmol) and (2,6-dimethoxyphenyl)boronic acid (180 mg, 0.992 mmol). The reaction time was 8 hours. Purification by silica-gel column chromatography (Et₂O/THF, 6/4, $R_f = 0.22$) gave 237 mg (0.632 mmol, 76 %) of a white solid, mp 200 - 202 °C; HPLC purity: 99 %, $t_R = 22.3$ min; $[\alpha]_D^{20} = -214.0$ (c 0.99, DMSO); ^1H NMR (400 MHz, DMSO- d_6) δ : 11.25 (s, 1H), 8.03 (s, 1H), 7.69 - 7.67 (m, 1H), 7.45 - 7.43 (m, 2H), 7.34 - 7.29 (m, 3H), 7.21 - 7.18 (m, 1H), 6.80 - 6.75 (m, 3H), 5.57 - 5.50 (m, 1H), 3.77 (s, 6H), 1.54 (d, $J = 7.0$, 3H); ^{13}C NMR (100 MHz, DMSO- d_6) δ : 157.9 (2C), 154.7, 150.9, 149.8, 145.7, 129.4, 128.1 (2C), 126.4, 126.1 (2C), 125.9, 110.0, 104.3 (2C), 102.9, 100.6, 55.77 (2C), 48.5, 22.8; IR (neat, cm^{-1}): 3411, 3253, 3090, 2967, 2840, 1579, 1473, 1235, 1105, 1033, 785, 728, 697; HRMS (APCI/ASAP, m/z): 375.1817 (calcd. $\text{C}_{22}\text{H}_{23}\text{N}_4\text{O}_2$, 375.1821 $[\text{M}+\text{H}]^+$).

4.9.8 (*R*)-3-Methoxy-4-(4-((1-phenylethyl)amino)-7*H*-pyrrolo[2,3-*d*]pyrimidin-6-yl)benzamide (47)

Compound **47** was prepared as described in Section 4.6.2, starting with **7a** (303 mg, 0.833 mmol) and (4-carbamoyl-2-methoxyphenyl)boronic acid (197 mg, 1.01 mmol). The reaction time was 7 hours. Purification by crystallization from acetonitrile (25 mL) gave 259 mg (0.668 mmol, 79 %) of a pale solid, mp 265 - 267 °C; HPLC purity: 99 %, $t_R = 17.9$ min; $[\alpha]_D^{20} = -361.3$ (c 0.99, DMSO); ^1H NMR (400 MHz, DMSO- d_6) δ : 11.78 (s, 1H),

8.07 (s, 1H), 8.03 (s, br, 1H), 7.89 (m, 1H), 7.87 - 7.82 (m, 1H), 7.606 - 7.602 (m, 1H), 7.57 - 7.54 (m, 1H), 7.44 - 7.36 (m, 4H), 7.33 - 7.29 (m, 2H), 7.22 - 7.18 (m, 1H), 5.54 - 5.49 (m, 1H), 4.00 (s, 3H), 1.55 (d, $J = 7.0$, 3H); ^{13}C NMR (100 MHz, DMSO- d_6) δ : 167.3, 155.8, 155.2, 152.0, 151.0, 145.4, 133.6, 129.2, 128.2 (2C), 126.6, 126.4, 126.1 (2C), 122.9, 119.8, 110.9, 103.7, 101.5, 55.7, 48.6, 22.8; IR (neat, cm^{-1}): 3392, 3165, 1664, 1591, 1503, 1398, 1249, 1152, 1038, 862, 776, 697; HRMS (APCI/ASAP, m/z): 388.1768 (calcd. $\text{C}_{22}\text{H}_{22}\text{N}_5\text{O}_2$, 388.1773 $[\text{M}+\text{H}]^+$).

4.9.9 (*R*)-*N*-(3-Methoxy-4-(4-((1-phenylethyl)amino)-7*H*-pyrrolo[2,3-*d*]pyrimidin-6-yl)phenyl)methanesulfonamide (**48**)

Compound **48** was prepared as described in Section 4.6.2, starting with **7a** (100 mg, 0.275 mmol) and *N*-(3-methoxy-4-(4,4,5,5-tetramethyl-1,3,2-dioxaborolan-2-yl)phenyl)methanesulfonamide (**10**) (90 mg, 0.275 mmol). The reaction time was 6 hours. Purification by silica-gel column chromatography (THF/Et₂O, 1/1, $R_f = 0.12$) gave 78 mg (0.178 mmol, 65 %) of a white solid, mp 157 - 160 °C; HPLC purity: 98 %, $t_R = 19.9$ min; $[\alpha]_D^{20} = -269.0$ (c 0.50, DMSO); ^1H NMR (400 MHz, DMSO- d_6) δ : 11.59 (s, 1H), 9.86 (s, 1H), 8.04 (s, 1H), 7.78 - 7.76 (m, 1H), 7.70 - 7.68 (m, 1H), 7.43 - 7.42 (m, 2H), 7.32 - 7.28 (m, 2H), 7.21 - 7.15 (m, 2H), 6.98 - 6.97 (m, 1H), 6.88 - 6.85 (m, 1H), 5.55 - 5.48 (m, 1H), 3.91 (s, 3H), 3.05 (s, 3H), 1.54 (d, $J = 7.0$, 3H); ^{13}C NMR (100 MHz, DMSO- d_6) δ : 156.7, 154.9, 151.4, 150.7, 145.6, 138.6, 129.8, 128.1 (2C), 127.8, 126.4, 126.1 (2C), 116.0, 112.2, 103.6, 103.1, 99.2, 55.5, 48.6, 39.4, 22.9; IR (neat, cm^{-1}): 3372, 2967, 2623, 1599, 1474, 1321, 1145, 977, 762, 700; HRMS (APCI/ASAP, m/z): 438.1592 (calcd. $\text{C}_{22}\text{H}_{24}\text{N}_5\text{O}_3\text{S}$, 438.1600 $[\text{M}+\text{H}]^+$).

4.9.10 (*R*)-*N*¹-(3-Methoxy-4-(4-((1-phenylethyl)amino)-7*H*-pyrrolo[2,3-*d*]pyrimidin-6-yl)benzyl)-*N*²,*N*²-dimethylethane-1,2-diamine (**49**)

To a solution of (*R*)-3-methoxy-4-(4-((1-phenylethyl)amino)-7*H*-pyrrolo[2,3-*d*]pyrimidin-6-yl)benzaldehyde (**31**) [20] (60 mg, 0.162 mmol) in anhydrous CH_2Cl_2 (3 mL) was added *N,N*'-dimethylethane-1,2-diamine (0.032 mL, 26 mg, 0.295 mmol). The reaction mixture was stirred at 20 °C for 2.5 hours at which time the solvent was removed *in vacuo*. The intermediate product was dissolved in a MeOH (5 mL), NaBH_4 (14 mg, 0.373) was added and the mixture was stirred for 3 hours. Upon completion, all solvent was removed and the crude material was extracted with EtOAc (2 × 25 mL) and H₂O (2 × 15 mL). The combined organic phases were washed with saturated aq. NaCl solution (15 mL), dried over anhydrous Na_2SO_4 , filtered and concentrated *in vacuo*. Purification was by silica-gel column chromatography ($\text{CH}_2\text{Cl}_2/\text{EtOH}/\text{NH}_3$, 80/20/1, $R_f = 0.08$). This gave 55 mg (0.124 mmol, 76 %) of **49** as a pale solid, mp 130 - 132 °C; HPLC purity: 99 %, $t_R = 21.8$ min; $[\alpha]_D^{20} = -276.9$ (c 0.51, DMSO); ^1H NMR (400 MHz, DMSO- d_6) δ : 11.60 (s, 1H), 8.04 (s, 1H), 7.79 - 7.76 (m, 1H), 7.69 - 7.76 (m, 1H), 7.44 - 7.42 (m, 3H), 7.32 - 7.28 (m, 3H), 7.12 - 7.11 (m, 1H), 6.99 - 6.95 (m, 1H), 5.53 - 5.48 (m, 1H), 3.93 (s, 3H), 3.74 - 3.73 (m, 2H), 2.55 (t, $J = 6.5$, 2H), 2.34 (t, $J = 6.5$, 2H), 2.12 (s, 6H), 1.54 (d, $J = 7.0$, 3H), NH was not

seen; ^{13}C NMR (100 MHz, DMSO- d_6) δ : 156.1, 154.9, 151.4, 150.7, 145.7, 141.8, 130.2, 128.2 (2C), 126.9, 126.4, 126.1 (2C), 120.1, 118.6, 111.3, 103.6, 99.5, 58.9, 55.5, 52.9, 48.6, 45.6, 45.4 (2C), 22.9; IR (neat, cm^{-1}): 3216, 3107, 2935, 2810, 2758, 1591, 1568, 1452, 1346, 1304, 1257, 1231, 1153, 1034, 1003, 805, 783, 696; HRMS (APCI/ASAP, m/z): 445.2710 (calcd. $\text{C}_{26}\text{H}_{33}\text{N}_6\text{O}$, 445.2716 $[\text{M}+\text{H}]^+$).

4.9.11 (*S*)-2-((6-(2-(Methoxy- d_3)phenyl)-7*H*-pyrrolo[2,3-*d*]pyrimidin-4-yl)amino)-2-phenylethan-1-ol (**52**)

Compound **52** was prepared as described in Section 4.6.4 starting with **13** (91 mg, 0.209 mmol). Purification by silica-gel column chromatography ($\text{CH}_2\text{Cl}_2/\text{MeOH}$, 9/1, $R_f = 0.35$) gave 59 mg (0.163 mmol, 78 %) of a white solid, mp 186 - 187 $^\circ\text{C}$; HPLC purity: 98 %, $t_R = 18.6$ min; $[\alpha]_{\text{D}}^{20} = -235.0$ (c 0.50, DMSO); ^1H NMR (400 MHz, DMSO- d_6) δ : 11.64 (s, 1H), 8.04 (s, 1H), 7.76 - 7.75 (m, 1H), 7.72 - 7.71 (m, 1H), 7.45 - 7.43 (m, 2H), 7.31 - 7.28 (m, 3H), 7.24 (s, br, 1H), 7.22 - 7.20 (m, 1H), 7.15 - 7.13 (m, 1H), 7.04 - 7.01 (m, 1H), 5.45 - 5.42 (m, 1H), 4.96 (t, $J = 5.7$, 1H), 3.79 - 3.71 (m, 2H); ^{13}C NMR (100 MHz, DMSO- d_6) δ : 156.1, 155.5, 151.5, 150.7, 142.1, 130.1, 128.3, 128.0 (2C), 127.2, 127.1 (2C), 126.6, 120.6, 120.3, 111.9, 103.7, 100.0, 65.0, 56.0, 54.8; IR (neat, cm^{-1}): 3451, 3234, 3140, 2928, 1592, 1536, 1482, 1305, 1275, 1112, 1063, 781, 746, 698; HRMS (APCI/ASAP, m/z): 364.1852 (calcd. $\text{C}_{21}\text{H}_{18}\text{D}_3\text{N}_4\text{O}_2$, 364.1853 $[\text{M}+\text{H}]^+$).

4.9.12 (*R*)-6-(2-Ethoxyphenyl)-*N*-(1-phenylethyl)-7*H*-pyrrolo[2,3-*d*]pyrimidin-4-amine (**53**)

Compound **53** was prepared as described in Section 4.6.4 starting with **14** (90 mg, 0.178 mmol). Purification by silica-gel column chromatography ($\text{CH}_2\text{Cl}_2/\text{MeOH}$, 90/10, $R_f = 0.35$) gave 58 mg (0.155 mmol, 78 %) of a white solid, mp 115 - 117 $^\circ\text{C}$; HPLC purity: 99 %, $t_R = 20.4$ min; $[\alpha]_{\text{D}}^{20} = -171.6$ (c 0.50, DMSO); ^1H NMR (400 MHz, $\text{CDCl}_3\text{-TMS}$) δ : 10.25 (s, 1H), 8.30 (1H), 7.73 - 7.70 (m, 1H), 7.46 - 7.39 (m, 4H), 7.37 - 7.35 (m, 1H), 7.30 - 7.26 (m, 2H), 7.04 - 7.00 (m, 2H), 6.69 - 6.68 (m, 1H), 5.58 - 5.57 (m, 1H), 5.38 - 5.34 (m, 1H), 4.34 (q, $J = 7.0$, 2H), 4.14 - 4.02 (m, 2H), 1.56 (t, $J = 7.0$, 3H); ^{13}C NMR (100 MHz, $\text{CDCl}_3\text{-TMS}$) δ : 155.9, 155.2, 151.5, 150.5, 140.1, 133.5, 129.3 (3C), 128.3, 127.9, 127.0 (2C), 121.7, 119.7, 113.1, 103.7, 95.2, 68.5, 64.8, 59.2, 15.1; IR (neat, cm^{-1}): 3418, 2971, 2868, 1590, 1470, 1452, 1235, 1125, 1036, 742, 699; HRMS (APCI/ASAP, m/z): 375.1817 (calcd. $\text{C}_{22}\text{H}_{23}\text{N}_4\text{O}_2$, 375.1821 $[\text{M}+\text{H}]^+$).

4.9.13 (*S*)-*N*-(4-(4-((2-Hydroxy-1-phenylethyl)amino)-7*H*-pyrrolo[2,3-*d*]pyrimidin-6-yl)phenyl)methanesulfonamide (**54**)

Compound **54** was prepared as described in Section 4.6.2, starting with **7b** (300 mg, 0.789 mmol) and (4-(methylsulfonamido)phenyl)boronic acid (204 mg, 0.947 mmol). The reaction time was 1 hour. Purification by silica-gel column chromatography ($\text{THF}/\text{Et}_2\text{O}$, 6/4, $R_f = 0.17$), followed by crystallization from acetonitrile (25 mL), gave 264 mg (0.623

mmol, 79 %) of a white solid, mp 245 - 246 °C; HPLC purity: 99 %, $t_R = 16.4$ min; $[\alpha]_D^{20} = -243.1$ (c 1.01, DMSO); $^1\text{H NMR}$ (400 MHz, DMSO- d_6) δ : 11.96 (s, 1H), 9.82 (s, br, 1H), 8.04 (s, 1H), 7.77 - 7.75 (m, 2H), 7.69 - 7.67 (m, 1H), 7.44 - 7.42 (m, 2H), 7.32 - 7.26 (m, 4H), 7.22 - 7.19 (m, 1H), 7.05 (s, 1H), 5.44 - 5.39 (m, 1H), 4.97 - 4.94 (m, 1H), 3.79 - 3.69 (m, 2H), 3.03 (s, 3H); $^{13}\text{C NMR}$ (100 MHz, DMSO- d_6) δ : 155.5, 151.6, 151.5, 142.0, 137.5, 133.1, 128.1 (2C), 127.5, 127.1 (2C), 126.7, 125.5 (2C), 120.1 (2C), 104.1, 95.6, 65.0, 56.1, 39.4; IR (neat, cm^{-1}): 3397, 3323, 3139, 2938, 1597, 1480, 1328, 1147, 967, 782, 757, 704; HRMS (APCI/ASAP, m/z): 424.1437 (calcd. $\text{C}_{21}\text{H}_{22}\text{N}_5\text{O}_3\text{S}$, 424.1443 $[\text{M}+\text{H}]^+$).

4.9.14 (*S*)-2-((6-(4-(Methylsulfonyl)phenyl)-7*H*-pyrrolo[2,3-*d*]pyrimidin-4-yl)amino)-2-phenylethan-1-ol (**55**)

Compound **55** was prepared as described in Section 4.6.2, starting with **7b** (304 mg, 0.800 mmol) and (4-(methylsulfonyl)phenyl)boronic acid (189 mg, 0.946 mmol). The reaction time was 3 hours. Purification by silica-gel column chromatography (THF/Et₂O, 1/1, $R_f = 0.18$), followed by crystallization from acetonitrile (23 mL), gave 200 mg (0.490 mmol, 62 %) of an off-white solid, mp 300 - 302 °C (dec.); HPLC purity: 99 %, $t_R = 16.9$ min; $[\alpha]_D^{20} = -283.6$ (c 0.99, DMSO); $^1\text{H NMR}$ (400 MHz, DMSO- d_6) δ : 12.26 (s, 1H), 8.10 (s, 1H), 8.04 - 7.97 (m, 4H), 7.91 - 7.89 (m, 1H), 7.45 - 7.43 (m, 2H), 7.37 (s, br, 1H), 7.33 - 7.29 (m, 2H), 7.23 - 7.20 (m, 1H), 5.46 - 5.41 (m, 1H), 5.00 - 4.98 (m, 1H), 3.80 - 3.70 (m, 2H), 3.25 (s, 3H); $^{13}\text{C NMR}$ (100 MHz, DMSO- d_6) δ : 155.9, 152.7, 152.0, 141.8, 138.7, 136.5, 131.5, 128.1 (2C), 127.8 (2C), 127.0 (2C), 126.7, 124.8 (2C), 104.2, 99.1, 65.0, 56.0, 43.6; IR (neat, cm^{-1}): 3362, 3105, 2997, 2864, 1593, 1477, 1314, 1278, 1141, 765, 703; HRMS (APCI/ASAP, m/z): 409.1331 (calcd. $\text{C}_{21}\text{H}_{21}\text{N}_4\text{O}_3\text{S}$, 409.1334 $[\text{M}+\text{H}]^+$).

4.9.15 (*S*)-2-(3-(4-((2-Hydroxy-1-phenylethyl)amino)-7*H*-pyrrolo[2,3-*d*]pyrimidin-6-yl)phenyl)acetamide (**56**)

Compound **56** was prepared as described in Section 4.6.4 starting with **15** (63 mg, 0.121 mmol). Purification by silica-gel column chromatography (THF/NH₃, 99/1, $R_f = 0.17$) gave 49 mg (0.125 mmol, 85 %) of a yellow solid, mp 172 - 174 °C; $[\alpha]_D^{20} = -242.7$ (c 1.10, DMSO); $^1\text{H NMR}$ (400 MHz, DMSO- d_6) δ : 12.00 (s, 1H), 8.04 (s, 1H), 7.85 - 7.83 (m, 1H), 7.75 - 7.73 (m, 1H), 7.71 - 7.65 (m, 3H), 7.44 - 7.43 (m, 2H), 7.35 - 7.28 (m, 3H), 7.22 - 7.17 (m, 2H), 6.93 (s, br, 1H), 5.87 (s, br, 2H), 5.44 - 5.39 (m, 1H), 5.03 - 5.02 (m, 1H), 3.75 - 3.71 (m, 2H); $^{13}\text{C NMR}$ (100 MHz, DMSO- d_6) δ : 177.9, 174.6, 155.4, 151.8, 151.5, 145.3, 137.8, 134.0, 131.9, 128.9, 128.0 (2C), 127.1 (2C), 126.7, 126.6, 124.3, 104.3, 97.2, 64.8, 56.0, 55.8; IR (neat, cm^{-1}): 3204, 2923, 2849, 1661, 1597, 1199, 1133, 759, 700; HRMS (APCI/ASAP, m/z): 388.1770 (calcd. $\text{C}_{22}\text{H}_{22}\text{N}_5\text{O}_2$, 388.1773 $[\text{M}+\text{H}]^+$).

4.9.16 (*S*)-4-(4-((2-Hydroxy-1-phenylethyl)amino)-7*H*-pyrrolo[2,3-*d*]pyrimidin-6-yl)-3-methoxybenzamide (**57**)

Compound **57** was prepared as described in Section 4.6.2, starting with **7b** (298 mg, 0.784 mmol) and (4-carbamoyl-2-methoxyphenyl)boronic acid (187 mg, 0.941 mmol). The reaction time was 4 hours. Purification by silica-gel column chromatography (THF, $R_f = 0.10$), followed by crystallization from acetonitrile (40 mL) gave 195 mg (0.483 mmol, 62 %) of an off-white solid, mp 213 - 215 °C; HPLC purity: 98 %, $t_R = 14.9$ min; $[\alpha]_D^{20} = -306.3$ (c 0.52, DMSO); $^1\text{H NMR}$ (400 MHz, DMSO- d_6) δ : 11.75 (s, 1H), 8.06 (s, 1H), 8.02 (s, br, 1H), 7.85 - 7.83 (m, 1H), 7.80 - 7.78 (m, 1H), 7.610 - 7.606 (m, 1H), 7.57 - 7.54 (m, 1H), 7.45 - 7.43 (m, 2H), 7.39 - 7.38 (m, 2H), 7.33 - 7.29 (m, 2H), 7.23 - 7.19 (m, 1H), 5.46 - 5.41 (m, 1H), 4.98 - 4.95 (m, 1H), 4.01 (s, 3H), 3.79 - 3.71 (m, 2H); $^{13}\text{C NMR}$ (100 MHz, DMSO- d_6) δ : 167.3, 155.8, 155.7, 152.0, 150.9, 142.0, 133.6, 129.2, 128.0 (2C), 127.0 (2C), 126.7, 126.5, 122.9, 119.8, 110.9, 103.8, 101.5, 64.9, 56.0, 55.8; IR (neat, cm^{-1}): 3421, 3283, 3165, 2923, 1734, 1670, 1591, 1556, 1403, 1245, 1157, 1033, 880, 761, 701; HRMS (APCI/ASAP, m/z): 404.1718 (calcd. $\text{C}_{22}\text{H}_{22}\text{N}_5\text{O}_3$, 404.1723 $[\text{M}+\text{H}]^+$).

4.9.17 (*S*)-*N*-(4-(4-((2-Hydroxy-1-phenylethyl)amino)-7*H*-pyrrolo[2,3-*d*]pyrimidin-6-yl)-3-methoxyphenyl)methanesulfonamide (**58**)

Compound **58** was prepared as described in Section 4.6.2, starting with **7b** (102 mg, 0.268 mmol) and *N*-(3-methoxy-4-(4,4,5,5-tetramethyl-1,3,2-dioxaborolan-2-yl)phenyl)methanesulfonamide (**10**) (88 mg, 0.268 mmol). The reaction time was 8 hours. Purification by silica-gel column chromatography (THF/Et₂O, 6/4, $R_f = 0.07$), followed by precipitation as HCl salt, gave 90 mg (0.184 mmol, 69 %) of a light yellow solid, mp 214 - 215 °C; HPLC purity: 99 %, $t_R = 16.8$ min; $[\alpha]_D^{20} = -99.4$ (c 0.50, DMSO); NMR spectra of HCl salt: $^1\text{H NMR}$ (400 MHz, DMSO- d_6) δ : 12.73 (s, 1H), 10.02 (s, 1H), 9.62 (s, br, 1H), 8.28 (s, br, 1H), 7.72 - 7.71 (m, 1H), 7.54 (s, br, 1H), 7.51 - 7.49 (m, 2H), 7.41 - 7.37 (m, 2H), 7.32 - 7.29 (m, 1H), 7.04 (s, 1H), 6.92 - 6.90 (m, 1H), 5.36 - 5.30 (m, 1H), 3.92 (s, 3H), 3.86 - 3.85 (m, 2H), 3.08 (s, 3H), OH not observed; $^{13}\text{C NMR}$ (100 MHz, DMSO- d_6) δ : 157.1, 154.7, 151.4, 150.0, 145.3, 139.9, 130.2, 128.6 (2C), 127.8 (2C), 127.1 (2C), 115.8, 111.0, 102.9, 101.9, 99.3, 64.4, 59.8, 55.7, 39.4; IR (neat, cm^{-1}): 3258, 2943, 1634, 1479, 1324, 1146, 979, 913, 761, 700; HRMS (APCI/ASAP, m/z): 454.1543 (calcd. $\text{C}_{22}\text{H}_{24}\text{N}_5\text{O}_4\text{S}$, 454.1549 $[\text{M}+\text{H}]^+$).

4.9.18 (*R*)-*N*-(4-(4-((1-Phenylethyl)amino)-7*H*-pyrrolo[2,3-*d*]pyrimidin-6-yl)phenyl)acetamide (**59**)

Compound **59** was prepared as described in Section 4.6.2, starting with **7b** (90 mg, 0.237 mmol) and *N*-(3-methoxy-4-(4,4,5,5-tetramethyl-1,3,2-dioxaborolan-2-yl)phenyl)acetamide (**11**) (82 mg, 0.284 mmol). The reaction time was 2 hours. Purification by silica-gel column chromatography (THF/Et₂O, 7/3, $R_f = 0.08$) gave 80 mg (0.192 mmol, 81 %) of a light yellow solid, mp 154 - 156 °C; HPLC purity: 97 %, $t_R = 17.2$ min; $[\alpha]_D^{20} = -238.9$ (c 0.99, DMSO); $^1\text{H NMR}$ (400 MHz, DMSO- d_6) δ : 11.55 (s, 1H), 10.05 (s, 1H),

8.02 (s, 1H), 7.67 - 7.65 (m, 2H), 7.47 - 7.43 (m, 3H), 7.32 - 7.28 (m, 2H), 7.24 - 7.18 (m, 2H), 7.15 (s, br, 1H), 5.43 - 5.40 (m, 1H), 4.96 - 4.94 (m, 1H), 3.90 (s, 3H), 3.74 - 3.71 (m, 2H), 2.07 (s, 3H); ^{13}C NMR (100 MHz, DMSO- d_6) δ : 168.4, 156.2, 155.4, 151.2, 150.6, 142.1, 139.6, 130.1, 128.0 (2C), 127.3, 127.0 (2C), 126.6, 115.2, 110.0, 103.7, 102.5, 98.9, 65.0, 55.4, 54.9, 24.1; IR (neat, cm^{-1}): 3283, 3110, 2718, 1763, 1675, 1596, 1448, 1319, 1255, 1157, 1033, 782, 700; HRMS (APCI/ASAP, m/z): 418.1876 (calcd. $\text{C}_{23}\text{H}_{24}\text{N}_5\text{O}_3$, 418.1879 $[\text{M}+\text{H}]^+$).

4.9.19 (*S*)-2-Phenyl-2-((6-(pyridin-4-yl)-7*H*-pyrrolo[2,3-*d*]pyrimidin-4-yl)amino)ethan-1-ol (60)

Compound **60** was prepared as described in Section 4.6.4 starting with **16** (124 mg, 0.271 mmol). Purification by silica-gel column chromatography ($\text{CH}_2\text{Cl}_2/\text{MeOH}$, 85/15, $R_f = 0.10$) gave 78 mg (0.140 mmol, 80 %) of a white solid, mp 226 - 228 °C (dec.); HPLC purity: 99 %, $t_R = 15.0$ min; $[\alpha]_D^{20} = -292.3$ (c 0.54, DMSO); ^1H NMR (400 MHz, DMSO- d_6) δ : 12.30 (s, 1H), 8.60 - 8.59 (m, 2H), 8.10 (s, 1H), 7.93 - 7.91 (m, 1H), 7.74 - 7.72 (m, 2H), 7.45 - 7.43 (m, 3H), 7.33 - 7.29 (m, 2H), 7.23 - 7.20 (m, 1H), 5.46 - 5.41 (m, 1H), 4.98 (t, $J = 5.6$, 1H), 3.78 - 3.71 (m, 2H); ^{13}C NMR (100 MHz, DMSO- d_6) δ : 156.0, 152.9, 152.0, 150.3 (2C), 141.7, 138.6, 130.4, 128.1 (2C), 127.0 (2C), 126.7, 118.5 (2C), 104.0, 99.5, 64.9, 56.0; IR (neat, cm^{-1}): 3216, 3112, 2940, 2847, 2727, 1592, 1537, 1479, 1311, 1143, 1070, 1027, 999, 821, 775, 698; HRMS (APCI/ASAP, m/z): 332.1512 (calcd. $\text{C}_{19}\text{H}_{18}\text{N}_5\text{O}$, 322.1511 $[\text{M}+\text{H}]^+$).

4.9.20 (*S*)-2-Phenyl-2-((6-(pyridin-3-yl)-7*H*-pyrrolo[2,3-*d*]pyrimidin-4-yl)amino)ethan-1-ol (61)

Compound **61** was prepared as described in Section 4.6.4 starting with **17** (70 mg, 0.151 mmol). Purification by silica-gel column chromatography ($\text{CH}_2\text{Cl}_2/\text{MeOH}$, 85/15, $R_f = 0.43$) gave 57 mg (0.140 mmol, 93 %) of a pale solid, mp 212 - 213 °C; HPLC purity: 99 %, $t_R = 14.9$ min; $[\alpha]_D^{20} = -301.2$ (c 0.52, DMSO); ^1H NMR (400 MHz, DMSO- d_6) δ : 12.19 (s, 1H), 9.02 - 9.01 (m, 1H), 8.49 - 8.48 (m, 1H), 8.15 - 8.12 (m, 1H), 8.08 (s, 1H), 7.83 - 7.81 (m, 1H), 7.49 - 7.43 (m, 3H), 7.33 - 7.31 (m, 2H), 7.25 (s, br, 1H), 7.23 - 7.19 (m, 1H), 5.46 - 5.40 (m, 1H), 4.99 (t, $J = 5.6$, 1H), 3.80 - 3.70 (m, 2H); ^{13}C NMR (100 MHz, DMSO- d_6) δ : 155.7, 152.2, 151.8, 148.0, 145.8, 141.9, 131.5, 130.3, 128.1 (2C), 127.8, 127.0 (2C), 126.7, 124.0, 104.0, 97.4, 65.0, 56.0; IR (neat, cm^{-1}): 3278, 3096, 3023, 2940, 2842, 1597, 1571, 1534, 1478, 1317, 1169, 1028, 924, 760, 696; HRMS (APCI/ASAP, m/z): 332.1509 (calcd. $\text{C}_{19}\text{H}_{18}\text{N}_5\text{O}$, 332.1511 $[\text{M}+\text{H}]^+$).

4.9.21 (*S*)-2-((6-(3-Methoxypyridin-4-yl)-7*H*-pyrrolo[2,3-*d*]pyrimidin-4-yl)amino)-2-phenylethan-1-ol (62)

Compound **62** was prepared as described in Section 4.6.4 starting with **18** (161 mg, 0.328 mmol). Purification by silica-gel column chromatography ($\text{CH}_2\text{Cl}_2/\text{MeOH}$, 85/15, $R_f =$

0.12) gave 95.0 mg (0.262 mmol, 89 %) of a white solid, mp 188 - 190 °C (dec.); HPLC purity: 98 %, $t_R = 15.6$ min; $[\alpha]_D^{20} = -266.2$ (c 1.00, DMSO); $^1\text{H NMR}$ (400 MHz, DMSO- d_6) δ : 11.99 (s, 1H), 8.48 (s, 1H), 8.25 (d, $J = 5.0$, 1H), 8.10 (s, 1H), 7.96 - 7.95 (m, 1H), 7.78 (d, $J = 5.0$, 1H), 7.56 (s, br, 1H), 7.45 - 7.43 (m, 2H), 7.33 - 7.29 (m, 2H), 7.23 - 7.19 (m, 1H), 5.48 - 5.43 (m, 1H), 4.99 (t, $J = 5.6$, 1H), 4.09 (s, 3H), 3.81 - 3.71 (m, 2H); $^{13}\text{C NMR}$ (100 MHz, DMSO- d_6) δ : 156.0, 153.6, 152.7, 151.4, 151.2, 142.4, 141.8, 134.8, 128.1 (2C), 127.1, 127.0 (2C), 126.7, 126.5, 119.5, 103.9, 64.9, 56.4, 56.1; IR (neat, cm^{-1}): 3205, 3107, 2993, 2935, 2842, 1590, 1477, 1309, 1259, 1157, 1019, 937, 812, 780, 748, 698; HRMS (APCI/ASAP, m/z): 362.1620 (calcd. $\text{C}_{20}\text{H}_{20}\text{N}_5\text{O}_2$, 362.1617 $[\text{M}+\text{H}]^+$).

4.9.22 (*S*)-2-((6-(4-(((2-(Dimethylamino)ethyl)amino)methyl)phenyl)-7*H*-pyrrolo[2,3-*d*]pyrimidin-4-yl)amino)-2-phenylethan-1-ol (63)

Compound **63** was prepared as described in Section 4.6.3, starting with (*S*)-4-(4-((2-hydroxy-1-phenylethyl)amino)-7*H*-pyrrolo[2,3-*d*]pyrimidin-6-yl)benzaldehyde (**32**) [20], (17 mg, 0.046 mmol) and *N,N'*-dimethylethane-1,2-diamine (0.015 mL, 12 mg, 0.137 mmol). Purification by silica-gel column chromatography ($\text{CH}_2\text{Cl}_2/\text{EtOH}/\text{NH}_3$, 70/30/2, $R_f = 0.16$) gave 16 mg (0.037 mmol, 80 %) of a light yellow solid, mp 198 - 200 °C; HPLC purity: 98 %, $t_R = 19.8$ min; $[\alpha]_D^{20} = 199.8$ (c 0.50, DMSO); $^1\text{H NMR}$ (400 MHz, DMSO- d_6) δ : 11.98 (s, 1H), 8.04 (s, 1H), 7.75 - 7.73 (m, 2H), 7.69 - 7.67 (m, 1H), 7.45 - 7.43 (m, 2H), 7.40 - 7.38 (m, 2H), 7.32 - 7.29 (m, 2H), 7.23 - 7.19 (m, 1H), 7.10 (s, br, 1H), 5.44 - 5.39 (m, 1H), 4.95 (s, br, 1H), 3.76 - 3.74 (m, 4H), 2.59 (t, $J = 6.4$, 2H), 2.36 (t, $J = 6.4$, 2H), 2.13 (s, 6H), NH was not seen; $^{13}\text{C NMR}$ (100 MHz, DMSO- d_6) δ : 155.3, 151.6, 151.4, 142.0, 139.9, 133.5, 129.7, 128.5 (2C), 128.0 (2C), 127.0 (2C), 126.6, 124.3 (2C), 104.2, 98.4, 95.7, 65.0, 58.6, 55.8, 52.6, 45.2 (2C); IR (neat, cm^{-1}): 3288, 3120, 2928, 2863, 1595, 1482, 1309, 1038, 780, 699; HRMS (APCI/ASAP, m/z): 431.2554 (calcd. $\text{C}_{25}\text{H}_{31}\text{N}_6\text{O}$, 431.2559 $[\text{M}+\text{H}]^+$).

4.9.23 (*S*)-2-((6-(2-Methoxy-4-(((2-(methylsulfonyl)ethyl)amino)methyl)phenyl)-7*H*-pyrrolo[2,3-*d*]pyrimidin-4-yl)amino)-2-phenylethan-1-ol (64)

A mixture of 2-(methylsulfonyl)ethan-1-amine hydrogen chloride (18 mg, 0.113 mmol), diisopropylethylamine (DIPEA) (0.020 mL, 15 mg, 0.113 mmol) and anhydrous CH_2Cl_2 (1 mL) were stirred for 30 min at 20 °C. (*S*)-4-(4-((2-Hydroxy-1-phenylethyl)amino)-7*H*-pyrrolo[2,3-*d*]pyrimidin-6-yl)-3-methoxybenzaldehyde (**33**) [20], (40 mg, 0.103 mmol) was then added and the mixture stirred for 6 hours at which time the solvent was removed *in vacuo*. The crude product was dissolved in a mixture of MeOH (4 mL) / THF (1 mL). NaBH_4 (6 mg, 0.159) was then added and the mixture stirred for 3 hours. Upon completion, all solvent was removed and the crude material was extracted with EtOAc (2×25 mL) and H_2O (2×10 mL). The combined organic phases were washed with saturated aq. NaCl solution (15 mL), dried over anhydrous Na_2SO_4 , filtered and concentrated *in vacuo*. Purification by silica-gel column chromatography ($\text{CH}_2\text{Cl}_2/\text{MeOH}/\text{NH}_3$, 90/10/1, $R_f = 0.46$) gave 43 mg (0.087 mmol, 77 %) of a yellow solid, mp 134 - 137 °C; HPLC purity: 98 %, $t_R = 15.6$ min; $[\alpha]_D^{20} = -266.2$ (c 1.00, DMSO); $^1\text{H NMR}$ (400 MHz, DMSO- d_6) δ : 11.99 (s, 1H), 8.48 (s, 1H), 8.25 (d, $J = 5.0$, 1H), 8.10 (s, 1H), 7.96 - 7.95 (m, 1H), 7.78 (d, $J = 5.0$, 1H), 7.56 (s, br, 1H), 7.45 - 7.43 (m, 2H), 7.33 - 7.29 (m, 2H), 7.23 - 7.19 (m, 1H), 5.48 - 5.43 (m, 1H), 4.99 (t, $J = 5.6$, 1H), 4.09 (s, 3H), 3.81 - 3.71 (m, 2H); $^{13}\text{C NMR}$ (100 MHz, DMSO- d_6) δ : 156.0, 153.6, 152.7, 151.4, 151.2, 142.4, 141.8, 134.8, 128.1 (2C), 127.1, 127.0 (2C), 126.7, 126.5, 119.5, 103.9, 64.9, 56.4, 56.1; IR (neat, cm^{-1}): 3205, 3107, 2993, 2935, 2842, 1590, 1477, 1309, 1259, 1157, 1019, 937, 812, 780, 748, 698; HRMS (APCI/ASAP, m/z): 362.1620 (calcd. $\text{C}_{20}\text{H}_{20}\text{N}_5\text{O}_2$, 362.1617 $[\text{M}+\text{H}]^+$).

$t_R = 15.7$ min; $[\alpha]_D^{20} = -224.1$ (c 0.99, DMSO); $^1\text{H NMR}$ (400 MHz, DMSO- d_6) δ : 11.61 (s, 1H), 8.03 (s, 1H), 7.70 - 7.68 (m, 2H), 7.45 - 7.43 (m, 2H), 7.32 - 7.28 (m, 2H), 7.22 - 7.18 (m, 2H), 7.12 (s, br, 1H), 6.99 - 6.97 (m, 1H), 5.45 - 5.40 (m, 1H), 4.96 - 4.94 (m, 1H), 3.95 (s, 3H), 3.77 - 3.71 (m, 4H), 3.27 (t, $J = 6.6$, 2H), 3.17-3.16 (m, 1H, NH), 3.04 (s, 3H), 2.93 (t, $J = 6.6$, 2H); $^{13}\text{C NMR}$ (100 MHz, DMSO- d_6) δ : 167.4, 156.1, 151.3, 149.1, 142.1, 130.1, 128.0 (2C), 127.1 (2C), 126.9, 126.5, 120.1, 118.9, 111.3, 104.5, 102.8, 99.6, 65.9, 55.5, 54.9, 53.9, 52.2, 42.1, 41.6; IR (neat, cm^{-1}): 3392, 3145, 2918, 1592, 1468, 1301, 1277, 1130, 1032, 808, 785, 703; HRMS (APCI/ASAP, m/z): 496.1940 (calcd. $\text{C}_{25}\text{H}_{30}\text{N}_5\text{O}_4\text{S}$, 496.1940 $[\text{M}+\text{H}]^+$).

4.9.24 (S)-2-((6-(4-(((2-(Dimethylamino)ethyl)amino)methyl)-2-methoxyphenyl)-7H-pyrrolo[2,3-d]pyrimidin-4-yl)amino)-2-phenylethan-1-ol (65)

Compound **65** was prepared as described in Section 4.6.3, starting with (S)-4-(4-((2-hydroxy-1-phenylethyl)amino)-7H-pyrrolo[2,3-d]pyrimidin-6-yl)-3-methoxybenzaldehyde (**33**) [20], (70 mg, 0.180 mmol) and *N,N'*-dimethylethane-1,2-diamine (0.023 mL, 18 mg, 0.148 mmol). Purification by silica-gel column chromatography ($\text{CH}_2\text{Cl}_2/\text{MeOH}/\text{NH}_3$, 90/10/1, $R_f = 0.46$) gave 64 mg (0.126 mmol, 77 %) of a light yellow solid, mp 119 - 121 $^\circ\text{C}$; HPLC purity: 98 %, $t_R = 17.9$ min; $[\alpha]_D^{20} = -192.9$ (c 0.50, DMSO); $^1\text{H NMR}$ (400 MHz, DMSO- d_6) δ : 11.6 (s, 1H), 8.03 (s, 1H), 7.70 - 7.68 (m, 2H), 7.44 - 7.42 (m, 3H), 7.32 - 7.28 (m, 3H), 7.22 - 7.19 (m, 2H), 7.13 (s, 1H), 6.99 - 6.97 (m, 1H), 5.43 - 5.42 (m, 1H), 4.98 (s, br, 1H), 3.94 (s, 3H), 3.76 - 3.73 (m, 2H), 2.62 (t, $J = 6.4$, 2H), 2.38 (t, $J = 6.4$, 2H), 2.15 (s, 6H), NH was not seen; $^{13}\text{C NMR}$ (100 MHz, DMSO- d_6) δ : 156.1, 155.6, 151.5, 150.7, 146.5, 142.1, 130.2, 128.1 (2C), 127.0, 127.1 (2C), 126.7, 120.3, 118.8, 111.5, 103.8, 99.7, 65.1, 58.5, 55.6, 52.7, 46.0, 45.5, 45.2 (2C); IR (neat, cm^{-1}): 3165, 2918, 2819, 1670, 1592, 1453, 1161, 1031, 821, 781, 700; HRMS (APCI/ASAP, m/z): 461.2663 (calcd. $\text{C}_{26}\text{H}_{33}\text{N}_6\text{O}_2$, 461.2665 $[\text{M}+\text{H}]^+$).

4.9.25 (S)-2-((6-(2-Methoxy-4-(((2-morpholinoethyl)amino)methyl)phenyl)-7H-pyrrolo[2,3-d]pyrimidin-4-yl)amino)-2-phenylethan-1-ol (66)

Compound **66** was prepared as described in Section 4.6.4 starting with **20** (217 mg, 0.343 mmol). Purification by silica-gel column chromatography ($\text{CH}_2\text{Cl}_2/\text{MeOH}$, 85/15, $R_f = 0.06$) gave 138 mg (0.274 mmol, 71%) of a light yellow solid, mp 191 - 193 $^\circ\text{C}$ (dec.); HPLC purity: 99 %, $t_R = 18.1$ min; $[\alpha]_D^{20} = -213.6$ (c 1.00, DMSO); $^1\text{H NMR}$ (400 MHz, DMSO- d_6) δ : 11.62 (s, 1H), 8.03 (s, 1H), 7.72 - 7.69 (m, 2H), 7.45 - 7.43 (m, 2H), 7.32 - 7.28 (m, 2H), 7.22 - 7.19 (m, 2H), 7.13 (s, br, 1H), 7.00 - 6.98 (m, 1H), 5.45 - 5.40 (m, 1H), 4.97 (s, br, 1H), 3.94 (s, 3H), 3.77 - 3.73 (m, 4H), 3.56 (t, $J = 4.6$, 4H), 2.65 (t, $J = 6.4$, 2H), 2.42 (t, $J = 6.4$, 2H), 2.35 - 2.33 (m, 4H), NH on solubility tail not found; $^{13}\text{C NMR}$ (100 MHz, DMSO- d_6) δ : 156.1, 155.5, 151.4, 150.7, 142.1, 130.1, 128.0 (2C), 127.1 (2C), 126.9, 126.6, 120.3, 118.8, 111.5, 107.1, 103.7, 99.7, 66.2 (2C), 65.0, 57.6, 56.1, 55.5, 53.4 (2C), 52.6, 45.0; IR (neat, cm^{-1}): 3232, 2940, 2816, 1591, 1451, 1306, 1256, 1114, 1067, 1031,

914, 814, 781, 754, 696; HRMS (APCI/ASAP, m/z): 503.2766 (calcd. C₂₈H₃₅N₆O₃, 503.2771 [M+H]⁺).

4.9.26 (S)-2-((6-(2-Methoxy-4-(((2-(piperidin-1-yl)ethyl)amino)methyl)phenyl)-7H-pyrrolo[2,3-d]pyrimidin-4-yl)amino)-2-phenylethan-1-ol (67)

Compound **67** was prepared as described in Section 4.6.4 starting with **21** (174 mg, 0.343 mmol). Purification by silica-gel column chromatography (CH₂Cl₂/MeOH, 85/15, R_f = 0.05) gave 110 mg (0.220 mmol, 72%) of a bright yellow solid, mp 180 - 182 °C (dec.); HPLC purity: 99%, t_R = 18.1 min; [α]_D²⁰ = -215.8 (c 1.01, DMSO); ¹H NMR (400 MHz, DMSO-*d*₆) δ: 11.61 (s, 1H), 8.03 (s, 1H), 7.71 - 7.68 (m, 2H), 7.45 - 7.43 (m, 2H), 7.32 - 7.28 (m, 2H), 7.22 - 7.19 (m, 2H), 7.11 (s, br, 1H), 6.98 - 6.96 (m, 1H), 5.44 - 5.40 (m, 1H), 4.97 (s, br, 1H), 3.94 (s, 3H), 3.77 - 3.73 (m, 4H), 2.59 (t, *J* = 6.5, 2H), 2.37 (t, *J* = 6.5, 2H), 2.31 - 2.29 (m, 4H), 1.50 - 1.45 (m, 4H), 1.37 - 1.36 (m, 2H), NH was not seen; ¹³C NMR (100 MHz, DMSO-*d*₆) δ: 156.1, 155.5, 151.4, 150.6, 142.1, 130.2, 128.0 (2C), 127.1 (2C), 126.9, 126.6, 120.1, 118.6, 111.3, 107.1, 103.7, 99.6, 65.0, 58.3, 56.0, 55.5, 54.2 (2C), 52.8, 45.6, 25.6 (2C), 24.1; IR (neat, cm⁻¹): 3253, 3108, 2926, 2838, 1591, 1451, 1307, 1255, 1156, 1032, 813, 780, 748, 700; HRMS (APCI/ASAP, m/z): 501.2973 (calcd. C₂₉H₃₇N₆O₂, 501.2978 [M+H]⁺).

4.9.27 (S)-2-((6-(2-Methoxy-4-(((2-(piperazin-1-yl)ethyl)amino)methyl)phenyl)-7H-pyrrolo[2,3-d]pyrimidin-4-yl)amino)-2-phenylethan-1-ol (68)

Compound **68** was prepared as described in Section 4.6.4 starting with **22** (186 mg, 0.296 mmol). Purification by silica-gel column chromatography (CH₂Cl₂/MeOH/NH₃, 90/10/1, R_f = 0.12) gave 99 mg (0.220 mmol, 64 %) of a bright yellow solid, mp 208 - 210 °C (dec.); HPLC purity: 99 %, t_R = 17.6 min; [α]_D²⁰ = -159.5 (c 1.00, DMSO); ¹H NMR (400 MHz, DMSO-*d*₆) δ: 11.60 (s, 1H), 8.02 (s, 1H), 7.76 - 7.74 (m, 1H), 7.69 - 7.67 (m, 1H), 7.44 - 7.42 (m, 2H), 7.32 - 7.28 (m, 2H), 7.22 - 7.18 (m, 2H), 7.10 (s, br, 1H), 6.97 - 6.95 (m, 1H), 5.44 - 5.39 (m, 1H), 5.03 (s, br, 1H), 3.93 (s, 3H), 3.76 - 3.72 (m, 8H), 2.81 (s, br, 1H), 2.59 (t, *J* = 6.1, 2H), 2.37 (t, *J* = 6.1, 2H), 2.36 - 2.32 (m, 4H), NH was not seen; ¹³C NMR (100 MHz, DMSO-*d*₆) δ: 156.4, 155.5, 151.4, 149.9, 142.1, 130.2, 128.0 (2C), 127.1 (2C), 126.9, 126.6, 120.1, 118.6, 111.3, 107.4, 103.7, 99.7, 65.0, 59.8, 56.7, 55.5, 52.9 (2C), 51.1, 45.6 (3C); IR (neat, cm⁻¹): 3243, 2937, 2817, 1593, 1451, 1348, 1307, 1253, 1156, 1030, 816, 781, 753, 700; HRMS (APCI/ASAP, m/z): 502.2924 (calcd. C₂₈H₃₆N₇O₂, 502.2930 [M+H]⁺).

4.9.28 (S)-2-((6-(3-(((2-(Dimethylamino)ethyl)amino)methyl)-4-fluorophenyl)-7H-pyrrolo[2,3-d]pyrimidin-4-yl)amino)-2-phenylethan-1-ol (69)

Compound **69** was prepared as described in Section 4.6.4 starting with **25** (127 mg, 0.219 mmol). Purification by silica-gel column chromatography (CH₂Cl₂/MeOH/NH₃, 90/10/1, R_f = 0.28) gave 80 mg (0.180 mmol, 82 %) of a bright yellow solid, mp 159 - 161 °C; HPLC

purity: 98 %, $t_R = 18.4$ min; $[\alpha]_D^{20} = -196.1$ (c 0.50, DMSO); $^1\text{H NMR}$ (400 MHz, DMSO- d_6) δ : 12.01 (s, 1H), 8.05 (s, 1H), 7.89 - 7.87 (m, 1H), 7.74 - 7.67 (m, 2H), 7.44 - 7.43 (m, 2H), 7.32 - 7.26 (m, 3H), 7.24 - 7.19 (m, 2H), 7.10 (s, br, 1H), 5.44 - 5.39 (m, 1H), 4.99 - 4.95 (m, 1H), 3.78 (s, 2H), 3.76 - 3.72 (m, 2H), 2.62 (t, $J = 6.3$, 2H), 2.35 (t, $J = 6.3$, 2H), 2.11 (s, 6H); $^{13}\text{C NMR}$ (100 MHz, DMSO- d_6) δ : 159.7 (d, $J = 244.3$), 155.6, 151.7, 142.0, 132.8, 128.3 (d, $J = 14.3$), 128.1, 128.0 (2C), 127.0 (2C), 126.7, 126.6 (d, $J = 4.6$), 124.5 (d, $J = 8.7$), 115.6 (d, $J = 24.0$), 96.0, 74.0, 73.8, 65.0, 58.8, 46.4, 46.2, 45.4, 45.3 (2C); IR (neat, cm^{-1}): 3117, 2935, 2810, 2758, 1597, 1475, 1320, 1231, 1023, 816, 696; HRMS (APCI/ASAP, m/z): 449.2462 (calcd. $\text{C}_{25}\text{H}_{30}\text{N}_6\text{OF}$, 449.2465 $[\text{M}+\text{H}]^+$).

4.9.29 (*S*)-2-((6-(4-Fluoro-3-(hydroxymethyl)phenyl)-7*H*-pyrrolo[2,3-*d*]pyrimidin-4-yl)amino)-2-phenylethan-1-ol (70)

Compound **70** was prepared as described in Section 4.6.4 starting with **26** (75 mg, 0.148 mmol). Purification by silica-gel column chromatography ($\text{CH}_2\text{Cl}_2/\text{MeOH}$, 90/10, $R_f = 0.12$) gave 58 mg (0.154 mmol, 78 %) of a white solid, mp 148 - 149 °C; HPLC purity: 98 %, $t_R = 16.5$ min; $[\alpha]_D^{20} = -246.9$ (c 0.50, DMSO); $^1\text{H NMR}$ (400 MHz, DMSO- d_6) δ : 12.04 (s, 1H), 8.05 (s, 1H), 7.94 - 7.92 (m, 1H), 7.74 - 7.70 (m, 2H), 7.44 - 7.42 (m, 2H), 7.32 - 7.29 (m, 2H), 7.26 - 7.19 (m, 2H), 7.13 (s, br, 1H), 5.44 - 5.1 (m, 1H), 5.39 (t, $J = 5.6$, 1H), 4.95 (t, $J = 5.6$, 1H), 4.61 (d, $J = 5.6$, 2H), 3.78 - 3.69 (m, 2H); $^{13}\text{C NMR}$ (100 MHz, DMSO- d_6) δ : 157.6 (d, $J = 245.1$), 155.5, 151.7, 151.5, 142.0, 132.8, 129.8 (d, $J = 15.5$), 128.1 (d, $J = 3.6$), 128.0 (2C), 127.0 (2C), 126.7, 125.2 (d, $J = 4.9$), 124.4 (d, $J = 8.6$), 115.4 (d, $J = 21.9$), 115.3, 109.6, 104.2, 96.0, 65.0, 56.8 (d, $J = 3.5$), 56.1; IR (neat, cm^{-1}): 3408, 3205, 3133, 2935, 2883, 1596, 1482, 1304, 1231, 1029, 768, 696; HRMS (APCI/ASAP, m/z): 389.1971 (calcd. $\text{C}_{23}\text{H}_{25}\text{N}_4\text{O}_2$, 389.1964 $[\text{M}+\text{H}]^+$). The hydroxyl proton at 5.39 disappeared after D_2O exchange.

4.9.30 (*S*)-2-((6-(4-(((2-(Dimethylamino)ethyl)amino)methyl)-3-fluorophenyl)-7*H*-pyrrolo[2,3-*d*]pyrimidin-4-yl)amino)-2-phenylethan-1-ol (71)

Compound **71** was prepared as described in Section 4.6.4 starting with **27** (107 mg, 0.183 mmol). Purification by silica-gel column chromatography ($\text{CH}_2\text{Cl}_2/\text{MeOH}/\text{NH}_3$, 85/15/2, $R_f = 0.15$) gave 69 mg (0.154 mmol, 84 %) of a white solid, mp 201 - 202 °C; HPLC purity: 99 %, $t_R = 17.8$ min; $[\alpha]_D^{20} = -232.7$ (c 1.00, DMSO); $^1\text{H NMR}$ (600 MHz, DMSO- d_6) δ : 12.05 (s, 1H), 8.06 (s, 1H), 7.73 - 7.72 (m, 1H), 7.60 - 7.58 (m, 1H), 7.58 - 7.55 (m, 1H), 7.51 - 7.48 (m, 1H), 7.44 - 7.43 (m, 2H), 7.32 - 7.29 (m, 2H), 7.22 - 7.20 (m, 1H), 7.18 (s, br, 1H), 5.44 - 5.40 (m, 1H), 4.96 (s, br, 1H), 3.77 - 3.71 (m, 2H), 3.75 (s, 2H), 3.32 (s, br, 1H), 2.58 (t, $J = 6.4$, 2H), 2.33 (t, $J = 6.4$, 2H), 2.11 (s, 6H); $^{13}\text{C NMR}$ (150 MHz, DMSO- d_6) δ : 160.8 (d, $J = 243.1$), 155.7, 152.0, 151.5, 141.9, 132.4 (d, $J = 8.5$), 132.1 (d, $J = 2.2$), 130.9 (d, $J = 5.4$), 128.0 (2C), 127.0 (2C), 126.7, 126.4 (d, $J = 15.5$), 120.2 (d, $J = 3.3$), 110.8 (d, $J = 24.1$), 104.0 (d, $J = 5.5$), 96.9, 65.0, 58.8 (2C), 56.0, 46.2, 45.9 (d, $J = 2.2$), 45.3; IR (neat, cm^{-1}): 3299, 3122, 2935, 2835, 2816, 2764, 1595, 1478, 1444, 1304, 1133, 1029, 777, 701; HRMS (APCI/ASAP, m/z): 449.2460 (calcd. $\text{C}_{25}\text{H}_{30}\text{N}_6\text{OF}$, 449.2465 $[\text{M}+\text{H}]^+$).

4.9.31 (*S*)-2-((6-(3-Fluoro-4-(hydroxymethyl)phenyl)-7*H*-pyrrolo[2,3-*d*]pyrimidin-4-yl)amino)-2-phenylethan-1-ol (72)

Compound **72** was prepared as described in Section 4.6.4 starting with **28** (95 mg, 0.187 mmol). Purification by silica-gel column chromatography (CH₂Cl₂/MeOH, 90/10, R_f = 0.23) gave 67 mg (0.175 mmol, 89 %) of a white solid, mp 273 - 275 °C; HPLC purity: 98 %, t_R = 15.7 min; [α]_D²⁰ = -279.6 (c 1.00, DMSO); ¹H NMR (600 MHz, DMSO-*d*₆) δ: 12.06 (s, 1H), 8.07 (s, 1H), 7.73 - 7.72 (m, 1H), 7.63 - 7.61 (m, 1H), 7.57 - 7.55 (m, 1H), 7.54 - 7.51 (m, 1H), 7.44 - 7.43 (m, 2H), 7.32 - 7.29 (m, 2H), 7.22 - 7.20 (m, 1H), 7.18 (s, br, 1H), 5.44 - 5.41 (m, 1H), 5.28 (t, *J* = 5.8, 1H), 4.96 (t, *J* = 5.6, 1H), 4.56 (d, *J* = 5.6, 2H), 3.77 - 3.71 (m, 2H); ¹³C NMR (150 MHz, DMSO-*d*₆) δ: 160.0 (d, *J* = 243.5), 155.7, 152.0, 151.6, 141.9, 132.6 (d, *J* = 8.4), 132.1 (d, *J* = 1.9), 129.7 (d, *J* = 5.5), 128.0 (2C), 127.8 (d, *J* = 15.4), 127.0 (2C), 126.7, 120.3 (d, *J* = 2.0), 110.7 (d, *J* = 23.5), 104.0, 97.0, 65.0, 56.6 (d, *J* = 3.3), 56.0; IR (neat, cm⁻¹): 3303, 3116, 3023, 2940, 2878, 1594, 1470, 1320, 1153, 994, 966, 868, 764, 700; HRMS (APCI/ASAP, m/z): 379.1570 (calcd. C₂₁H₂₀N₄O₂F, 379.1570 [M+H]⁺). The hydroxyl proton at 5.28 disappeared after D₂O exchange.

4.9.32 (*S*)-2-((6-(4-(((2-(Dimethylamino)ethyl)(methyl)amino)methyl)-2-methoxyphenyl)-7*H*-pyrrolo[2,3-*d*]pyrimidin-4-yl)amino)-2-phenylethan-1-ol (73)

Compound **73** was prepared as described in Section 4.6.4 starting with **29** (93 mg, 0.154 mmol). Purification by silica-gel column chromatography (CH₂Cl₂/MeOH/NH₃, 90/10/1, R_f = 0.09) gave 74 mg (0.156 mmol, 81 %) of a yellow solid, mp 116 - 118 °C; HPLC purity: 99 %; t_R = 17.5 min; [α]_D²⁰ = -234.6 (c 0.50, DMSO); ¹H NMR (400 MHz, DMSO-*d*₆) δ: 11.63 - 11.62 (m, 1H), 8.03 (s, 1H), 7.72 - 7.68 (m, 2H), 7.45 - 7.43 (m, 2H), 7.32 - 7.30 (m, 2H), 7.23 - 7.18 (m, 2H), 7.07 (s, 1H), 6.96 - 6.93 (m, 1H), 5.45 - 5.40 (m, 1H), 4.98 - 4.95 (m, 1H), 3.93 (s, 3H), 3.80 - 3.69 (m, 2H), 3.51 (s, 2H), 2.47 - 2.37 (m, 4H), 2.19 (s, 3H), 2.14 (s, 6H); ¹³C NMR (100 MHz, DMSO-*d*₆) δ: 156.0, 155.5, 151.4, 150.7, 142.1, 139.9, 130.1, 128.0 (2C), 127.1 (2C), 126.9, 126.6, 122.2, 120.8, 118.9, 111.8, 99.7, 65.0, 61.7, 58.3, 57.1, 55.5, 54.8, 45.6 (2C), 42.4; IR (neat, cm⁻¹): 3100, 2939, 2824, 2772, 1590, 1446, 1305, 1253, 1159, 1034, 780, 753, 696; HRMS (APCI/ASAP, m/z): 475.2823 (calcd. C₂₇H₃₅N₆O₂, 475.2821 [M+H]⁺).

4.9.33 (*S*)-(3-Methoxy-4-(4-((2-methoxy-1-phenylethyl)amino)-7*H*-pyrrolo[2,3-*d*]pyrimidin-6-yl)phenyl)methanol (74)

Compound **74** was prepared as described in Section 4.6.2, starting with **7d** (220 mg, 0.560 mmol) and (4-formyl-2-methoxyphenyl)boronic acid (121 mg, 0.670 mmol). Purification by silica-gel column chromatography (diethyl ether/MeOH, 19/1, R_f = 0.31) gave 107 mg (0.270 mmol, 49 %) of (*S*)-3-methoxy-4-(4-((2-methoxy-1-phenylethyl)amino)-7*H*-pyrrolo[2,3-*d*]pyrimidin-6-yl)benzaldehyde as a pale green solid, mp 185 - 187 °C; HPLC

purity: 99 %, $t_R = 20.3$ min; $[\alpha]_D^{20} = -318.6$ (c 0.80, DMSO); ^1H NMR (600 MHz, DMSO- d_6) δ : 11.06 (s, 1H), 9.97 (s, 1H), 8.30 (s, 1H), 7.90 - 7.89 (m, 1H), 7.53 - 7.52 (m, 1H), 7.52 (m, 1H), 7.47 - 7.46 (m, 2H), 7.36 - 7.34 (m, 2H), 7.28 - 7.26 (m, 1H), 6.95 (s, 1H), 5.65 - 5.64 (m, 1H), 4.02 (s, 3H), 3.87 - 3.83 (m, 2H), 3.41 (s, 3H); ^{13}C NMR (150 MHz, DMSO- d_6) δ : 191.3, 156.3, 156.0, 152.9, 151.3, 140.6, 136.3, 131.0, 128.7 (2C), 127.8, 127.6, 126.8, (2C), 126.2, 124.7, 110.7, 104.0, 99.2, 75.8, 59.3, 56.2, 54.1; IR (neat, cm^{-1}): 3117, 2826, 2360, 1682, 1592, 1474, 1309, 1146, 1031, 784, 700; HRMS (APCI/ASAP, m/z): 403.1767 (calcd. $\text{C}_{23}\text{H}_{22}\text{N}_4\text{O}_3$, 403.1770 $[\text{M}+\text{H}]^+$). Aldehyde reduction was performed as described in Section 4.8.34 and the product was purified by silica-gel column chromatography (THF/Et₂O, 1/1, $R_f = 0.24$). This gave 73 mg (0.180 mmol, 75 %) of **74** as a yellow solid, mp 203 - 204 °C; HPLC purity: 98 %, $t_R = 17.8$ min; $[\alpha]_D^{20} = -216.3$ (c 1.00, DMSO); ^1H NMR (600 MHz, DMSO- d_6) δ : 10.23 (s, 1H), 8.25 (s, 1H), 7.68 - 7.66 (m, 1H), 7.47 - 7.45 (m, 2H), 7.36 - 7.33 (m, 2H), 7.28 - 7.25 (m, 1H), 7.05 (s, 1H), 7.01 - 7.00 (m, 1H), 6.72 (s, 1H), 5.91 (s, 1H), 5.62 - 5.60 (m, 1H), 4.73 (s, 2H), 3.98 (s, 3H), 3.86 - 3.82 (m, 2H), 3.41 (s, 3H); ^{13}C NMR (150 MHz, DMSO- d_6) δ : 156.1, 155.6, 151.9, 150.5, 142.3, 140.7, 132.5, 128.7 (2C), 127.7, 127.6, 126.9 (2C), 119.9, 119.0, 110.5, 108.1, 103.7, 75.9, 65.1, 59.3, 55.9, 54.1; IR (neat, cm^{-1}): 3423, 3169, 2873, 1604, 1474, 1319, 1159, 1035, 997, 777, 670; HRMS (APCI/ASAP, m/z): 405.1923 (calcd. $\text{C}_{23}\text{H}_{25}\text{N}_4\text{O}_3$, 405.1927 $[\text{M}+\text{H}]^+$). The hydroxyl proton at 5.91 ppm disappeared after D₂O exchange.

4.9.34 (*S*)-6-(2-(Difluoromethoxy)phenyl)-*N*-(2-methoxy-1-phenylethyl)-7*H*-pyrrolo[2,3-*d*]pyrimidin-4-amine (**75**)

Compound **75** was prepared as described in Section 4.6.2, starting with **7d** (92 mg, 0.230 mmol) and 2-(2-(difluoromethoxy)phenyl)-4,4,5,5-tetramethyl-1,3,2-dioxaborolane (**9**) (320 mg, 0.119 mmol). The reaction time was 1 hour. Purification by silica-gel column chromatography (EtOAc/*n*-pentane, 5/1, $R_f = 0.19$) gave 62 mg (0.150 mmol, 64 %) of a pale brown solid, mp 95 - 97 °C; HPLC purity: 99 %, $t_R = 21.8$ min; $[\alpha]_D^{20} = -212.0$ (c 0.90, DMSO); ^1H NMR (600 MHz, DMSO- d_6) δ : 11.89 (s, 1H), 8.10 (s, 1H), 7.98 (d, $J = 8.3$, 1H), 7.83 - 7.82 (m, 1H), 7.48 - 7.46 (m, 2H), 7.40 - 7.37 (m, 1H), 7.35 - 7.30 (m, 4H), 7.27 (t, $J = 73.7$, 1H), 7.24 - 7.22 (m, 1H), 7.20 (s, 1H), 5.59 - 5.68 (m, 1H), 3.78 - 3.75 (m, 1H), 3.65 - 3.62 (m, 1H), 3.31 (s, 3H); ^{13}C NMR (150 MHz, DMSO- d_6) δ : 155.6, 151.9, 151.1, 147.7, 141.3, 128.7, 128.5, 128.4, 128.2 (2C), 127.0 (2C), 126.9, 125.5, 123.6, 119.0, 116.7 (t, $J = 258.1$), 103.8, 100.7, 75.0, 58.0, 52.7; ^{19}F NMR (564 MHz, DMSO- d_6) δ : -83.1 (d, $J = 73.1$); IR (neat, cm^{-1}): 3325, 3106, 2826, 1592, 1477, 1311, 1104, 1035, 751, 698; HRMS (APCI/ASAP, m/z): 411.1634 (calcd. $\text{C}_{22}\text{H}_{21}\text{N}_4\text{O}_2\text{F}_2$, 411.1633 $[\text{M}+\text{H}]^+$).

4.9.35 (*R*)-3-Phenyl-3-((6-phenyl-7*H*-pyrrolo[2,3-*d*]pyrimidin-4-yl)amino)propan-1-ol (**76**)

Compound **76** was prepared as described in Section 4.6.1, starting with 4-chloro-6-phenyl-7*H*-pyrrolo[2,3-*d*]pyrimidine [19] (50 mg, 0.218 mmol) and (*R*)-3-amino-3-phenylpropan-

1-ol (99 mg, 0.653 mmol). The reaction time was 28 hours. Purification by silica-gel column chromatography (EtOAc/MeOH, 95/5, R_f = 0.18) gave 68 mg (0.198 mmol, 91 %) of a white solid, mp 208 - 209 °C; HPLC purity: 98 %, t_R = 18.6 min; $[\alpha]_D^{20}$ = -289.4 (c 1.00, DMSO); ^1H NMR (400 MHz, DMSO- d_6) δ : 12.02 (s, 1H), 8.05 (s, 1H), 7.80 - 7.77 (m, 3H), 7.46 - 7.42 (m, 4H), 7.32 - 7.28 (m, 3H), 7.21 - 7.17 (m, 1H), 7.09 (s, br, 1H), 5.52 - 5.47 (m, 1H), 4.58 - 4.56 (m, 1H), 3.54 - 3.42 (m, 2H), 2.12 - 2.03 (m, 1H), 1.98 - 1.91 (m, 1H); ^{13}C NMR (100 MHz, DMSO- d_6) δ : 155.4, 151.7, 151.5, 144.7, 133.4, 131.8, 128.9 (2C), 128.1 (2C), 127.2, 126.5 (2C), 126.4, 124.5 (2C), 103.9, 96.0, 57.9, 50.4, 39.8; IR (neat, cm^{-1}): 3337, 3125, 3026, 2922, 1597, 1522, 1452, 1319, 1033. 787, 748, 702; HRMS (APCI/ASAP, m/z): 344.1634 (calcd. $\text{C}_{21}\text{H}_{20}\text{N}_4\text{O}$, 344.1637 $[\text{M}]^+$). The hydroxyl proton at 4.58 - 4.56 ppm disappeared after D_2O exchange.

4.9.36 (*R*)-3-((6-(2-Ethoxyphenyl)-7*H*-pyrrolo[2,3-*d*]pyrimidin-4-yl)amino)-3-phenylpropan-1-ol (77)

Compound **77** was prepared as described in Section 4.6.4 starting with **30** (97 mg, 0.187 mmol). Purification by silica-gel column chromatography ($\text{CH}_2\text{Cl}_2/\text{MeOH}$, 90/10, R_f = 0.38) gave 72 mg (0.186 mmol, 97 %) of a white solid, mp 116 - 117 °C; HPLC purity: 98 %, t_R = 21.0 min; $[\alpha]_D^{20}$ = -151.9 (c 1.00, DMSO); ^1H NMR (400 MHz, $\text{CDCl}_3\text{-TMS}$) δ : 10.23 (s, 1H), 8.33 (1H), 7.72 - 7.70 (m, 1H), 7.47 - 7.38 (m, 4H), 7.35 - 7.25 (m, 3H), 7.04 - 7.00 (m, 2H), 6.65 - 6.64 (m, 1H), 5.66 - 5.60 (m, 1H), 5.24 - 5.23 (m, 1H), 4.24 (q, J = 7.0, 2H), 3.79 - 3.69 (m, 2H), 2.33 - 2.25 (m, 1H), 2.05 - 1.98 (m, 1H), 1.56 (t, J = 7.0, 3H); ^{13}C NMR (100 MHz, $\text{CDCl}_3\text{-TMS}$) δ : 155.8, 155.2, 151.8, 150.3, 142.6, 133.3, 129.3, 129.2 (2C), 127.9, 127.8, 126.9 (2C), 121.6, 119.6, 113.3, 103.7, 95.0, 64.7, 58.4, 51.8, 39.6, 15.1; IR (neat, cm^{-1}): 3107, 2971, 2925, 2862, 1593, 1465, 1450, 1309, 1236, 1122, 1034, 748, 699; HRMS (APCI/ASAP, m/z): 389.1971 (calcd. $\text{C}_{23}\text{H}_{25}\text{N}_4\text{O}_2$, 389.1964 $[\text{M}+\text{H}]^+$). The hydroxyl proton at 5.24-5.23 ppm disappeared after D_2O exchange.

4.9.37 (*S*)-2-((7-Methyl-6-phenyl-7*H*-pyrrolo[2,3-*d*]pyrimidin-4-yl)amino)-2-phenylethan-1-ol (78)

4-Chloro-6-phenyl-7*H*-pyrrolo[2,3-*d*]pyrimidine [**19**] (150 mg, 0.653 mmol) and cesium carbonate (319 mg, 0.980 mmol) were dissolved in anhydrous DMF (2 mL). Iodomethane (0.65 mL, 1.31 mmol, 2 M in *tert*-butyl methyl ether) was added over 30 min and the solution stirred at room temperature for 90 min. The reaction mixture was then quenched with H_2O (50 mL), and extracted with EtOAc (2 \times 30 mL). The combined organic phases were washed with saturated aq NaHCO_3 (15 mL), saturated aq NaCl (20 mL), dried over anhydrous Na_2SO_4 , filtered and concentrated *in vacuo*. Purification by silica-gel column chromatography (EtOAc/*n*-pentane, 1/1, R_f = 0.46). This gave 143 mg (0.587 mmol, 90 %) of 4-chloro-7-methyl-6-phenyl-7*H*-pyrrolo[2,3-*d*]pyrimidine as a white solid, mp 150 - 152 °C (lit.[57] 151 - 153 °C); ^1H NMR (400 MHz, DMSO- d_6) δ : 8.68 (s, 1H), 7.74 - 7.71 (m, 2H), 7.60 - 7.54 (m, 3H), 6.79 (s, 1H), 3.84 (s, 3H); ^1H NMR data are in agreement with

those previously reported [57]. Compound **78** was then made as described in Section 4.6.1, starting with 4-chloro-7-methyl-6-phenyl-7*H*-pyrrolo[2,3-*d*]pyrimidine (120 mg, 0.492 mmol) and (*S*)-2-amino-2-phenylethan-1-ol (203 mg, 1.48 mmol). The reaction time was 26 hours. The crude product was purified by silica-gel column chromatography (EtOAc, $R_f = 0.13$). This gave 150 mg (0.436 mmol, 88 %) of **78** as a white solid. mp 133 - 135 °C; HPLC purity: 99 %, $t_R = 19.9$ min; $[\alpha]_D^{20} = -227.3$ (c 0.99, DMSO); ^1H NMR (400 MHz, DMSO- d_6) δ : 8.12 (s, 1H), 7.77 - 7.75 (m, 1H), 7.61 - 7.59 (m, 2H), 7.54 - 7.50 (m, 2H), 7.45 - 7.42 (m, 3H), 7.32 - 7.28 (m, 2H), 7.22 - 7.19 (m, 1H), 6.86 (s, br, 1H), 5.46 - 5.41 (m, 1H), 4.97 - 4.94 (m, 1H), 3.76 - 3.72 (m, 2H), 3.70 (s, 3H); ^{13}C NMR (100 MHz, DMSO- d_6) δ : 155.6, 151.4, 150.9, 141.9, 136.5, 131.9, 128.8 (2C), 128.4 (2C), 128.0 (2C), 127.9, 127.0 (2C), 126.6, 101.7, 98.4, 64.9, 56.1, 29.6; IR (neat, cm^{-1}): 3288, 3026, 2913, 1724, 1596, 1471, 1306, 1070, 757, 698; HRMS (APCI/ASAP, m/z): 345.1714 (calcd. $\text{C}_{21}\text{H}_{21}\text{N}_4\text{O}$, 345.1715 $[\text{M}+\text{H}]^+$).

4.10 Docking and dynamics

The X-ray crystal structures of the protein 4WKQ (Wild-type EGFR) [35] were prepared using the protein preparation wizard, which is part of the Maestro software package (Maestro, v8.5; Schrödinger, LLC, New York, NY, USA) using the OPLS-3 force field. The resulting protein structures were used in the following docking study. Ligands were drawn using ChemBioDraw (ChemBioDraw Ultra 13.0, CambridgeSoft, PerkinElmer) or the Maestro 2D Sketcher tool and were prepared using LigPrep2.2 (LigPrep, v2.2; Schrödinger, LLC). For the computational investigation of the receptor-inhibitor structures, the energy minimized structures of 4WKQ and ligands were subsequently docked using induced-fit docking (IFD) of Schrödinger [32-34]. Briefly this was achieved by doing an initial docking for each ligand using Glide and a softened potential (van der Waals radii scaling). A maximum of 20 poses per ligand were retained. Side-chain prediction for each protein-ligand complex on residues within 5 Å of the ligands were then calculated using Prime and the same set of ligands and residues were subsequently minimized using Prime minimization. Finally, the ligands within a specified energy from the lowest-energy structure (30 kcal/mol) were redocked on the modified receptor structure using default Glide settings. The resulting docked poses were analysed using Glide pose viewer tool. For dynamic simulation, the best poses from docking were used as starting points when building the model systems. Dynamic simulations were conducted for 10 ns simulation time using Maestros Desmond suite [36], the OPLS-3 force field and a TIP4P solvent model. Briefly, this was performed by putting the docked protein-ligand complex inside a minimized solvent box and adding ions (Na^+ or Cl^-) in order to have an electrical neutral system. Finally, NaCl was added to a total concentration of 0.15 M, which is approximately the physiological concentration of monovalent ions. This gave normally a system of approximately 39 000 atoms. Molecular dynamics were then calculated on these systems using the isothermal-isobaric (NPT) ensemble at 300K and 1.01325 bar. Trajectory analysis were performed using Desmond's Simulation Interactions Diagram tool and all the

graphical pictures were made using Maestro or Pymol (The PyMOL Molecular Graphics System, Version 1.8 Schrödinger, LLC).

4.11 Conformational search

Compounds **50**, **53** and **77** were subjected to a conformational search using MacroModel, version 11.3, Schrödinger, LLC, New York, NY, 2016. Conformations in water were calculated using the OPLS3 force field.

Acknowledgements

Susana Villa Gonzalez is thanked for the HRMS experiments. Roger Aarvik and Steffen Bugge are acknowledged for their kind help and support. Prof. Dr. Justus Duyster and Dr. Nikolas von Bubnoff, Technical University of Munich, Munich, Germany kindly provided EGFR Ba/F3 cells. The research was financially supported by Anders Jahres foundation and Technology Transfer Office (TTO-NTNU Trondheim). NOTUR is acknowledged for CPU-time.

Author Contributions

The synthetic work was mainly performed by J. Han and some compounds were synthesised by S. Henriksen. Molecular docking and dynamics performed by E. Sundby. The Ba/F3 cellular experiments were performed by K. Nørsett. J. Han and B. Hoff planed the work and wrote the paper.

Supplementary Material: This file contains *in vitro* kinase data with standard deviations, kinase selectivity data, EGFR-ligand interactions maps following dynamics and selected NMR spectra. The material is available free of charge.

5. References

- [1] W. Pao, J. Chmielecki, Rational, biologically based treatment of EGFR-mutant non-small-cell lung cancer, *Nat. Rev. Cancer*, 10 (2010) 760-774.
- [2] H.J. Lee, A.N. Seo, E.J. Kim, M.H. Jang, Y.J. Kim, J.H. Kim, S.W. Kim, H.S. Ryu, I.A. Park, S.A. Im, G. Gong, K.H. Jung, H.J. Kim, S.Y. Park, Prognostic and predictive values of EGFR overexpression and EGFR copy number alteration in HER2-positive breast cancer, *Br. J. Cancer*, 112 (2015) 103-111.

- [3] M.R. Brewer, C.H. Yun, D. Lai, M.A. Lemmon, M.J. Eck, W. Pao, Mechanism for activation of mutated epidermal growth factor receptors in lung cancer, *Proc. Natl. Acad. Sci. U. S. A.*, 110 (2013) E3595-E3604.
- [4] N. Cook, K.K. Frese, M. Moore, Assessing the role of the EGF receptor in the development and progression of pancreatic cancer, *Gastrointest. Cancer: Targets Ther.*, 4 (2014) 23-37.
- [5] D.R. Siwak, M. Carey, B.T. Hennessy, C.T. Nguyen, M.J. McGahren Murray, L. Nolden, G.B. Mills, Targeting the epidermal growth factor receptor in epithelial ovarian cancer: current knowledge and future challenges, *J. Oncol.*, 2010 (2010) Article ID 568938.
- [6] T. Zellweger, C. Ninck, M. Bloch, M. Mirlacher, P.A. Koivisto, H.J. Helin, M.J. Mihatsch, T.C. Gasser, L. Bubendorf, Expression patterns of potential therapeutic targets in prostate cancer, *Int. J. Cancer*, 113 (2005) 619-628.
- [7] F.J. Hendler, B.W. Ozanne, Human squamous cell lung cancers express increased epidermal growth factor receptors, *J. Clin. Invest.*, 74 (1984) 647-651.
- [8] D. Schuster, C. Laggner, T. Langer, Why drugs fail - a study on side effects in new chemical entities, *Curr. Pharm. Des.*, 11 (2005) 3545-3559.
- [9] M.D. Segall, A.P. Beresford, J.M.R. Gola, D. Hawksley, M.H. Tarbit, Focus on success: using a probabilistic approach to achieve an optimal balance of compound properties in drug discovery, *Expert Opin. Drug Metab. Toxicol.*, 2 (2006) 325-337.
- [10] A.L. Gill, M. Verdonk, R.G. Boyle, R. Taylor, A comparison of physicochemical property profiles of marketed oral drugs and orally bioavailable anti-cancer protein kinase inhibitors in clinical development, *Curr. Top. Med. Chem.*, 7 (2007) 1408-1422.
- [11] Z. O'Brien, M. Fallah Moghaddam, Small molecule kinase inhibitors approved by the FDA from 2000 to 2011: a systematic review of preclinical ADME data, *Expert Opin. Drug Metab. Toxicol.*, 9 (2013) 1597-1612.
- [12] N.A. Meanwell, Improving Drug Candidates by Design: A Focus on Physicochemical Properties As a Means of Improving Compound Disposition and Safety, *Chem. Res. Toxicol.*, 24 (2011) 1420-1456.
- [13] J. Bain, L. Plater, M. Elliott, N. Shpiro, C.J. Hastie, H. McLauchlan, I. Klevernic, J.S. Arthur, D.R. Alessi, P. Cohen, The selectivity of protein kinase inhibitors: a further update, *Biochem. J.*, 408 (2007) 297-315.
- [14] D. Kitagawa, K. Yokota, M. Gouda, Y. Narumi, H. Ohmoto, E. Nishiwaki, K. Akita, Y. Kirii, Activity-based kinase profiling of approved tyrosine kinase inhibitors, *Genes Cells*, 18 (2013) 110-122.
- [15] N. Yamamoto, M. Honma, H. Suzuki, Off-target serine/threonine kinase 10 inhibition by erlotinib enhances lymphocytic activity leading to severe skin disorders, *Mol. Pharmacol.*, 80 (2011) 466-475.
- [16] T. Schneider-Merck, M. Trepel, Lapatinib, *Recent Results Cancer Res.*, 184 (2010) 45-59.
- [17] P. Marathe, Y. Tang, B. Slecicka, D. Rodrigues, A. Gavai, T. Wong, L. Christopher, H. Zhang, Preclinical pharmacokinetics and in vitro metabolism of BMS-690514, a potent inhibitor of EGFR and VEGFR2, *J. Pharm. Sci.*, 99 (2010) 3579-3593.
- [18] J. Ling, K.A. Johnson, Z. Miao, A. Rakhit, M.P. Pantze, M. Hamilton, B.L. Lum, C. Prakash, Metabolism and excretion of erlotinib, a small molecule inhibitor of epidermal growth factor receptor tyrosine kinase, in healthy male volunteers, *Drug Metab. Dispos.*, 34 (2006) 420-426.
- [19] S.J. Kaspersen, C. Sørum, V. Willassen, E. Fuglseth, E. Kjøbli, G. Bjørkøy, E. Sundby, B.H. Hoff, Synthesis and in vitro EGFR (ErbB1) tyrosine kinase inhibitory activity of 4-N-substituted 6-aryl-7H-pyrrolo[2,3-d]pyrimidine-4-amines, *Eur. J. Med. Chem.*, 46 (2011) 6002-6014.

- [20] S.J. Kaspersen, J. Han, K.G. Nørsett, L. Rydså, E.B. Kjøbli, S., G. Bjørkøy, E. Sundby, B.H. Hoff, Identification of new 4-*N*-substituted 6-aryl-7*H*-pyrrolo[2,3-*d*]pyrimidine-4-amines as highly potent EGFR-TK inhibitors with Src-family activity, *Eur. J. Pharm. Sci.*, 59 (2014) 69-82.
- [21] E. Sundby, J. Han, S.J. Kaspersen, B.H. Hoff, *In vitro* baselining of new pyrrolopyrimidine EGFR-TK inhibitors with Erlotinib, *Eur. J. Pharm. Sci.*, 80 (2015) 56-65.
- [22] P. Traxler, Tyrosine kinases as targets in cancer therapy - successes and failures, *Expert Opin. Ther. Targets*, 7 (2003) 215-234.
- [23] P. Traxler, P.R. Allegrini, R. Brandt, J. Brueggen, R. Cozens, D. Fabbro, K. Grosios, H.A. Lane, P. McSheehy, J. Mestan, T. Meyer, C. Tang, M. Wartmann, J. Wood, G. Caravatti, AEE788: A Dual Family Epidermal Growth Factor Receptor/ErbB2 and Vascular Endothelial Growth Factor Receptor Tyrosine Kinase Inhibitor with Antitumor and Antiangiogenic Activity, *Cancer Res.*, 64 (2004) 4931-4941.
- [24] Y.W. Park, M.N. Younes, S.A. Jasser, O.G. Yigitbasi, G. Zhou, C.D. Bucana, B.N. Bekele, J.N. Myers, AEE788, a dual tyrosine kinase receptor inhibitor, induces endothelial cell apoptosis in human cutaneous squamous cell carcinoma xenografts in nude mice, *Clin. Cancer Res.*, 11 (2005) 1963-1973.
- [25] P. LoRusso, K. Venkatakrishnan, E.G. Chiorean, D. Noe, J.T. Wu, S. Sankoh, M. Corvez, E.A. Sausville, Phase 1 dose-escalation, pharmacokinetic, and cerebrospinal fluid distribution study of TAK-285, an investigational inhibitor of EGFR and HER2, *Invest. New Drugs*, 32 (2014) 160-170.
- [26] T. Doi, H. Takiuchi, A. Ohtsu, N. Fuse, M. Goto, M. Yoshida, N. Dote, Y. Kuze, F. Jinno, M. Fujimoto, T. Takubo, N. Nakayama, R. Tsutsumi, Phase I first-in-human study of TAK-285, a novel investigational dual HER2/EGFR inhibitor, in cancer patients, *Br. J. Cancer*, 106 (2012) 666-672.
- [27] K.L. Billingsley, S.L. Buchwald, An Improved System for the Palladium-Catalyzed Borylation of Aryl Halides with Pinacol Borane, *J. Org. Chem.*, 73 (2008) 5589-5591.
- [28] J.D. Dunitz, Win some, lose some: enthalpy-entropy compensation in weak intermolecular interactions, *Chem. Biol.*, 2 (1995) 709-712.
- [29] C. Krintel, P. Francotte, D.S. Pickering, L. Juknaite, J. Poehlsgaard, L. Olsen, K. Frydenvang, E. Goffin, B. Pirotte, J.S. Kastrop, Enthalpy-entropy compensation in the binding of modulators at ionotropic glutamate receptor GluA2, *Biophys. J.*, 110 (2016) 2397-2406.
- [30] P.V. Desai, T.J. Raub, M.-J. Blanco, How hydrogen bonds impact P-glycoprotein transport and permeability, *Bioorg. Med. Chem. Lett.*, 22 (2012) 6540-6548.
- [31] S. Bugge, I.U. Moen, K.O. Kragseth Sylte, E. Sundby, B.H. Hoff, Truncated structures used in search for new lead compounds and in a retrospective analysis of thienopyrimidine-based EGFR inhibitors, *Eur. J. Med. Chem.*, 94 (2015) 175-194.
- [32] Induced fit docking protocol 2013-3, Glide version 6.1, Prime version 3.4, Schrödinger, LLC, New York, NY, (2013).
- [33] W. Sherman, H.S. Beard, R. Farid, Use of an induced fit receptor structure in virtual screening, *Chem. Biol. Drug Des.*, 67 (2006) 83-84.
- [34] W. Sherman, T. Day, M.P. Jacobson, R.A. Friesner, R. Farid, Novel Procedure for Modeling Ligand/Receptor Induced Fit Effects, *J. Med. Chem.*, 49 (2006) 534-553.
- [35] Y. Yosaatmadja, C.J. Squire, M. McKeage, J.U. Flanagan, 4WKQ: 1.85 angstrom structure of EGFR kinase domain with gefitinib, To be published: DOI: 10.2210/pdb4wkq/pdb, (2014).
- [36] v. Desmond Molecular Dynamics System, D. E. Shaw Research, Maestro-Desmond Interoperability Tools, version 3.9, Schrödinger, New York, NY, 2014.

- [37] Y. Kawakita, K. Miwa, M. Seto, H. Banno, Y. Ohta, T. Tamura, T. Yusa, H. Miki, H. Kamiguchi, Y. Ikeda, T. Tanaka, K. Kamiyama, T. Ishikawa, Design and synthesis of pyrrolo[3,2-d]pyrimidine HER2/EGFR dual inhibitors: Improvement of the physicochemical and pharmacokinetic profiles for potent in vivo anti-tumor efficacy, *Bioorg. Med. Chem*, 20 (2012) 6171-6180.
- [38] M. Falasca, K.J. Linton, Investigational ABC transporter inhibitors, *Expert Opin. Invest. Drugs*, 21 (2012) 657-666.
- [39] G. Szakacs, J.P. Annereau, S. Lababidi, U. Shankavaram, A. Arciello, K.J. Bussey, W. Reinhold, Y. Guo, G.D. Kruh, M. Reimers, J.N. Weinstein, M.M. Gottesman, Predicting drug sensitivity and resistance: Profiling ABC transporter genes in cancer cells, *Cancer Cell*, 6 (2004) 129-137.
- [40] H. Xie, L. Zeng, S. Zeng, X. Lu, G. Zhang, X. Zhao, N. Cheng, Z. Tu, Z. Li, H. Xu, L. Yang, X. Zhang, M. Huang, J. Zhao, W. Hu, Novel pyrrolopyrimidine analogues as potent dipeptidyl peptidase IV inhibitors based on pharmacokinetic property-driven optimization, *Eur. J. Med. Chem*, 52 (2012) 205-212.
- [41] J.P. Hughes, S. Rees, S.B. Kalindjian, K.L. Philpott, Principles of early drug discovery, *Br. J. Pharmacol*, 162 (2011) 1239-1249.
- [42] L. Shao, M.C. Hewitt, The kinetic isotope effect in the search for deuterated drugs, *Drug News Perspect.*, 23 (2010) 398-404.
- [43] R.A. Hartz, V.T. Ahuja, X. Zhuo, R.J. Mattson, D.J. Denhart, J.A. Deskus, V.M. Vrudhula, S. Pan, J.L. Ditta, Y.-Z. Shu, J.E. Grace, K.A. Lentz, S. Lelas, Y.-W. Li, T.F. Molski, S. Krishnananthan, H. Wong, J. Qian-Cutrone, R. Schartman, R. Denton, N.J. Lodge, R. Zaczek, J.E. Macor, J.J. Bronson, A Strategy to Minimize Reactive Metabolite Formation: Discovery of (S)-4-(1-Cyclopropyl-2-methoxyethyl)-6-[6-(difluoromethoxy)-2,5-dimethylpyridin-3-ylamino]-5-oxo-4,5-dihydropyrazine-2-carbonitrile as a Potent, Orally Bioavailable Corticotropin-Releasing Factor-1 Receptor Antagonist, *J. Med. Chem.*, 52 (2009) 7653-7668.
- [44] D.J. St.Jean, C. Fotsch, Mitigating Heterocycle Metabolism in Drug Discovery, *J. Med. Chem*, 55 (2012) 6002-6020.
- [45] A.K. Mandagere, T.N. Thompson, K.-K. Hwang, Graphical Model for Estimating Oral Bioavailability of Drugs in Humans and Other Species from Their Caco-2 Permeability and in Vitro Liver Enzyme Metabolic Stability Rates, *J. Med. Chem.*, 45 (2002) 304-311.
- [46] X. Liu, M. Wright, C.E.C.A. Hop, Rational Use of Plasma Protein and Tissue Binding Data in Drug Design, *J. Med. Chem*, 57 (2014) 8238-8248.
- [47] P.P. Graczyk, Gini Coefficient: A New Way To Express Selectivity of Kinase Inhibitors against a Family of Kinases, *J. Med. Chem*, 50 (2007) 5773-5779.
- [48] M.W. Karaman, S. Herrgard, D.K. Treiber, P. Gallant, C.E. Atteridge, B.T. Campbell, K.W. Chan, P. Ciceri, M.I. Davis, P.T. Edeen, R. Faraoni, M. Floyd, J.P. Hunt, D.J. Lockhart, Z.V. Milanov, M.J. Morrison, G. Pallares, H.K. Patel, S. Pritchard, L.M. Wodicka, P.P. Zarrinkar, A quantitative analysis of kinase inhibitor selectivity, *Nat. Biotechnol.*, 26 (2008) 127-132.
- [49] J. Han, S.J. Kaspersen, S. Nervik, K.G. Nørsett, E. Sundby, B.H. Hoff, Chiral 6-aryl-furo[2,3-d]pyrimidin-4-amines as EGFR inhibitors, *Eur. J. Med. Chem*, 119 (2016) 2778-2799.
- [50] A. Cavazzoni, R.R. Alfieri, D. Cretella, F. Saccani, L. Ampollini, M. Galetti, F. Quaini, G. Graiani, D. Madeddu, P. Mozzoni, E. Galvani, S. La Monica, M. Bonelli, C. Fumarola, A. Mutti, P. Carbognani, M. Tiseo, E. Barocelli, P.G. Petronini, A. Ardizzoni, Combined use of anti-ErbB monoclonal antibodies and erlotinib enhances antibody-dependent cellular cytotoxicity of wild-type erlotinib-sensitive NSCLC cell lines, *Mol. Cancer*, 11 (2012) 91.

- [51] M. Eiblmaier, L.A. Meyer, M.A. Watson, P.M. Fracasso, L.J. Pike, C.J. Anderson, Correlating EGFR expression with receptor-binding properties and internalization of ⁶⁴Cu-DOTA-cetuximab in 5 cervical cancer cell lines, *J. Nucl. Med.*, 49 (2008) 1472-1479.
- [52] D.T. Hendricks, R. Taylor, M. Reed, M.J. Birrer, FHIT gene expression in human ovarian, endometrial, and cervical cancer cell lines, *Cancer Res.*, 57 (1997) 2112-2115.
- [53] M. Scheffner, K. Munger, J.C. Byrne, P.M. Howley, The state of the p53 and retinoblastoma genes in human cervical carcinoma cell lines, *Proc. Natl. Acad. Sci. U. S. A.*, 88 (1991) 5523-5527.
- [54] S. Bugge, S.J. Kaspersen, S. Larsen, U. Nonstad, G. Bjørkøy, E. Sundby, B.H. Hoff, Structure-activity study leading to identification of a highly active thienopyrimidine based EGFR inhibitor, *Eur. J. Med. Chem.*, 75 (2014) 354-374.
- [55] B.A. Pollok, B.D. Hamman, S.M. Rodems, L.R. Makings, Optical probes and assays, WO 2000066766 A1, (2000).
- [56] K.E. Frank, A. Burchat, P. Cox, D.C. Ihle, K.D. Mullen, G. Somal, A. Vasudevan, L. Wang, N.S. Wilson, Preparation of tricyclic compounds for the treatment of immunological and oncological conditions, WO2012149280A2, (2012).
- [57] V. Prieur, J. Rubio-Martinez, M. Font-Bardia, G. Guillaumet, M.D. Pujol, Microwave-Assisted Synthesis of Substituted Pyrrolo[2,3-d]pyrimidines, *Eur. J. Org. Chem.*, 2014 (2014) 1514-1524.

Figure 1. Pyrrolopyrimidine-based EGFR inhibitors

Figure 2. Lead structure **I**, and structural elements subjected to further evaluation.

Figure 3. Effect of variation of the 6-aryl group on the EGFR IC₅₀ value (nM) for pyrrolopyrimidines containing (*R*)-1-phenylethan-1-amine as C-4 substituent.

Figure 4. Effect of variation of the 6-aryl group on EGFR IC₅₀ value (nM) for pyrrolopyrimidines containing (*S*)-2-amino-2-phenylethan-1-ol as C-4 substituent.

Figure 5. EGFR IC₅₀ value (nM) for pyrrolopyrimidines **74-78**.

Figure 6. Structure-activity relationships identified in this and previous study [19, 20]. Colour code: green: induce potency; black: minor effects; red: reduce potency.

Figure 7. Docking of compound **77** using crystal structure 4WKQ [35].

Figure 8. Ligand-EGFR contacts for compound **77** during 10 ns of molecular dynamics. Highlighted amino acids are within 5 Å distance from the docked ligand. (Dynamics for compounds **50**, **53** and **76** are given in the Supplementary Material). The colours indicate residue type: green – lipophilic residues; red – acidic residues; blue – polar residues; purple – basic residues. The lines indicate contacts with the enzyme. Only interactions that occur more than 10 % of the 10 ns simulation time are shown. Ligand atoms that are exposed to solvent are marked with grey spheres.

Figure 9. Ligand-EGFR contacts for compound **65** during 10 ns of molecular dynamics. Highlighted amino acids are within 5 Å distance from the docked ligand. The colours indicate residue type: green – lipophilic residues; red – acidic residues; blue – polar residues; purple – basic residues. The lines indicate contacts with the enzyme. Only interactions that occur more than 10 % of the 10 ns simulation time are shown. Ligand atoms that are exposed to solvent are marked with grey spheres.

Figure 10. Efflux ratio (Caco-2) as a function polar surface area (n = 28).

Figure 11. Metabolic stability illustrated with respect of compound **50**.
 $HLM_{t_{1/2}}$ (Erlotinib) = 31.7 min.

Figure 12. Estimation of bioavailability using a graphical oral bioavailability map.

Figure 13. Inhibition profile of compounds **71**, **50**, **76** and Erlotinib towards 15 kinases sorted by the activity of compound **71**. Data for additional kinases for these compounds, **51** and **53** is provided in Supplementary Material)

Scheme 1. Synthesis of functionalized pyrrolo[2,3-*d*]pyrimidines. Reagents: SEM-deprotection i) TFA, CH₂Cl₂, ii) sat. Aqueous NaHCO₃, THF.

Scheme 2. Synthesis of boronic esters **8-11**. Functionalisation to: **10**: CH₃SO₂Cl, CH₂Cl₂; **11**: Ac₂O, CH₂Cl₂.

Table 1. Summary of key ADME data for the new EGFR inhibitors. Compounds are sorted by the P_{app} values. Additional data is provided in Supplementary Material.

Table 2. hERG inhibition data for the new EGFR inhibitors. Additional data is provided in Supplementary Material.

Table 3. Cell proliferation study of selected pyrrolopyrimidines towards Ba/F3-EGFR^{L858R} and A-431 cells.

Table 4. Cell proliferation data of compound **50** and Erlotinib towards various cancer cell lines.